National Library of Canada
Acquisitions and Bibliographic Services Branch
395 Wellington Street
Ottawa, Ontario
K1A 0N4

Bibliothèque nationale du Canada
Direction des acquisitions et des services bibliographiques
395, rue Wellington
Ottawa (Ontario)
K1A 0N4

Your file  Votre référence

Our file  Notre référence

## NOTICE

The quality of this microform is heavily dependent upon the quality of the original thesis submitted for microfilming. Every effort has been made to ensure the highest quality of reproduction possible.

If pages are missing, contact the university which granted the degree.

Some pages may have indistinct print especially if the original pages were typed with a poor typewriter ribbon or if the university sent us an inferior photocopy.



## AVIS

La qualité de cette microforme dépend grandement de la qualité de la thèse soumise au microfilmage. Nous avons tout fait pour assurer une qualité supérieure de reproduction.

S'il manque des pages, veuillez communiquer avec l'université qui a conféré le grade.

La qualite d'impression de certaines pages peut laisser à désirer, surtout si les pages originales ont été dactylographiées à l'aide d'un ruban usé ou si l'université nous a fait parvenir une photocopie de qualité inférieure.



Canada

# Neural Network Application To Vehicle System Dynamics

Choucri-Gabriel Taraboulsi

A Thesis
in
The Department
of
Mechanical Engineering

Presented in Partial Fulfilment of the Requirements
for the Degree of Master of Applied Science at
Concordia University
Montreal, Quebec
Canada

June 1995

ISBN 0-612-05139-0

**ABSTRACT**

**Neural Network Application**

**to**

**Vehicle System Dynamics**

Choucri-Gabriel Taraboulsi

Neural Network (N.N.) and Neurocomputing have been applied as a tool with artificial intelligence in many areas such as pattern recognition, control, classification, diagnostics, automation, etc. With the advancement of parallel processing and computational speed, N.N. has become an efficient tool for predicting and simulating input-output relationship for complex systems with large number of variables with poorly defined relationships. Vehicle dynamics is such a complex system when tire mechanics is included under steering input. N.N. is developed using a commercial software Neural-Works Professional II Plus to evaluate its potential for simulation and control of vehicle system under steering input. A three degree of freedom vehicle model under steering input is developed to train N.N. on the relationship between the tire parameter and vehicle yaw velocity. Inverse dynamics is then used to predict tire property for given vehicle yaw response, including a minimum feasible yaw response. A six degrees of freedom complete vehicle model is then used to study the potential of N.N. for roll dynamics and its control, under steering input. From this preliminary study, it is concluded

that N.N. can be used effectively in vehicle dynamics applications, however, with some inherent limitations. Its potential is significant in application to control of vehicle system dynamics. A major limitation being the inability of the N.N. to learn when different combination of parameters lead to same response.

**ACKNOWLEDGMENTS.**

The author wishes to express his sincere appreciation to his thesis supervisor, Dr. A. K. W. Ahmed for providing guidance throughout the course of his investigation.

Thanks are due to the faculty members, staff, and other graduate students of CONCAVE Research Centre, and the Department of Mechanical Engineering for their help during the course of his work.

Finally, the author would like to express his special thanks to his family members for their love, encouragement and support.

**TABLE OF CONTENT.**

## LIST OF FIGURES.

## LIST OF TABLES.

## NOMENCLATURE.

| | |
|---|---|
| $a_X$ | acceleration along the longitudinal axis |
| $a_Y$ | acceleration along the lateral axis |
| $a_Z$ | acceleration along the vertical axis |
| $C_F$ | equivalent front damping coefficient |
| $C_R$ | equivalent rear damping coefficient |
| $C_\alpha$ | cornering stiffness of tire |
| $C_{\alpha F}$ | cornering stiffness of front tire |
| $C_{\alpha R}$ | cornering stiffness of rear tire |
| $C_\gamma$ | camber stiffness of tire |
| $F_S$ | suspension force |
| $F_X$ | force component along the $X$ axis |
| $F_Y$ | force component along the $Y$ axis |
| $F_{YF}$ | cornering force of front tire |
| $F_{YR}$ | cornering force of rear tire |
| $F_{Y\alpha}$ | cornering force of tire |
| $F_{Y\gamma}$ | camber thrust of tire |
| $F_Z$ | force component along the $Z$ axis |
| $f_r$ | coefficient of rolling resistance |
| $h_A$ | displacement of the centre of gravity due to rolling |
| $h_B$ | displacement of the centre of gravity relatively to the roll centre |
| $h_C$ | displacement of the centre of gravity relatively to the ground |
| $h_o$ | distance between the roll centre and the centre of gravity |

| | |
|---|---|
| $I_X$ | moment of inertia about the $X$ axis |
| | moment of inertia about the rolling centre |
| $I_Y$ | moment of inertia about the $Y$ axis |
| $I_Z$ | moment of inertia about the $Z$ axis |
| $K_F$ | front equivalent spring stiffness. |
| $K_R$ | rear equivalent spring stiffness. |
| $K_t$ | equivalent torsion bar stiffness. |
| $L$ | vehicle wheel base |
| $L_1$ | distance between the centre of gravity and the front tire |
| $L_2$ | distance between the centre of gravity and the rear tire |
| $m$ | mass of the vehicle |
| $M_X$ | moment about the $X$ axis |
| $M_Y$ | moment about the $Y$ axis |
| $M_Z$ | moment about the $Z$ axis |
| N.N. | Neural Network |
| $S$ | vehicle tread |
| $V_X$ | velocity along the vehicle fixed $X$ axis |
| $\dot{V}_X$ | acceleration along the vehicle fixed $X$ axis |
| $V_Y$ | velocity along the vehicle fixed $Y$ axis |
| $\dot{V}_Y$ | acceleration along the vehicle fixed $Y$ axis |
| $V_Z$ | velocity along the vehicle fixed $Z$ axis |
| $\dot{V}_Z$ | acceleration along the vehicle fixed $Z$ axis |
| $X$ | displacement along the $X$ axis direction |
| $\dot{X}$ | velocity along the $X$ axis direction |

| | |
|---|---|
| $\ddot{X}$ | acceleration along the $X$ axis direction |
| $Y$ | displacement along the $Y$ axis direction |
| $\dot{Y}$ | velocity along the $Y$ axis direction |
| $\ddot{Y}$ | acceleration along the $Y$ axis direction |
| $Z$ | displacement along the $Z$ axis direction |
| $\dot{Z}$ | velocity along the $Z$ axis direction |
| $\ddot{Z}$ | acceleration along the $Z$ axis direction |
| $\alpha$ | slip angle |
| $\alpha_F$ | front slip angle (3 d.o.f. vehicle model) |
| $\alpha_R$ | rear slip angle (3 d.o.f. vehicle model) |
| $\alpha_1$ | front right slip angle (6 d.o.f. vehicle model) |
| $\alpha_2$ | front left slip angle (6 d.o.f. vehicle model) |
| $\alpha_3$ | rear right slip angle (6 d.o.f. vehicle model) |
| $\alpha_4$ | rear left slip angle (6 d.o.f. vehicle model) |
| $\gamma$ | camber angle |
| $\delta_F$ | steering angle ( 3 d.o.f. vehicle model) |
| $\Delta_i$ | deflection of the suspension at each tire (6 d.o.f. vehicle model) |
| $\dot{\Delta}_i$ | deflection rate of the suspension at each tire (6 d.o.f. vehicle model) |
| $\theta$ | mean steering angle |
| $\theta_L$, $\theta_{FL}$ | left front steering angle |
| $\theta_R$, $\theta_{FR}$ | right front steering angle |
| $\Omega_X$ | roll angle |
| $\dot{\Omega}_X$ | roll velocity |
| $\ddot{\Omega}_X$ | roll acceleration |

| | |
|---|---|
| $\Omega_y$ | pitch angle |
| $\dot{\Omega}_y$ | pitch velocity |
| $\ddot{\Omega}_y$ | pitch acceleration |
| $\Omega_z$ | Yaw angle |
| $\dot{\Omega}_z$ | Yaw velocity |
| $\ddot{\Omega}_z$ | Yaw acceleration |

# CHAPTER 1

## 1. INTRODUCTION AND LITERATURE REVIEW.

### 1.1 GENERAL

Neurocomputing and neural networks (N.N.) in simple term are an attempt in simulation of the human brain. It is, however important to mention that in no way the N.N. is a match to the human brain. Human brain is formed of neurons, where each neuron is formed of an input area the dendrites, a processing area the synapse and an output area the axons which is connected to other neurons. Similarly, the N.N. is formed of artificial neurons (A.N.), where each neuron is formed of an input area, a processing element and an output area. A systematically linked network of A.N. is carried out in the construction of N.N. The present research is focused on the application of the advance neurocomputing technology to a complex dynamical system such as road vehicle dynamics.

The beginning of neural computing and N.N. is often considered to be the 1943 paper of Warren McCulloh and Walter Pitts [1]. In this work, although practical application of such work was not apparent, they were able to show that a simple type of N.N. could compute any arithmetic or logical function. Other researchers like Norbert Wiener and John von

Neuman [2, 3] suggested that research in brain-like computers might have wide applications. In 1949 D.O. Hebb [4] proposed that the connectivity of the brain neuron is continually changing as an organism learns. He proposed that a specific learning law be introduced for processing area or the synapses of neurons. The first successful neurocomputer (the Mark I Perceptron) was developed during 1957 and 1958 by Frank Rosenblatt, Charles Wightman and others [5]. Following that period, N.N. research went into a quiet phase from 1967 to 1982. In the early 1980s the Defence Advanced Research Projects Agency (DARPA) began funding neurocomputing research. DARPA funding opened the door for neurocomputing to demonstrate its potential and effectiveness in a wide range of applications. Today neurocomputing and N.N. have found their ways into various types of applications like system modelling, control, classification, medical diagnostics, robotics, automation and many other fields. Several articles and books [6, 7, 8, 9] have appeared on various aspects of N.N. algorithms, applications and software in the 1990s.

N.N. is most effective when the problem to be solved depend on many parameters and where physical properties could not be expressed in equations. A good example is the vehicle tire, where properties and behaviour depend on many variables such as road surface and friction, vehicle speed, slip, braking or driving force, inflation pressure, steering angle

etc. Similarly the dynamic behaviour of a vehicle under steering input is highly complex and depends on the suspension design, spring rate, damping characteristics, tire properties, torsion bar design, forward velocity steering angle etc. Study of the tire mechanics and transient vehicle dynamics under steering input are therefore, potential candidates for the application of N.N. for vehicle systems.

For a vehicle system the tire and suspension are the connection between road and vehicle structure, where all major forces and moments are developed at the tire-road interface. The tire and suspension parameters, therefore, have the most influence on the dynamic behaviour of a road vehicle. These parameters have a well known conflicting requirement between ride quality and handling (stability) performance of a vehicle. Furthermore, the characteristics of these components are significantly influenced by a large number of variables, which often make it very difficult to model realistically. One of the major difficulty is in estimating an appropriate property for the component, and providing a control of the property to satisfy conflicting requirements.

This study is aimed at addressing some of the issues that poses difficulty in modeling vehicle system dynamics, by applying neurocomputational tool. The study examines the potential of N.N. in simulating a tire and a simple vehicle

model with four suspensions under steering input. The N.N. is further used to estimate optimal parameter through inverse dynamics and for parameters control. For the application to tire model a simple three degrees-of-freedom (DOF) bicycle model [10, 11, 12] with identical front and rear tire parameter is considered. The in-plane vehicle motions include forward, lateral and yaw. Since tire parameters have the most influence on yaw velocity, the model is used to simulate vehicle yaw velocity for a wide range of tire parameters. Based on the simulated result the N.N. is trained to gain artificial intelligence on the relationship between vehicle yaw velocity and tire parameters. The trained N.N. is then utilized to predict tire property for a given vehicle yaw response in time domain. The network is further used to establish tire parameters for maximum stability.

The application of N.N. is next extended for a complex six DOF vehicle model suspended on four suspensions. Under a steering input vehicle roll is the critical mode which is a measure of handling performance. Similar to the 3 DOF model, the 6 DOF vehicle model is used to simulate the roll motion for a range of suspension parameters, to train the N.N. The inverse dynamics of N.N. is then used to predict suspension parameters for a given transient roll performance under a steering input. Finally a controller based on N.N. is proposed and used to estimate suspension damping for a given steering

input, and forward velocity, and a roll reduction parameter. Simulation results for the six DOF model with and without the open loop controller are compared.

## 1.2 REVIEW OF RELEVANT LITERATURE

The literature used in this research could be divided into two categories:

1) literature concerned with vehicle dynamics and formulation of the mathematical models of the three and six DOF vehicle models,

2) literature concerned with N.N. and neural computing in application to system modelling, inverse dynamic, optimization and control.

### 1.2.1 VEHICLE DYNAMICS:

The vehicle dynamics could be defined as the behaviour and performance of the vehicle under different road and operating conditions, for example: performance at different velocities under road irregularities and side winds; performance at different velocity under a steering input; as well as performance under braking and acceleration. The analytical study of the vehicle dynamics is based on

formulating a mathematical model which effectively represent the vehicle system, identification of performance indices and solution of the mathematical model using an appropriate and suitable tool.

To formulate the mathematical models of the vehicle one must study the mechanics of tires, suspension and steering since they are the connections between the vehicle and the road. Validity of a model largely depend on validity of the component characteristics used in the model. In this study, tire, suspension and steering system are the critical components.

The tire is the most complicated part of the vehicle, its behaviour has been studied for a long time and is still being studied extensively. The tire is the primary running gear-ground contact through which forces are transmitted from the vehicle to the road and vice versa. Ellis [10] presents different tire mathematical models for the study of the cornering forces. The first model is the stretched string model, where the tire is assumed to be a stretched string retained by lateral springs representing the tire wall. In the second model, the tread band is represented as an equivalent beam supported by an elastic foundation. These models with linear or nonlinear stiffness are not adequate to represent accurately the tire behaviour in cornering. For the vertical

and ride dynamic studies [13] tire is often considered as a parallel combination of a linear spring and damper. Nonlinear spring, however, must be used to simulate wheel lift off. The cornering properties of the tire depend on the lateral force developed at the road-tire interface, which is a function of a wide range of parameters [11]. For a free rolling tire, the tire-road interface forces and moments can be expressed in terms of: lateral force; rolling resistance; and self aligning moment. Wong [11] has presented a through treatment of all the above forces and moments, which must be incorporated in the tire model for simulation of cornering performance.

The suspension of the vehicle is a mechanism which dictates the ride quality and handling performance of the vehicle. The design of the suspension poses conflicting requirement between stability and ride comfort of the vehicle. Newton, Steeds and Garett, [14] and Ellis [11] present different types of suspension, which could be divided into two distinctive categories. The first is the axle suspension where the left and the right wheels are connected by a rigid axle, and the second type is the independent suspension in which the left and right wheels are not connected. Despite the different types of suspension the analysis always results in calculating the equivalent spring stiffness, equivalent damping coefficient, equivalent roll stiffness and the roll centre location. Although the suspension equivalent stiffness and

damping characteristics are often considered to be linear, nonlinear elements are used in reality for a compromise between ride and handling performance [15].

The steering mechanism in most vehicles is the Ackerman steering mechanism. Due to physical constraint this steering mechanism can not provide perfect steering. A perfect steering is defined as one, where all wheels can have pure rolling around a curve. Since rear wheels are not steered, perfect steering can not be achieved. This leads to wheel side slip which can be minimized through an Ackerman geometry. In analysing vehicle motion, perfect steering is assumed when the steering angle is small. Bevan [17] presents the steering mechanism its limitations and a way to calculate the left and right steering angle according to a mean steering angle. The mean steering angle is the steering input or the angle of an imaginary wheel positioned in the middle of the vehicle. This imaginary wheel acting alone would produce the same effect of the two other wheels, assuming perfect steering.

The mathematical models of a vehicle under steering input could vary from simple one like the three DOF model formulated by Ellis [10], Wong [11], Gilespie [12] to complex ones. This vehicle model is referred to as a bicycle model where the vehicle mass is situated between the front and the rear tires. This model is effectively used to evaluate steady state

curving performance of a vehicle. The influence of tire parameters on the lateral and yaw velocity of the vehicle can be easily examined using this model. This model, however cannot simulate the roll performance of the vehicle under a steering input. A six DOF model formulated by Lugner [17, 18] is a three dimensional model of the vehicle capable of exhibiting more realistic behaviour.

### 1.2.2 NEURAL NETWORKS:

The theoretical concept of N.N. has been around since 1940s, but its development has been slow due to computational limitations. With the development of algorithms, programming techniques and fast computers, it gained momentum in the 1980s. Since then, through defence funding and extensive research N.N. and neurocomputing have been explored for application in a wide range of areas including pattern recognition, control, classification, diagnostics, automation, etc.

Zurada [6], Hechlt-Nielsen [7] and Freeman [8] have recently published books in the area of N.N. These books present a complete introduction to N.N. along with different types and their applications. Some of these N.N. types are:

Adaline and Madaline: has gained application in adaptive signal processing. It is a N.N. that can be implemented as

filters to perform noise removal from information-bearing signals.

Back-propagation: has application in problems requiring recognition of complex patterns and performing non-trivial mapping. It is a network that adapts itself to "learn" the relationship between a set of example patterns, and able to apply the same relationship to a new input pattern. Back-propagation network, therefore, has potential application in simulation, control of dynamical systems and reverse dynamics.

General regression network: is a general purpose network. It gained applications in system modeling and prediction.

Modular neural network: is a generalization of back-propagation neural network. It is applied to system modeling, prediction, classification and filtering.

Among various N.N. developed to date, back-propagation network can be easily adapted for application to simulation of dynamical system, control and optimization. Hunt and Sbarbro [19] presents the use of N.N. as a controller. The N.N. is used as a representation framework for modelling nonlinear dynamical systems, it is then possible to use these nonlinear models within nonlinear feedback control structure.

In recent years, there have been few applications of N.N. in vehicle system modeling and control. Moran and Nagai [20] in the control of a vehicle rear suspension. In this paper the authors demonstrate the ability of N.N. to formulate a vehicle

model. This neuro-vehicle model is used to train both front and rear suspension neuro-controller under a nonlinear rear preview control scheme. To do that a N.N. is trained to identify the inverse dynamics of the front suspension and determine the road disturbances. Knowing the road disturbances the rear wheel controller can improve the rear suspension response.

Palkovics and El-Guindy [21] used the back-propagation N.N. to model the vehicle tire. The data file used in the learning process is obtained from tests. The side force for a given slip angle predicted by the N.N. is compared with that of magic formula of Pacejka. Furthermore, they implemented the neuro-tire in a vehicle mathematical model to demonstrate the effectiveness of the N.N. The software used in this study is a simple N.N. feature in the MATLAB.

In developing a N.N. application one should take in consideration that success of N.N. to learn is not guaranteed. Sometimes for no apparent reason N.N. might not learn and will not give adequate results [7]. Developing a N.N. application is carried out by trial and error until the best results are obtained. It is important to note that there should be no similar inputs to the N.N. with different outputs, if such a case is presented to the N.N. learning would be impossible.

## 1.3 SCOPE AND OBJECTIVE OF THE PRESENT RESEARCH

As discussed in the literature review, neurocomputing and N.N. are a fast growing computational tool with a scope for a wide range of applications. It has already claimed a tremendous success in pattern recognition. Its application in vehicle dynamics however, has been limited.

The primary objective of this investigation is to examine the potential of N.N. namely, back-propagation network in applications to vehicle dynamics. As an initial stage, the application is focused on a model to predict or estimate tire parameters based on vehicle yaw response to steering input. Furthermore, to determine the tire parameter to minimize yaw response or improve stability in time domain. For this a three DOF bicycle model discussed in the literature review is utilized.

Next, the model is extended to relatively complex six DOF multi variable vehicle model. The objective is to evaluate the potential and limitation of back-propagation N.N. in application to multi-variable complex system. In this case N.N. simulation is carried out for relationship between time-roll response and suspension parameters. The application of N.N. is then extended as a controller to control the roll of the vehicle by controlling the suspension damping coefficient.

Such a controller if implemented would not require a compromise between ride quality and handling performance of the vehicle.

The thesis presents systematic development of tire and suspension forces, leading to the development of the three and six DOF vehicle models. The result for each model and roll control study are discussed as outlined in the following subsection.

### 1.3.1 Organization of the thesis

In chapter 2, the forces and moments developed at the tire-road interface due to rolling resistance, slip, camber angle and self alignment are discussed and formulated. Evaluation of roll centre and characteristics of suspension component are discussed. The expressions for suspension forces are formulated. This chapter also presents the steering system along with explanation of perfect steering. Expressions for left and right wheel angle for a mean steering angle is formulated.

In chapter 3, N.N. is introduced along with a brief review of back-propagation N.N. The "learning" rule and N.N. parameters are discussed. The procedure for building a N.N. application is outlined.

Chapter 4 presents the N.N. application of the three DOF model. The system parameters are listed and the N.N. results are presented. All results computed from N.N. based on system response are compared with simulation results for the N.N. predicted parameter. Various training schemes are evaluated. Finally, the N.N. is tested for estimating the parameter corresponding to minimum response corresponding to all "learning" cycles.

The procedure in chapter 4 is repeated for a six DOF vehicle model in chapter 5. The expressions developed in chapter 2 are used to develop the model. N.N. is applied for multi-variable and single variable design objective. Results are presented similar to the 3 DOF model. This chapter also presents development and application of N.N. for control of suspension damping to improve roll response.

Finally chapter 6 presents general and specific conclusions related to the present study. A list of recommendations for further is work also included in this chapter.

# CHAPTER 2

## 2. VEHICLE SYSTEM MODELING CONSIDERATIONS.

### 2.1 INTRODUCTION

Major components that significantly influence vehicle dynamics response include tires, suspension and steering system. Most of ground vehicles use tires as the running gear-ground contact. Except aerodynamic and gravitational forces, almost all other forces and moments to the complicated vehicle system are induced through the tire-ground contact. A through understanding and representation of the dynamic tire characteristic is, therefore, essential to study the performance of a vehicle.

The primary function of a vehicle suspension system is to isolate the sprung mass (structure and occupant) from shock and vibrations generated by the road surface. The suspension also has a major influence on the stability, steering control and the overall handling of the vehicle under dynamic conditions. Each wheel of the vehicle is connected to the sprung mass through a system of linkages, spring and damper elements, referred to as suspension.

A vehicle under steering input may be subjected to many

different degrees of free movement. The interaction of these movements, along with their velocity, acceleration and frequency makes the vehicle one of the most complex system in the field of dynamics [10, 11, 12, 14, 22]. Researchers and designers in the field of vehicle system, therefore, simplify the model to study different aspects of vehicle dynamics.

In this investigation two different vehicle models, namely: a 3 DOF in-plane bicycle model; and a six DOF three dimensional model are considered for application of N.N. This section presents the characteristics of tires, suspension and steering systems toward the development of vehicle models developed in chapters 4 and 5.

## 2.2 TIRE CHARACTERISTICS

In general the tire is required to fulfil several functions, namely, to support the vehicle weight, transmit tractive and braking forces to the ground, provide steering control and directional stability and to provide a first barrier to road irregularities. Although tires are often modeled as a linear spring, all tire characteristics are highly nonlinear, and in reality is far more complex than a simple spring.

Tire performance and characteristics depend on many

factors such as construction, working pressure and temperature, surface hardness, static load, tread condition and geometry, and road surface conditions which may vary widely. Depending on the above factors and operator inputs such as steer angle, velocity, acceleration, etc. the tire develops forces and moments at the tire-ground interface. Various input-output quantities for a tire are shown in Fig. (2.1). Tire-ground contact forces $F_X$, $F_Y$, $F_Z$ and moments $M_X$, $M_Y$, $M_Z$ developed depend on the slip angle $\alpha$ , camber angle $\gamma$ , tire deflection $\delta$ , forward speed $V$ and slip $s$ . The resulting forces and moments are also influenced by a number of uncertain parameters as listed in Fig. (2.1). The inherent non-linearity and wide range of factors influencing tire characteristics makes it one of the most difficult component in the modelling of vehicle systems.

### 2.2.1 TIRE AXIS SYSTEM

Various tire forces and moments, as well as its geometric parameters are defined in terms of a tire axis system. The most commonly used axis system is the one recommended by the Society of Automotive Engineers (SAE) [33] is shown in Fig. (2.2)

The origin of the axis system $O$ is the centre of tire-ground contact. Positive $X$ axis is defined on the ground

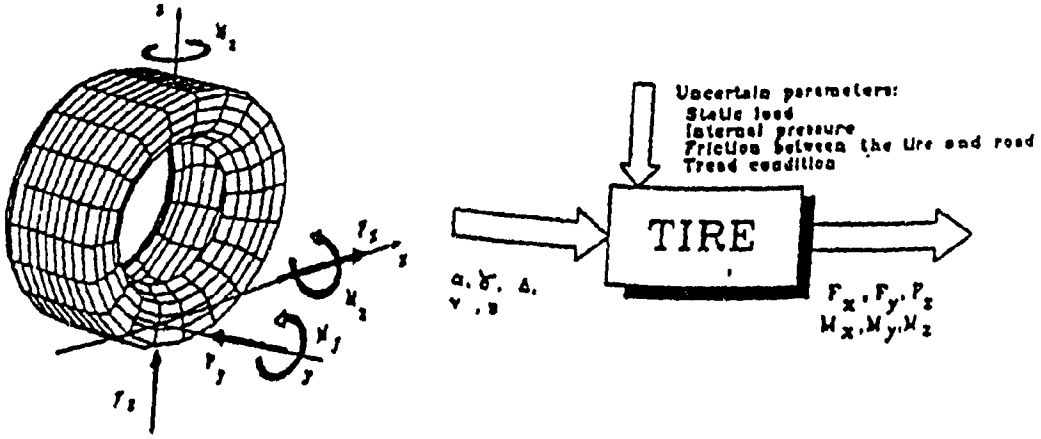


Fig. (2.1) Various tire quantities. [21]

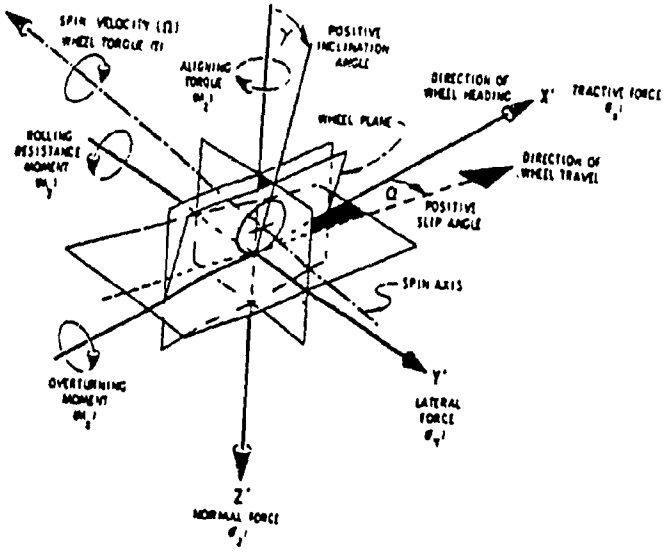


Fig. (2.2) S.A.E. Axis. [33]

plane in the direction of wheel heading. $Y$ axis is also in the ground plane and is perpendicular to the $X$ axis in the lateral direction. $Z$ axis is in the vertical direction perpendicular to the ground plane, with the positive direction toward the ground. Camber angle $\gamma$ is the angle formed between the $XZ$ plane and the wheel plane. The slip angle $\alpha$ is the angle between the direction of wheel heading $X$ and direction of wheel travel.

### 2.2.2 TIRE FORCES AND MOMENTS

Various forces and moments acting at the tire-road interface in the plane X-Y can be classified under three categories. Thy are: Longitudinal force ( $F_X$ in Fig. 2.2) which result from tractive or braking effort and rolling resistance; Lateral force ( $F_Y$ in Fig. 2.2) at the interface which result from the camber angle and cornering; and aligning torque ( $M_Z$ in Fig. 2.2) that results due to the lateral force acting at the contact with a pneumatic trail. These forces and moments are discussed and formulated in the following subsections.

#### 2.2.2.1 LONGITUDINAL FORCE

For a tire under tractive or braking effort, the longitudinal force can be expressed as:

$$For\ driving \quad F_x = F_d - F_r \tag{2.1}$$

$$For\ braking \quad F_x = F_b + F_r \tag{2.2}$$

where $F_d$ and $F_b$ are the tractive and braking effort respectively and $F_r$ is the rolling resistance.

TRACTIVE (BRAKING) EFFORT

When a driving torque is applied to a pneumatic tire, the front of tire contact patch is compressed. Therefore, the distance the tire travels under a driving torque is less than that of free rolling condition. As a result a phenomenon of longitudinal slip takes place, which is defined in terms of the difference between actual velocity and free rolling velocity [17]. The slip $S$ can be expressed as:

$$For\ dreiving \quad S_d = \frac{r\omega - V}{r\omega} \tag{2.3}$$

$$For\ braking \quad S_b = \frac{V - r\omega}{V} \tag{2.4}$$

where $V$ is the linear velocity of the tire centre, $\omega$ is the angular velocity, and $r$ is the radius of free rolling tire. The tractive effort $F_d$ is a function of slip $S_d$, trend of which based on experimental data is shown in Fig. (2.3). As the figure shows, the tractive effort initially increases with slip and reaches a maximum value around 20% slip ($S_d$=0.2). The peak attainable tractive effort is $\mu_p W$ , where $\mu_p$ is the

peek coefficient of road adhesion and $W$ is the normal tire load. For slip greater that 20%, the tractive effort decrease drastically to a value of $\mu_s W$ at 100% slip, where $\mu_s$ is the slip coefficient of adhesion. As the Fig. (2.3) shows, a linear relationship between tractive effort and slip can be considered in the presence of small slip:

$$F_d = C_1 S_d \tag{2.5}$$

where $C_1$ is the slope of the linear range as shown in Fig. (2.3).

ROLLING RESISTANCE

An inflated tire under load deforms in the area of ground contact. Due to the rotation of the tire the deflected area is not symmetric and the normal force $F_z$ does not act at the origin of the tire. Fig. (2.4) shows a force diagram during rolling under load, where $F_z$ acts at a distance $X$ in the direction of rolling. The shift produces a moment equal to $F_z X$, which is known as the rolling resistance moment. For a free wheel, therefore, a horizontal force at the tire-ground contact must exist to maintain equilibrium. this resulting force is referred to as the rolling resistance $F_r$ acting against the direction of travel can be expressed as:

$$F_r = F_z \frac{X}{r_e} \tag{2.6}$$

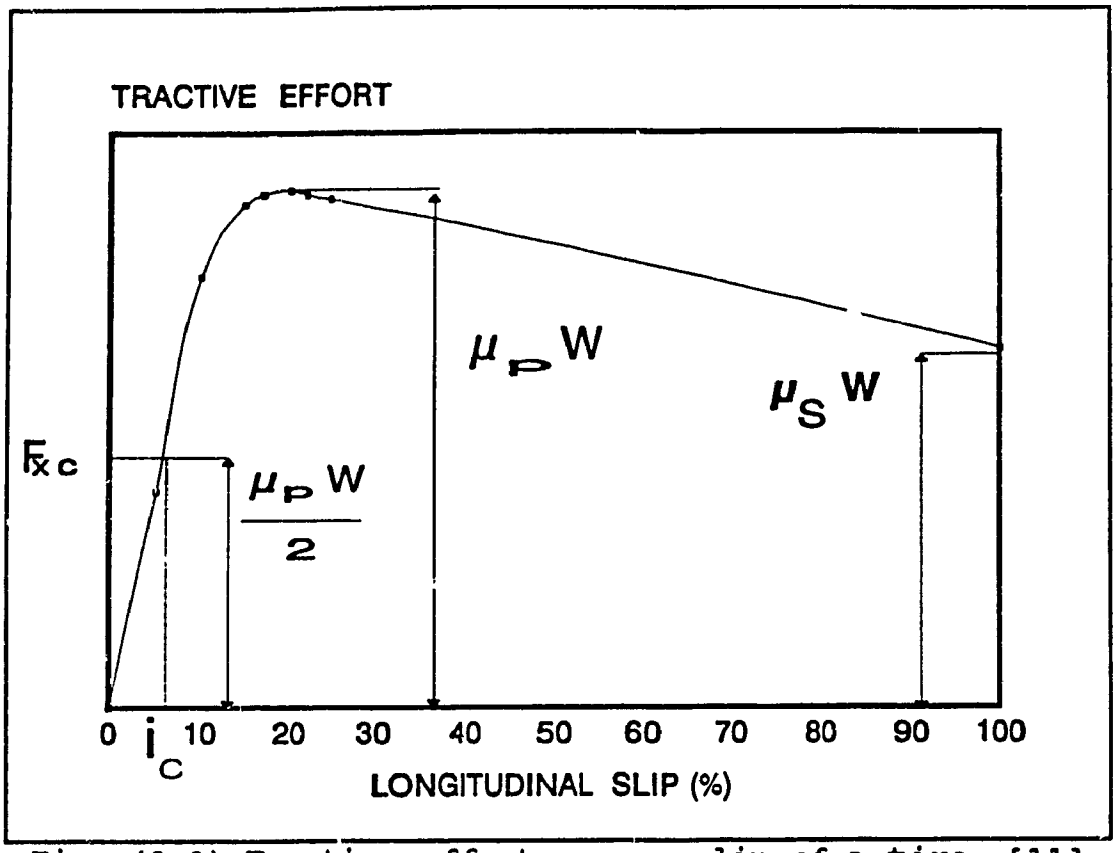


Fig. (2.3) Tractive effort versus slip of a tire. [11]

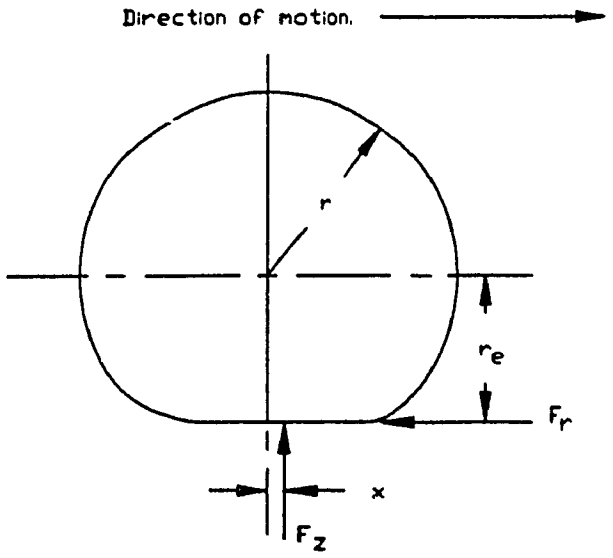


Fig. (2.4) Rolling resistance.

where $X$ is the arm of rolling resistance moment and $r_e$ is the effective rolling radius of the tire as shown in Fig. (2.4). Equation (2.6) is commonly expressed as:

$$F_r = F_Z f_r \quad where \quad f_r = \frac{X}{r_e} \tag{2.7}$$

$f_r = x/r_e$ is the coefficient of rolling resistance. The value of this coefficient depends on the tire diameter the vehicle velocity, tire inflation pressure, tire tread geometry, tire type, tire temperature, and the surface condition.

The complex relationship between tire, its operational parameters and the resulting rolling resistance coefficient make it extremely difficult to develop analytical method for predicting the rolling resistance. The rolling resistance is, therefore, primarily determined through experiments [11]. Based on experimental results, many empirical formulas have been proposed. One such simple and widely accepted expression that represent the influence of pressure and forward speed is given by [11]:

$$f_r = f_0 + f_s \left(\frac{V}{100}\right)^{2.5} \tag{2.8}$$

where $V$ is in km./h

$f_s$ and $f_0$ depend on the inflation pressure as shown in Fig. (2.5).

Since most of passenger vehicles have an inflation pressure around 207 KPa (30 psi), the expression (equation 2.8) can be simplified to

$$f_r = 0.01\,(1+\frac{V}{160}) \qquad (2.9)$$

This equation is acceptable for speeds up to 128 Km/h (80 mph) on concrete surfaces.

Preliminary performance on different road surface can be evaluated ignoring the effect of speed. In this case, the rolling resistance coefficient can be taken as an average value for different tire on different surface given in table (2.1) [11].

2.2.2.2 LATERAL FORCE

The lateral force at the tire-road interface is developed due to the cornering and the presence of camber angle. Tire models had been developed to calculate the lateral forces. The tire lateral force characteristics has been developed based on tire mechanics and experiments. The tire lateral force also known as cornering force can be expressed as a nonlinear function of slip angle (angle between wheel heading and direction of travel). Another component of the lateral force is due to the camber angle (angle of inclination from the vertical plane). The lateral force at tire road interface do not pass at the centre of rotation but behind the centre at

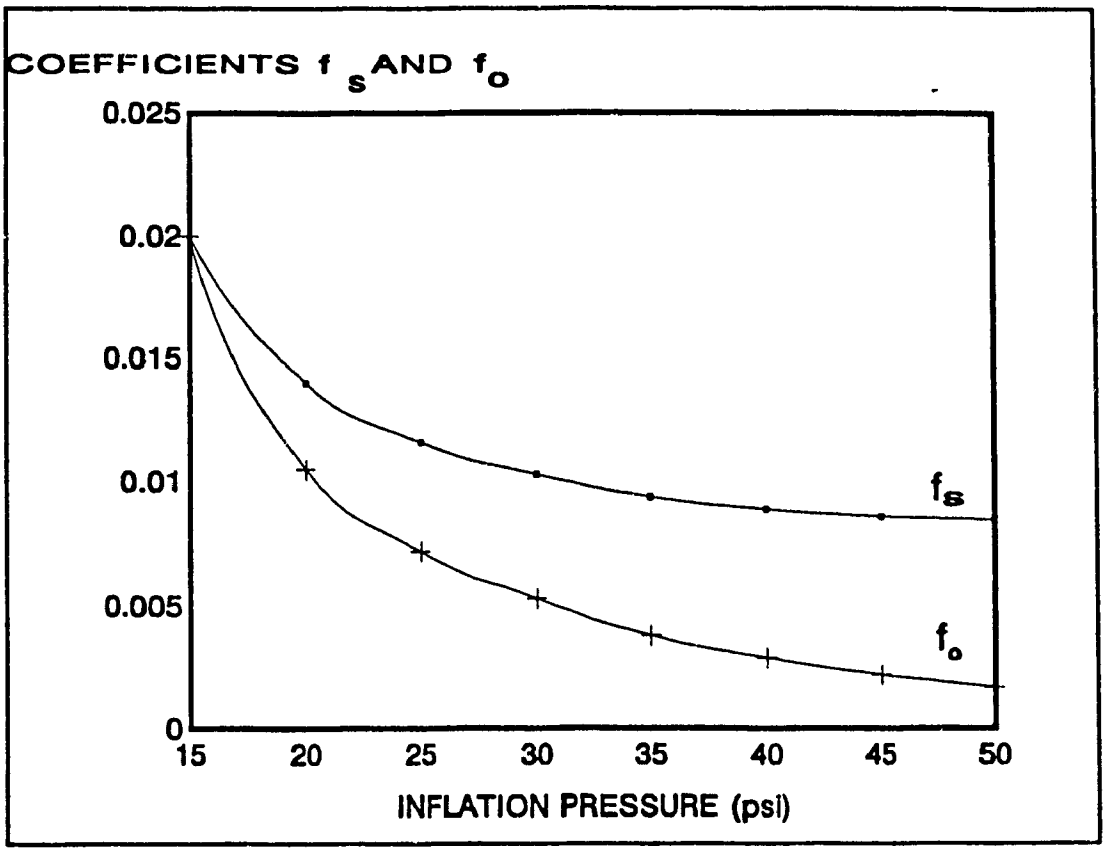


Fig. (2.5) Effect of tire inflation pressure on $f_s$ and $f_o$ . [11]

| Vehicle Type. | Concrete. | Medium hard soil. | Sand. |
|---|---|---|---|
| Passenger cars. | 0.015 | 0.08 | 0.30 |
| Trucks. | 0.012 | 0.06 | 0.25 |
| Tractors | 0.02 | 0.04 | 0.20 |

Table (2.1) Coefficient of rolling resistance. [11]

a small distance $t_p$ , referred to as pneumatic trail [10, 11, 12]. This causes a moment about the vertical axis referred to as aligning torque.

LATERAL FORCE DUE TO CORNERING

During cornering when a perpendicular force to the wheel plane is applied, a lateral force ( $F_{Y\alpha}$ ) is developed at the contact patch and the tire is forced to move along a path at an angle $\alpha$ with the wheel plane referred to as slip angle. The characteristics of cornering force can be expressed as a nonlinear function of slip angle for a given tire construction. The trend can, however, be considered linear for slip angle in the range of 0 to 4° . For this range the cornering force can be estimated from:

$$F_{Y\alpha} = C_\alpha \alpha \qquad (2.10)$$

where $C_\alpha$ is referred to as tire cornering stiffness

LATERAL FORCE DUE TO CAMBER ANGLE

Camber angle as defined in section 2.2.1 is the angle of wheel plane inclination from the X-Z plane. The camber angle is introduced to achieve axle bearing pressure and to decrease king pin offset. The camber angle can be positive or negative as defined in Fig. (2.2). In a rolling tire, the camber ( $\gamma$ ) introduces a lateral force at the tire-road interface which

can be expressed as a linear function of the camber angle given by [11]:

$$F_{y\gamma} = \pm C_\gamma \gamma \qquad (2.11)$$

Where $C_\gamma$ is referred to as a camber stiffness of the tire determined experimentally. The total lateral force at the tire-road interface can, therefore, be expressed as:

$$F_y = F_{y\alpha} + F_{y\gamma} \qquad (2.12)$$

By substituting equation (2.10) and (2.11) the total lateral force is:

$$F_y = C_\alpha \alpha \pm C_\gamma \gamma \qquad (2.13)$$

The camber angle in passenger cars is limited to around 1°, since it tends to promote tire wear [11], and for simplification its effect can be neglected.

ALIGNING TORQUE

As explained previously, the lateral force at the tire-road interface acts at a distance $t_p$ behind the wheel centre. This causes a moment $M_z$ about the Z-axis, referred to as self aligning torque:

$$M_z = F_x t_p \qquad (2.14)$$

where $t_p$ is the pneumatic trail usually considered as 1/6 of the tire contact patch. The aligning torque is comparatively small and can be ignored for most analysis.

## 2.3 SUSPENSION SYSTEM.

One of the objective in the present study is to examine the potential of N.N. in predicting suspension parameters, and possible application of N.N. as a dynamic controller of suspension parameter. For this, a six DOF complete vehicle with four wheels and suspension is considered, while subjected to a steering input.

The vehicle suspension system primarily consists of a spring and damper placed between each wheel and vehicle body. In addition to basic suspension, modern vehicles utilizes a torsional spring that connects the left and right wheels. This torsional spring also referred to as a stabilizer bar or an anti roll bar acts as a spring only in the presence of roll thus increasing the roll stiffness of the vehicle. The force developed by various suspension elements are presented in this section.

### 2.3.1 SUSPENSION COMPONENTS:

Vehicle system suspension can be represented by a

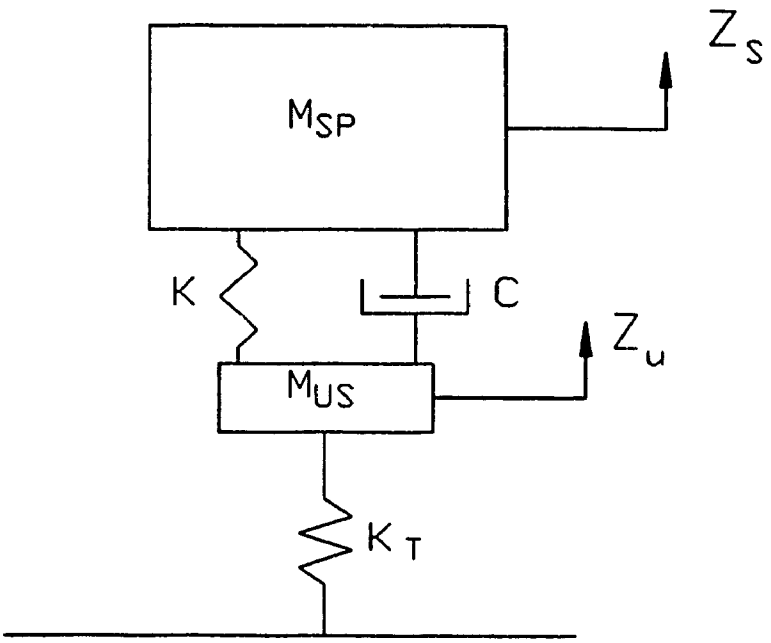


**Fig. (2.6) Simple suspension model.**

combination of several elements as shown in Fig. (2.6), where $M_{SP}$ is the sprung mass representing vehicle body, $M_{US}$ is the unsprung mass representing the axle, $K$ is the stiffness of the spring, $K_T$ is the tyre stiffness and $C$ is the damping coefficient of the shock absorber. The springs of the suspension supports the sprung mass, the shock absorber provides the dissipation of energy and the tire acts as a secondary suspension between the axle and ground. Although friction is present in the suspension system, it is often neglected.

SUSPENSION SPRING:

The primary function of the suspension spring is to support the vehicle sprung mass. There are two major types of springs used in cars and light weight trucks, namely coil spring and leaf spring. The spring is characterized by its stiffness, which can be linear or nonlinear (progressive). In general, the suspension force for the spring can be expressed as: [22]

$$F_s = K_s(Z)\,Z \qquad (2.15)$$

where $Z$ is the vertical deflection across the spring. $K_s(Z)$ is the stiffness which is constant for a linear spring.

SUSPENSION DAMPER:

The primary function of the suspension damper is to isolate sprung mass from shock and vibration generated at the wheel or axle. It dissipates energy by pushing oil through a small orifice as the relative position across the damper is changed. For constant area orifice, the damper is considered linear where the force across the damper is proportional to the relative velocity.

Dampers are often designed with valves to provide variable effective orifice and nonlinear characteristics to achieve better performance over a wide frequency range. In general, the force developed across a damper can be expressed as:

$$F_D = C(Z)\dot{Z} \qquad (2.16)$$

where $\dot{Z}$ is the velocity across the damper. $C(Z)$ is the coefficient of damping which is constant for a linear damper.

ANTI-ROLL BAR:

Anti-roll bar is a torsional spring attached to left and right wheels to resist roll motion of the sprung mass. The bar is only active when there is a relative motion between the left and right wheels, thus affecting only the roll motion. A detailed model for anti-roll bar is presented in [13]. The

stiffness of the bar can be obtained based on material property and bar geometry. Knowing the torsion bar stiffness, $K_T$ in N/rad. suspension force due to anti-roll bar can be expressed as:

$$F_S = K_T \Omega_X \qquad (2.17)$$

where $\Omega_X$ is the roll motion of the sprung mass. Here the characteristic of the bar is considered linear.

ROLL CENTRE:

The roll centre of the vehicle is the point at which the vertical forces act upon the sprung mass. To model a vehicle system the roll centre location must, therefore, be determined. As shown in Fig. (2.7) the determination of the roll centre is based on finding the instantaneous centre of the suspension mechanism which in this case is denoted by points A and A'. The roll centre for the suspension is found from the intersection of lines connecting tire-road contact C and C' to A and A', respectively (Fig. (2.7)). If the vehicle is on a level road, the point R is located on the centre line of the vehicle. But if the vehicle is subjected to roll it is clear that the roll centre will migrate. If the roll angle is small, the change in the suspension geometry can be neglected in order to assume a fixed roll centre.

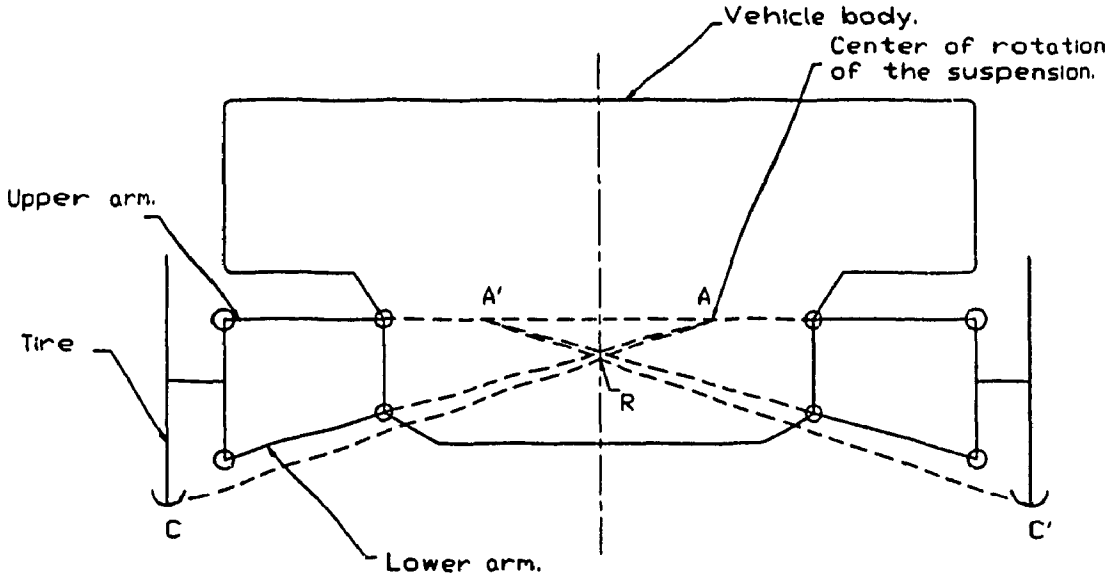


**Fig. (2.7) Determining the roll centre.**

### 2.3.2 SUSPENSION FORCES

The suspension force can be determined based on the relative motion and the relative velocity across the suspension elements. With reference to Fig. (2.6), the suspension force can be expressed as:

$$F_s = K_{eq.} Z + C_{eq.} \dot{Z} \qquad (2.18)$$

where $K_{eq.}$ and $C_{eq.}$ are the equivalent suspension stiffness and damping coefficients. These are function of element characteristics and suspension geometry. The variables $Z$ and $\dot{Z}$ are relative position and velocity across the suspension, which is given by:

$$Z = Z_S - Z_u$$
$$\dot{Z} = \dot{Z}_S - \dot{Z}_u$$

The variables $Z_S$ and $Z_u$ are function of sprung mass bounce, roll, pitch and wheel bounce. In the presence of anti-roll bar the suspension force can be evaluated from equations (2.15) to (2.17) to give an expression:

$$F_s = K_{eq.} Z + C_{eq.} \dot{Z} + K_{t.eq.} \Omega_x \qquad (2.19)$$

where $K_{t.eq.}$ is the equivalent torsion stiffness (roll stiffness expressed in N/rad.) and $\Omega_x$ is the roll angle.

A simplified linear expression is considered in this study to systematically evaluate the potential of N.N. in vehicle dynamics applications.

## 2.4 STEERING SYSTEM

The steering system is a mechanism that allow the driver to introduce a rotation to the front tires around the Z axis (Fig. (2.2)). The steering mechanism gives the driver the ability to control the vehicle direction of motion. This also allows the driver to correct the vehicle motion if external forces (Like side wind) disturb it.

In the study of vehicle dynamics, the tire-ground forces developed are a function of slip angle as discussed earlier. The slip angle is in turn a function of steering angle. It is, therefore, necessary to know the steer angle of each wheel for a given steering input. The steering geometry, and relationship between steering input and wheels angles are discussed in the following subsection.

### 2.4.1 CORRECT STEERING

The relative motion between the wheels of a vehicle and the road should be of pure rolling in order to avoid wheel scrub. To satisfy this condition when a vehicle is moving along a curved path, the path of each wheel should be concentric circular arcs [11, 16]. This condition as shown in Fig. (2.8) indicate that the perpendicular from each wheel must coincide at $G$ for a vehicle with front steerable wheels.

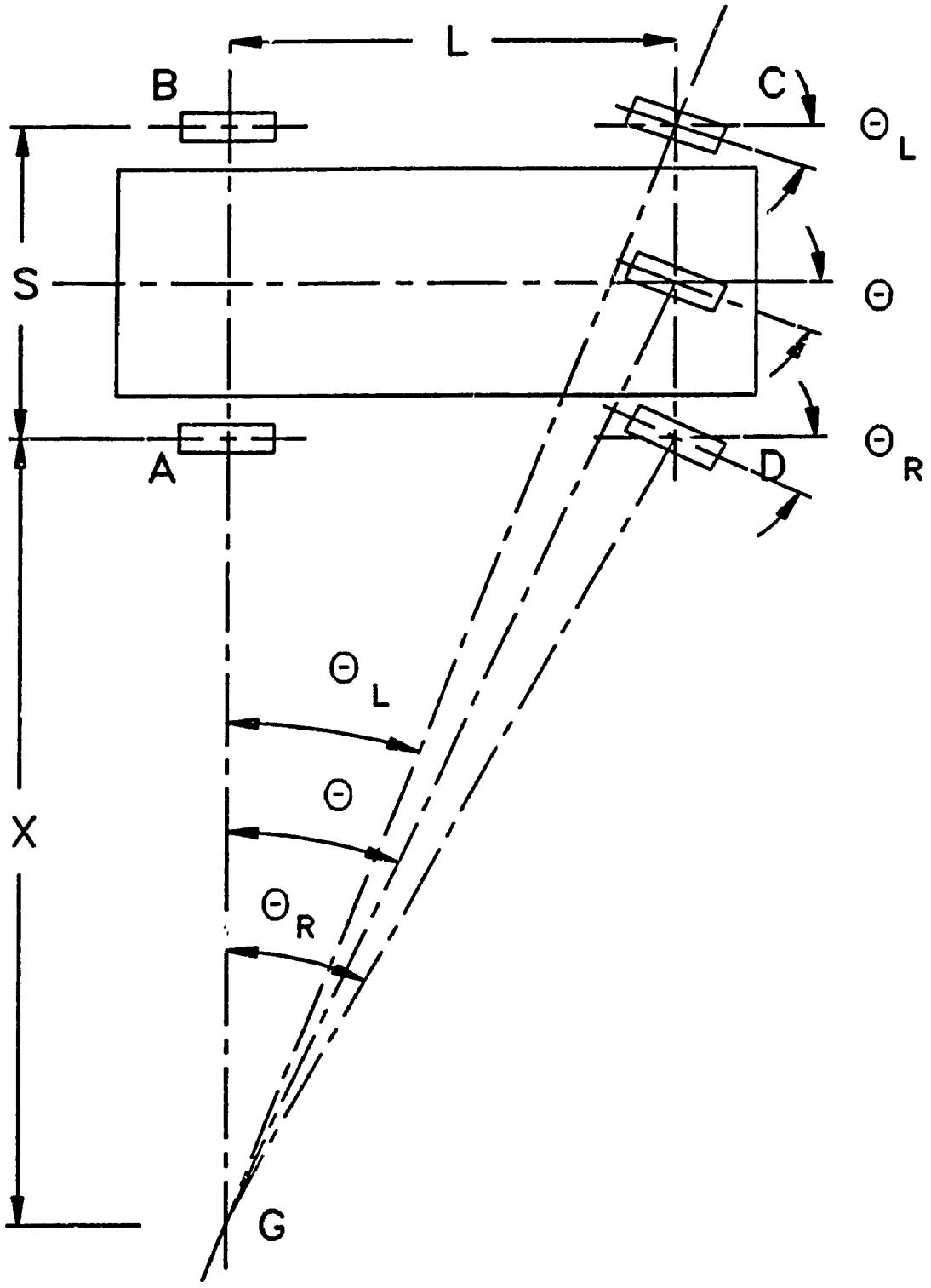


Fig. (2.8) Correct steering.

The figure also indicates that in order to achieve a steering angle of $\theta$ , there is an angle $\theta_R$ and $\theta_L$ for the inner and outer wheels, respectively, to give correct steering.

### 2.4.2 STEERING ANGLE VERSUS WHEEL ANGLE:

In deriving the steering angle of inner and outer wheels in terms of steering input, correct steering input is assumed. With reference to Fig. (2.8), the steering input is the angle of the imaginary wheel placed at the centre of track width, referred to as mean steering angle. From the geometric relationship:

$$\tan\theta = \frac{L}{0.5S+X} \qquad (2.20)$$

For the right (Inner) wheel:

$$\tan\theta_R = \frac{L}{X} \qquad (2.21)$$

For the left (Outer) wheel:

$$\tan\theta_L = \frac{L}{S+X} \qquad (2.22)$$

Combining equations (2.20) and (2.22), and equations (2.20) and (2.21), the wheel angle for left and right wheels can be expressed in terms of mean steering input $\theta$. Assuming small

angle $(\tan\theta-\theta)$ , these expressions are:

$$\theta_L = \frac{\theta}{\frac{S\theta}{2L}+1} \tag{2.23}$$

and

$$\theta_R = \frac{\theta}{1-\frac{S\theta}{2L}} \tag{2.24}$$

where $S$ and $L$ represent the track width and wheel base, respectively. $\theta$ is the mean steering angle or the steering input seen by the wheels.

### 2.4.3 STEERING INPUT

Transient response of the vehicle will be considered in the application of N.N. in this study. For this a simple steering represented by a ramp function is utilized. Two such ramp function for mean steering angle used are shown in Figs. (2.9) and (2.10). The mean steering angle shown in Fig. (2.9) represents a steering rate of 1.14 deg/sec. for a duration of 0.5 sec. The mean steering angle shown in Fig. (2.10) represents a steering rate of 10 deg/sec. for a duration of 0.5 sec. Fig. (2.10) also shows the angle for inner and outer wheels obtained from equations (2.23) and (2.24) to be used for the left and right wheels of a four wheel vehicle model.

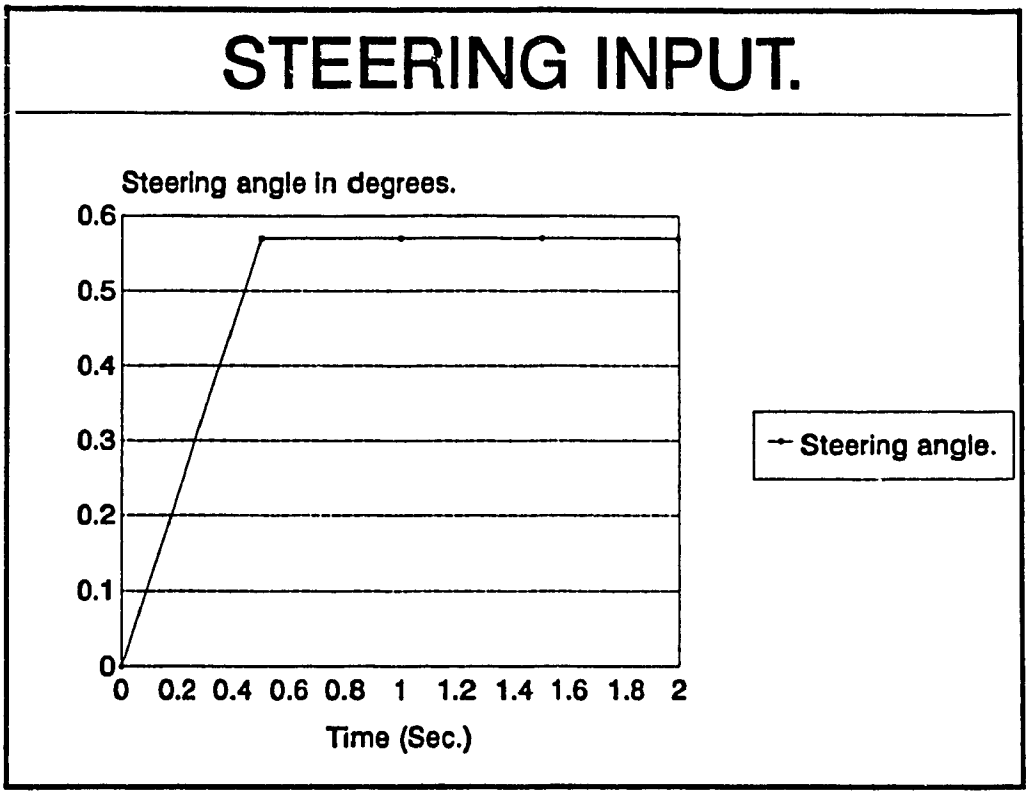


Fig. (2.9) Steering angle versus time graph (Three degrees of freedom).

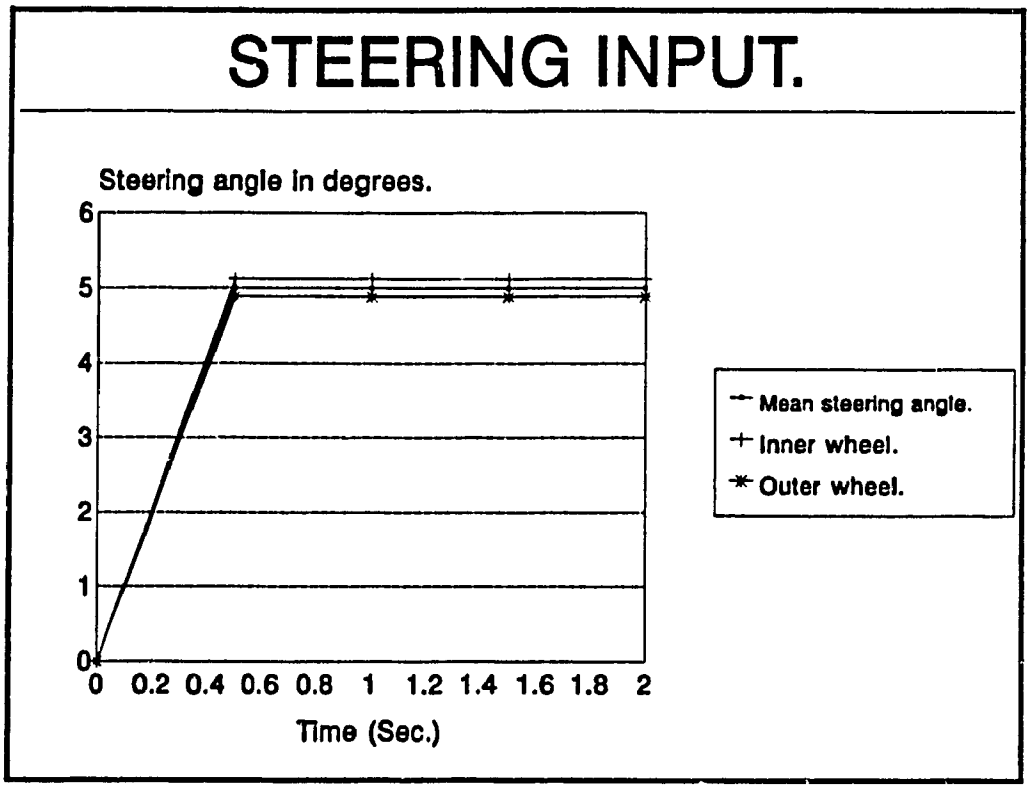


Fig. (2.10) Steering angle versus time graph showing the mean as well as inner and outer wheels angles in time domain.

## 2.5 SUMMARY

This chapter primarily presented the vehicle tire system, and tire mechanics. Major forces and moments developed by a rolling tire are discussed along with its axis system. The tire-road interaction forces in the contact plane and moments about vertical axis are formulated. The longitudinal force due to driving or braking effort and rolling resistance is expressed. The lateral force resulting from cornering and camber angle is formulated.

For the suspension and steering system various assumptions such as linear suspension, fixed roll centre and perfect steering to be considered in this study are discussed. For the suspension system, springs, dampers, stabilizer bar and roll centre are reviewed to show their importance in vehicle modeling. For the steering system, perfect steering assumption that will be used in the simulation of six DOF vehicle model is explained. The relationship between the steering input and steer angles for the left and right wheels are developed. The expression developed and presented in this chapter will be used to develop the vehicle models used in this investigation.

# CHAPTER 3

## 3. NEUROCOMPUTING AND NEURAL NETWORK.

### 3.1 INTRODUCTION

As mentioned in chapter 1, Neurocomputing and Neural Network (N.N.) is an attempt in emulation of the human brain at a very basic level. Like the human brain, N.N. is formed of a number of interconnected artificial neurons, where each neuron has an input, processing and output areas. The technology for N.N.has been around for some time, but its application are being explored only over the last few years. This is made possible with the advancement of computers with fast and parallel processing capabilities. Neurocomputing and N.N. has been defined by experts as follows:

Neurocomputing: "is the technological discipline concerned with information processing systems that autonomously develop operational capabilities in adaptive response to an information environment" [7]

Neural Network: "is a parallel, distributed information processing structure consisting of processing elements interconnected via unidirectional signal channels called connections." [7]

Neurocomputing by itself is a subject of research extensively investigated by computer scientist, and is not within the scope of the present investigation. Several version of the N.N. technology has been developed as a tool, and applied to a wide range of applications including pattern recognition, control classification, diagnostics, automation, system dynamics, etc.

The application of N.N. in dynamical system has been carried out by few researchers only in the very recent years as discussed in the literature review. The objective here is to apply an appropriate N.N. to the study of some complex aspects in vehicle dynamics. As discussed in the literature rHxiew, there are many types of N.N. that are suitable for specific types of applications. In selecting a N.N. various aspects that must be considered include:

- Types of N.N. and their possible applications.
- Types of learning rules for the N.N.
- Transfer functions that can be used in the network.
- Various N.N. parameters and their selection.
- The procedure and steps used in building a N.N.

Each of these aspects are discussed in the following subsections in relation to the present application of N.N. in vehicle dynamics simulation and control.

## 3.2 TYPES OF N.N. AND THEIR APPLICATION

As discussed in the literature review, different types of N.N. have been developed over the years. Some books [6, 7, 8] have been published in the recent years with detail introduction to various types of N.N. and their possible applications. Some of the well known N.N. include:

Adaline and Madaline: has gained application in adaptive signal processing. It is a N.N. that can be implemented as filters to perform noise removal from information-bearing signals.

Back-propagation: has application in problems requiring recognition of complex patterns and performing non-trivial mapping. It is a network that adapts itself to "learn" the relationship between a set of examples patterns, and able to apply the same relationship to a new input pattern. Back-propagation network, therefore, has potential application in simulation, control of dynamical systems and reverse dynamics.

General regression network: is a general purpose network. It gained applications in system modeling and prediction.

Modular neural network: is a generalization of back-propagation neural network. It is applied to system modeling, prediction, classification and filtering.

Among various N.N. developed to date, back-propagation network (BPN) is most applicable to simulation of dynamical

systems, control and optimization. It can be used in addressing problems requiring recognition of complex patterns and performing non-trivial mapping function. This network has been demonstrated to be most successful in system modeling, control, and pattern recognition [7]. In basic terms a BPN can be trained through a set of input-output relationship to develop artificial intelligence. An adequately trained BPN can then be used to make prediction of the network output by providing the network input, and/or provide an optimal parameter for control.

For the application of N.N. to vehicle system model and control in this investigation BPN is selected. Rest of this chapter is devoted to description of BPN; selection of learning rule, transfer function and parameters for its use; and a flow chart for the BPN algorithm.

## 3.3 BACK-PROPAGATION NETWORK (BPN)

Back-propagation network (BPN), formalized by Werbos [34], and later by Parker [35], Rumelhart and McClelland [36], operate as a multi layer feed forward network using supervised learning. A detailed discussion of BPN and its architecture is not discussed here and is available in references [6, 7, 8].

The network architecture is formed of a number of layers the first one is the input layer, the last one is the output layer and ones between them are called intermediate layers. Fig. (3.1) shows a BPN formed of an input layer, two intermediate layers and an output layer. Each node of the network has a variable weight, and there are a predefined transfer function between nodes. In general terms, after an input pattern with known output has been applied to the first layer of the network, it is propagated through each upper layer until the network output is generated. The process of propagation through each layer is also shown in Fig. (3.1), where $x$ is the input to the network, $x'$ and $x''$ are the output of the first and second layers, and $y$ is the network output. Here $f$ represents the transfer function, where $W$ is the weight and $\theta$ represents noise. The network output is compared to the desired known output and the mean square error is calculated for each output unit. The error is then transmitted backward to each node of intermediate layers that contribute directly to the output. The process is repeated and the internal values (weights) of the network are updated until a reasonable error is achieved.

After training, when presented with an arbitrary input pattern the network should be able to calculate the correct output. It however must be noted, that trained network can not work properly if the relation between the arbitrary input and

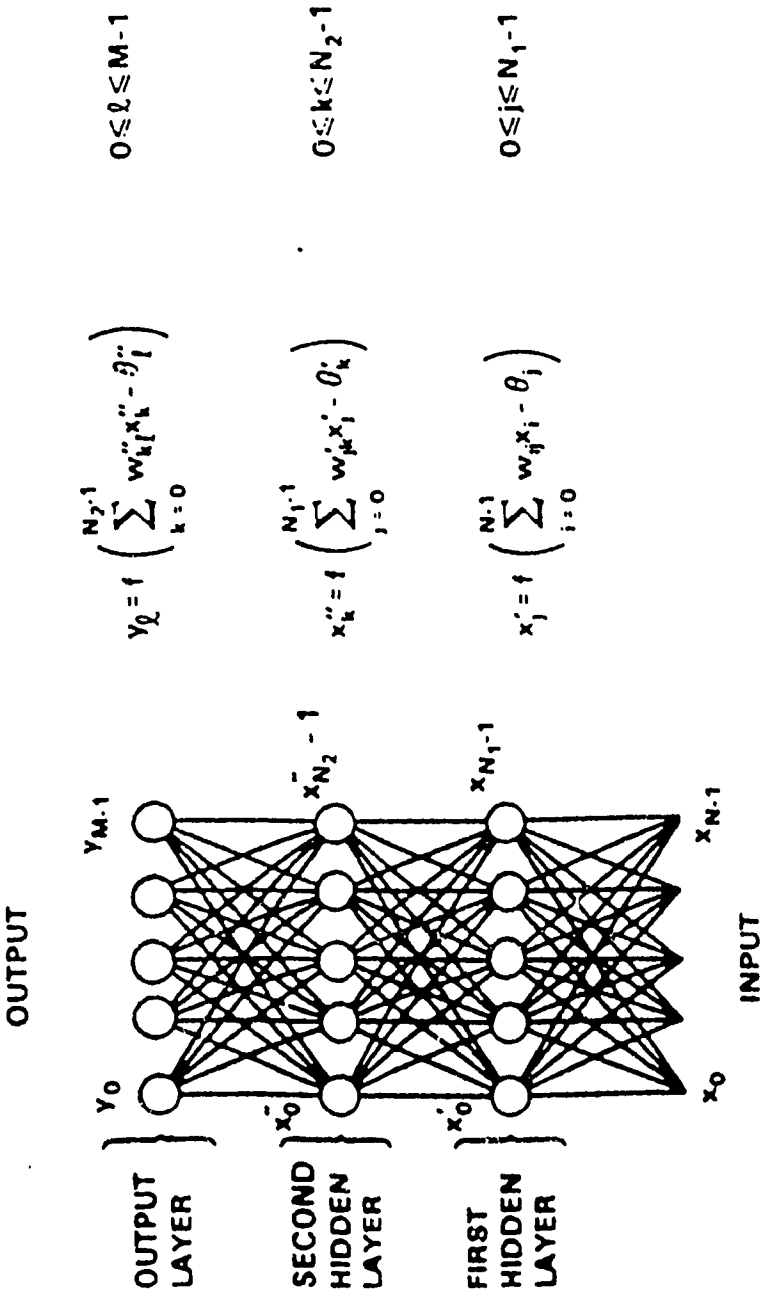


Fig. (3.1) A Four layer BPN. [27]

the required output is not similar to what it learned. Also sometimes a N.N. would not learn and minimize the error without any apparent reason [7].

In the implementation of the BPN, one should choose two major specification of the network. These specifications are the learning rule and the transfer function. The following subsections discuss each one of them briefly.

### 3.3.1 N.N. LEARNING RULES

The N.N. learning rules are used to adjust the weights and biases of the N.N. that minimizes the error between the network output and the desired output during training. There are several learning rules available [6, 27] that can be applied. Some of them include:

1) delta rule,
2) normal cumulative,
3) extended delta-bar-delta,
4) delta-bar-delta,

One of the difficulty in using a N.N. is that their behaviour is not very well understood. In practice, the learning rule is selected based on trial, where the rule that leads to lowest error is used. For the present application, delta rule and normal cumulative were found to be most efficient.

### 3.3.1.1 DELTA LEARNING RULE

The BPN error in the output layer is calculated as the difference between the desired output and the network output. This error, transformed by the derivative of the transfer function is back-propagated to prior layers where it is accumulated. This back-propagated and transformed error becomes the error term for that prior layer. The process of back-propaHxting the errors continues until the first layer is reached. The Delta learning rule change the weights of the network by multiplying the error at each weight by the learning coefficient. The difference between the current weight and the previous weight is multiplied by a momentum to accelerate the minimization of the error. The following equation illustrate how the delta rule updates the weights of the BPN:

$$W(t+1) = W(t) + \alpha \delta x'_i + \gamma (W(t) - W(t-1)) \qquad (3.1)$$

where $W(t+1)$ is the updated weight, $W(t)$ is the current weight, $W(t-1)$ is the previous weight, $\alpha$ is the learning coefficient, $\delta$ is the error, $x'_i$ is the input to that connection and $\gamma$ is the momentum.

### 3.3.1.2 NORMAL CUMULATIVE LEARNING RULE

The normal cumulative learning rule is similar to the delta rule, the only difference is that instead of updating

the weight for every set of data presented, the user specify a number of presentation (Epoch) after which the weights are updated. The weight are update in two phases:

1) at each data presentation:

$$m(t+1) = m(t) + \alpha\delta x'_i \tag{3.2}$$

where $m(t+1)$ is the updated dummy weight, $m(t)$ is the current weight $\alpha$ is the learning coefficient, $\delta$ is the error and $x'_i$ is the input to that connection.

2) after a certain number of presentation when the epoch number is reached,

$$\begin{aligned} W(t+1) &= W(t) + m(t) + \gamma a(t) \\ a(t) &= m(t) \\ m(t+1) &= 0 \end{aligned} \tag{3.3}$$

where $\gamma$ is the momentum and $a(t)$ is the dummy load at the beginning of the cycle.

### 3.3.2 TYPES OF TRANSFER FUNCTIONS

The transfer function is the function that relates the neuron output to the net output. Fig. (3.2) shows the location of a transfer function in a N.N., from the figure the neuron output $X$ is defined as [27]:

$$X = \sum_{i=0}^{N-1} W_i x_i - \theta \tag{3.4}$$

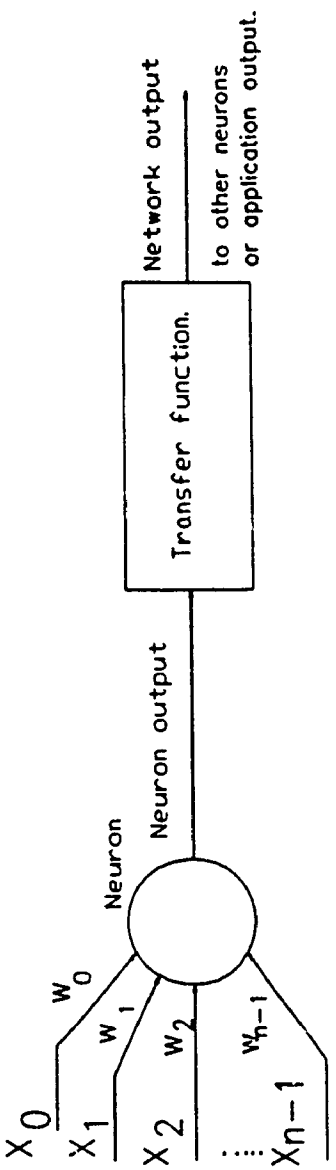


Fig. (3.2) Transfer function location in an A.N.

where $W_i$ is the weight, $x_i$ is the input and $\theta$ is an offset or a noise function. The transfer function is applied to the neuron output and the network output is:

$$Y = transf(X) = transf(\sum_{i=0}^{N-1} W_i x_i - \theta) \qquad (3.5)$$

BPN is based on continuous change of the biases and weights of the network in the direction of steepest descent with respect to the error. It therefore requires a function with continuous differentiable non-linearity. Different transfer functions can be used [6, 7], some of which include: linear transfer function, Sigmoid transfer function, tanh transfer function, etc. Although any continuous differentiable non-linear function can be used, Sigmoid transfer function was found to give, the best results in the present application. The sigmoid transfer function is a 'S' shaped continuous differentiable function shown in Fig. (3.3), which can be expressed as:

$$f(x) = \frac{1}{1+e^{-x}} \qquad (3.6)$$

## 3.4 THE BPN PARAMETERS

As expressed in equation (3.1), there are two main parameters required to operate the N.N., they are the learning coefficient $\alpha$ , and the momentum $\gamma$ .

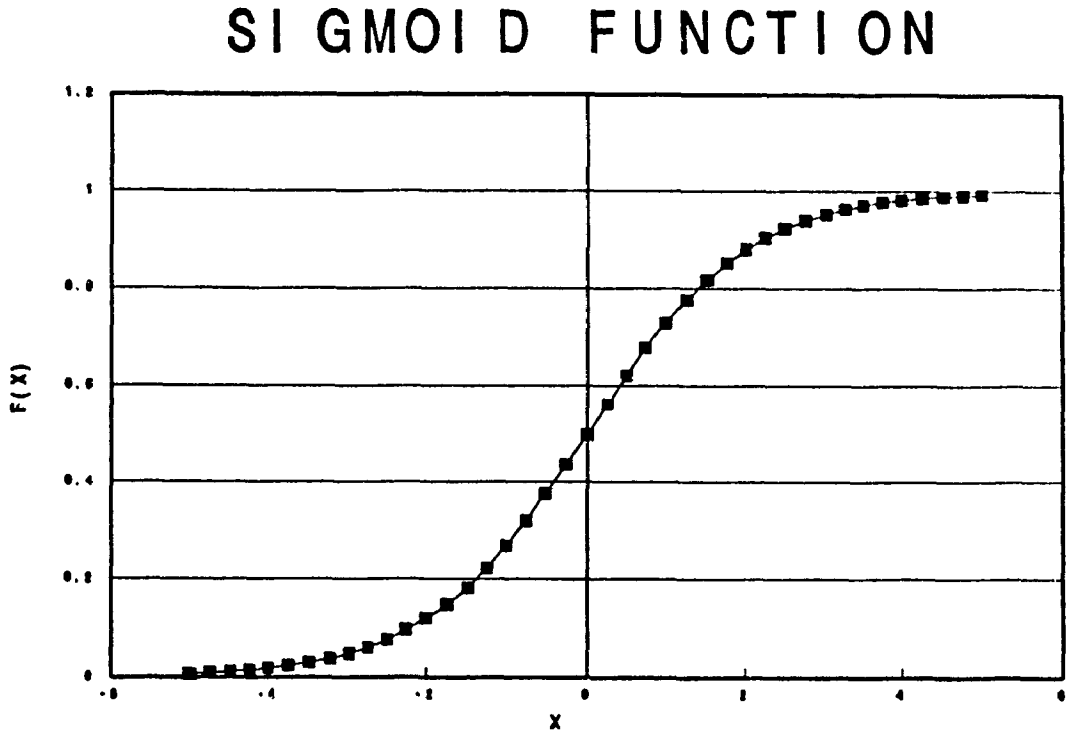


Fig. (3.3) Sigmoid function.

The learning coefficient $\alpha$ , controls the rate at which the error modify the weights. If the value of the learning rate is too high, the network can become unstable. On the other hand, if the rate is too low, a extremely long training period is required. The value of the learning coefficient between 0 and 1 is best selected by trial to achieve fast learning of stable network [6].

The other parameter, momentum $\gamma$ is a factor that dictates the speed of error minimization. This allows the network to respond not only to the local gradient but also to recent trend in error minimization. The momentum parameter is also selected by trial to achieve satisfying performance of the network [6].

## 3.4 BPN ALGORITHM AND FLOW CHART

The back-propagation N.N. learns by propagating the error between the N.N.output and the desired output. The propagHxed error is used to modify the weights, the rate by which the weights are modified depends on the learning coefficient and the momentum.

The method by which the back-propagation N.N. works is shown in the flow chart Fig. (3.4) and the following steps. (The learning rule and the transfer function in the following

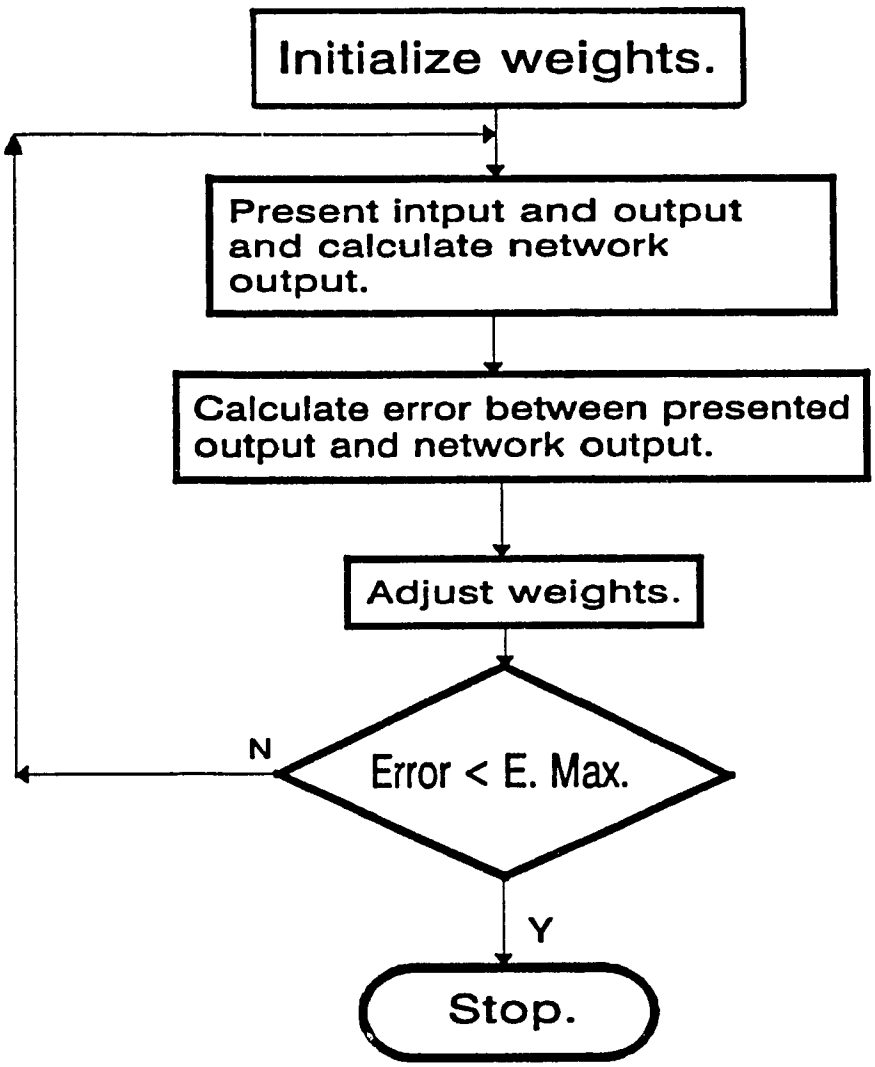


Fig. (3.4) BPN Flow chart.

steps are respectively the delta rule and Sigmoid).

STEP 1: Specify the number of inputs, outputs, nodes (layers) and number of neuron per layer, Fig. (3.1)

STEP 2: Initialize the weights and offsets,

STEP 3: Present inputs $x_0, x_1, \ldots, x_{N-1}$ and desired outputs $d_0, d_1, \ldots, d_{M-1}$ to the N.N.,

STEP 4: Calculate the error between the N.N. output $y_0, y_1, \ldots, y_{M-1}$ and the desired output. The N.N. output is calculated by summing the weights at each node then the transfer function is used to transfer the summation to the next node if there is any, or to get the N.N. output.

STEP 5: Back-propagate the error to all the nodes and neurons. The weights are updated using the calculated error, the learning coefficient and the momentum,

$$W(t+1) = W(t) + \alpha \delta_j x_i' \qquad (3.7)$$

where $W(t+1)$ is the updated weight, $W(t)$ is the initial weight from hidden node $i$ or from an input to node $j$, $\alpha$ is the learning rate, $\delta_j$ is an error term of node $j$ and $x_i'$ is either the output of node $i$ or is an input. If node is an output node, then

$$\delta_j = y_j(1-y_j)(d_j-y_j) \qquad (3.8)$$

where $d_j$ is the desired output of node $j$ and $y_j$ is the actual output. (N.N. output)

If node $j$ is an internal hidden node, then

$$\delta_j = x_j'(1-x_j')\sum_k \delta_k W_{jk} \qquad (3.9)$$

where $k$ is over all nodes in the layer above node $j$. Convergence is sometimes faster if a momentum $\gamma$ term is added and weight changes are smoothened by:

$$W(t+1) = W(t) + \alpha \delta_j x_i + \gamma(W(t) - W(t-1)) \qquad (3.10)$$

where

$$0 < \gamma < 1$$

and $W(t-1)$ is the previous weight.

STEP 6: Repeat the steps from 3 to 5 until the error calculated is acceptable.

## 3.5 STEPS IN BUILDING A N.N.

The way to build a N.N. could be stated in the following steps:

1) Determine the problem type the inputs and the outputs that will be given to the N.N. to learn. It is important that the inputs and outputs be related.

2) Construct a data training file and a testing file, the training file could be used as a testing file. Be sure not to have similar inputs with different outputs or vice versa.
3) Determine the purpose of building the N.N. For this research the N.N. was needed for system modelling and for control this helped to determine that back-propagation N.N. is the most suitable for this problem.

4) Determine the number of neuron needed, the input and output neurons are equal to the number of inputs and outputs of the problem. The number of neuron and the number of layers are chosen by trial and error.
5) Determine a learning rule that will update the weights of the N.N., and achieve learning. For the N.N. the choice of the learning rule is done by trial.
6) Determine the most suitable transfer function.
7) Determine the N.N. parameters by trial.
8) Start the learning process and test the N.N. if error is acceptable the training is over if not change parameters and restart training until reaching the minimum error.
9) The trained N.N. could now be used for the application needed.

## 3.6 SUMMARY

This chapter primarily presented the N.N. and specially the BPN. The chapter gave a general idea about the N.N. and

the BPN parameters which are essential in building a BPN. The learning rules used in the research are explained. The transfer function are explained and the Sigmoid transfer function is formulated. The BPN algorithm and flow chart are explained in detail. The steps to build a N.N. application are explained in a simple manner. The BPN will be applied to the three and six DOF vehicle model in the following two chapters.

# CHAPTER 4

## 4. APPLICATION OF N.N. TO A THREE DOF VEHICLE MODEL

### 4.1 INTRODUCTION

As discussed in chapter 1, there has been very limited application of N.N. to vehicle system dynamics. The objective of this part of the study is to attempt simulation of the tire property in cornering. For this, a simplified three degrees of freedom vehicle model often refereed to as a bicycle model [10, 11] is considered. Since tire parameters have the most influence on vehicle yaw velocity, the model is used to simulate yaw velocity for a steering input until steady state is reached.

The tire parameters and simulation results are used to train a back propagation N.N. described in chapter 3. Using inverse dynamics, the trained network was then used to predict the tire parameter for a given vehicle response. The performance of N.N. is evaluated by comparing the response given to the N.N. with that of simulation with N.N. predicted parameter.

The results are tested for different training scheme and wide range of responses. The N.N. is finally tested for

prediction of tire parameters corresponding to minimum feasible yaw response of the vehicle model. This chapter presents: the development of the three degrees of freedom model; simulation parameters and results; and N.N. results as compared to those of simulation.

## 4.2 THREE DEGREES OF FREEDOM VEHICLE MODEL

A simplified vehicle model in negotiating a curve can be modeled as a bicycle-model, where the pair of tires on an axle are represented by a single tire with double the cornering stiffness. The mass of the vehicle in this case is concentrated between the front and the rear axles as shown in Fig. (4.1). When the vehicle negotiates a curve at moderate or higher speeds under a steer angle $\delta_F$, lateral forces ( $F_{YF}$ and $F_{YR}$ ) at the tire-road interface are developed. This also leads to a slip angle $\alpha_F$ and $\alpha_R$ for the front and rear wheels as was discussed in chapter 2. The expressions developed in that chapter for the tire forces are used here to develop the vehicle model.

Two sets of axis system are used to formulate the equations of motion of the vehicle. The first set of axis is fixed to the vehicle so that the inertia properties of the vehicle are constant. The other set is fixed in the space to express the absolute acceleration of the vehicle as shown in

Fig.(4.2).

As shown in Fig. (4.2) when the vehicle is turning along a curved path, it is subjected to a translation and a rotation motion. $ox$ and $oy$ are the longitudinal and lateral fixed axis and point $O$ is the centre of gravity of the vehicle. At time $t$, $V$ is the velocity of the centre of gravity, which has component $V_X$ and $V_Y$ with respect to body fixed axis system. At time $t+\Delta t$ the velocity of the vehicle is $V+\Delta V$ with component $V_X+\Delta V_X$ and $V_Y+\Delta V_Y$ along the $X$ and $Y$ axis of the vehicle respectively.

As further shown in Fig. (4.2), the translation of body fixed axis in time $\Delta t$ is accompanied by a rotation $\Delta\Omega_Z$. The corresponding transformation matrix about $z$ axis is,

$$\begin{pmatrix} \cos\Delta\Omega_Z & -\sin\Delta\Omega_Z & 0 \\ \sin\Delta\Omega_Z & \cos\Delta\Omega_Z & 0 \\ 0 & 0 & 1 \end{pmatrix}$$

The change in the velocity in time $\Delta t$ can therefore be expressed as:

$$\Delta V = \begin{pmatrix} \cos\Delta\Omega_Z & -\sin\Delta\Omega_Z & 0 \\ \sin\Delta\Omega_Z & \cos\Delta\Omega_Z & 0 \\ 0 & 0 & 1 \end{pmatrix} * \begin{pmatrix} V_X+\Delta V_X \\ V_Y+\Delta V_Y \\ 0 \end{pmatrix} - \begin{pmatrix} V_X \\ V_Y \\ 0 \end{pmatrix} -$$

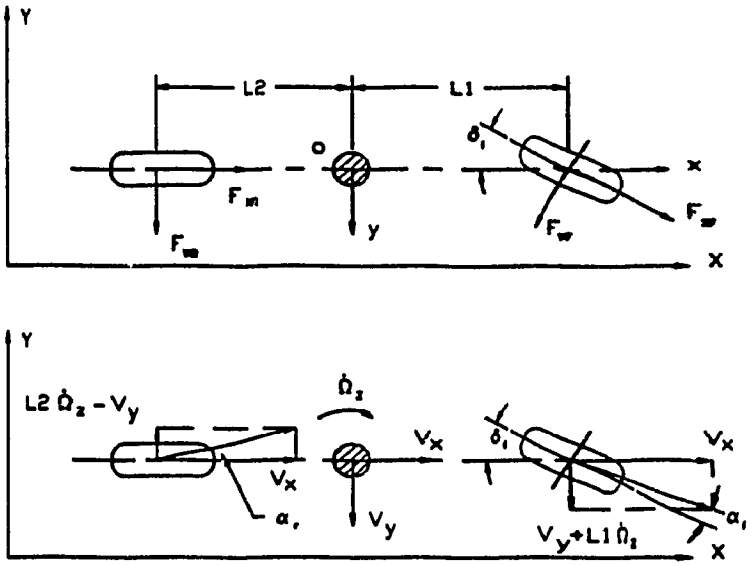


Fig. (4.1) Three degrees of freedom vehicle model.

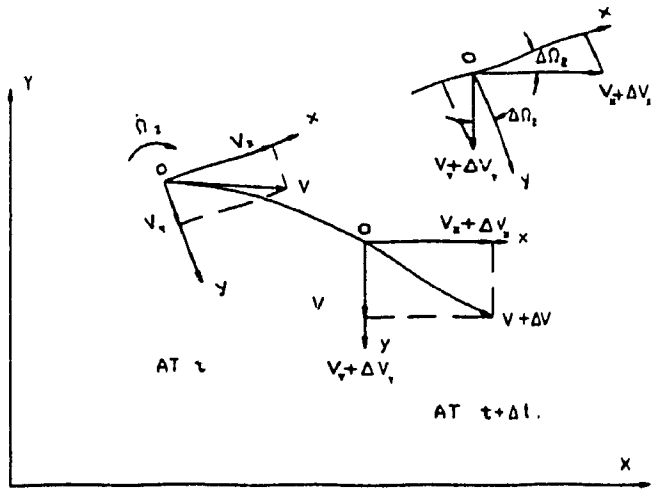


Fig. (4.2) Axis used for analyzing vehicle motion.

$$\begin{pmatrix} \cos\Delta\Omega_Z(V_X+\Delta V_X)-\sin\Delta\Omega_Z(V_Y+\Delta V_Y)-V_X \\ \sin\Delta\Omega_Z(V_X+\Delta V_X)+\cos\Delta\Omega_Z(V_Y+\Delta V_Y)-V_Y \\ 0 \end{pmatrix} \tag{4.1}$$

since $\Delta\Omega_z$ is very small the following

$$\sin\Delta\Omega_z=\Delta\Omega_Z$$

$$\cos\Delta\Omega_Z=1$$

$$\Delta V_X\,\Delta\Omega_Z=0$$

can be substituted in equation (4.1) to express the change in velocity as:

$$\Delta V=\begin{pmatrix} \Delta V_X-V_Y\Delta\Omega_Z \\ \Delta V_Y+V_X\Delta\Omega_Z \\ 0 \end{pmatrix} \tag{4.2}$$

The absolute acceleration can now be found by dividing equation (4.2) by $\Delta t$ and taking the limit when $\Delta t=0$ .

$$\begin{pmatrix} a_X \\ a_Y \\ a_Z \end{pmatrix}=\begin{pmatrix} \dot{V}_X-V_Y\dot{\Omega}_Z \\ \dot{V}_Y+V_X\dot{\Omega}_Z \\ 0 \end{pmatrix} \tag{4.3}$$

where $\dot{\Omega}_Z$ is the arqular velocity $d\Omega/dt$ as shown in Figs. (4.1) and (4.2). With reference to Fig. (4.1) using axes fixed to the vehicle, the equations of motion in the longitudinal, lateral and yaw directions can be expressed as:

$$m * a_X = F_{XF}\cos\delta_F + F_{XR} - F_{YF}\sin\delta_F$$

$$m * a_Y = F_{YR} + F_{YF}\cos\delta_F + F_{XF}\sin\delta_F$$

$$I_z\dot{\Omega}_Z = L_1 F_{YF}\cos\delta_F - L_2 F_{YR} + L_1 F_{XF}\sin\delta_F$$

where $\delta_F$ is the steering angle. Substituting equation (4.3) into the previous equations lead to the equation of motion as:

$$m * (\dot{V}_X - V_Y\dot{\Omega}_Z) = F_{XF}\cos\delta_F + F_{XR} - F_{YF}\sin\delta_F \qquad (4.4)$$

$$m * (\dot{V}_Y + V_X\dot{\Omega}_Z) = F_{YR} + F_{YF}\cos\delta_F + F_{XF}\sin\delta_F \qquad (4.5)$$

$$I_Z\dot{\Omega}_Z = L_1 F_{YF}\cos\delta_F - L_2 F_{YR} + L_1 F_{XF}\sin\delta_F \qquad (4.6)$$

The lateral forces $F_{YF}$ and $F_{YR}$ (in equations (4.4) to (4.6)) at the front and rear tire-road interface expressed by equation (2.12) are: (neglecting the camber effect)

$$F_{YF} = 2C_{\alpha F}\alpha_F \qquad (4.7)$$

$$F_{YR} = 2C_{\alpha R}\alpha_R \qquad (4.8)$$

where $C_{\alpha F}$ and $C_{\alpha R}$ are the cornering stiffness of each tire. $\alpha_F$ and $\alpha_R$ are the slip angle of front and rear tires defined in chapter 2 and also shown in Fig. (4.1). With reference to Fig. (4.1), the slip angles can be defined in terms of vehicle motion variables. For small angles, the expressions for slip angles are:

$$\alpha_F = \delta_F - \frac{L_1 \dot{\Omega}_Z + V_Y}{V_X} \tag{4.9}$$

$$\alpha_R = \frac{L_2 \dot{\Omega}_Z + V_Y}{V_X} \tag{4.10}$$

The longitudinal force $F_{XF}$ and $F_{XR}$ (in equations (4.4) to (4.6)) at the tire-road interface is the rolling resistance of the tire in the absence of tractive or braking effort (Equation (2.1) and (2.2)). The tire rolling resistance expressed in equation (2.7) is:

$$F_{XF} = F_{rF} = F_{ZF} f_r \tag{4.11}$$

$$F_{XR} = F_{rR} = F_{ZR} f_r \tag{4.12}$$

where $F_Z$ is the normal tire load, which can be expressed in terms of vehicle weight $mg$ as:

$$F_{ZF} = \frac{L_2}{L_1 + L_2} mg \tag{4.13}$$

$$F_{ZR} = \frac{L_1}{L_1 + L_2} mg \tag{4.14}$$

The term $f_r$ in equations (4.11) and (4.12) referred to as coefficient of rolling resistance is expressed by equation (2.9) as a function of velocity is:

$$f_r = 0.01 \left(1 + \frac{V}{160}\right) \tag{4.15}$$

Substituting equations (4.7), (4.8), (4.11) and (4.12) into equations (4.4) to (4.6) completely defines the motion of the vehicle for a steering input $\delta_F$ .

## 4.3 SIMULATION OF THREE DOF VEHICLE MODEL

The three DOF vehicle model expressed by equations (4.4) to (4.6) is solved in time domain using fourth order Runge-Kutta. The steering used for simulation is a ramp function as discussed in section (3.8) and described in Fig. (3.12). The vehicle parameters used for the simulation are representative of a passenger car [11] as presented in Table (4.1). For the given ramp function steering input, the vehicle response is computed in time domain for various combination of tire cornering stiffness.

Sample results of yaw, forward and lateral velocity for two sets of tire cornering stiffness are shown in Figs (4.3) to (4.5). As the results show, (Fig. (4.3)) the yaw velocity increases with time, and for the given steering input a steady state is reached in less than 3 seconds. As shown in Fig. (4.4), the forward velocity decreases with time because the vehicle is subjected to a rolling resistance with no drive force. The lateral velocity response of the vehicle is shown in Fig. (4.5).

| | |
|---|---|
| Mass $m$ | 2000 $kg.$ |
| Inertia | 2880 $kg.m^2$ |
| $L_1$ | 1.035 $m.$ |
| $L_2$ | 1.265 $m.$ |
| $f_r$ | 0.03 |
| $C_{\alpha F}$ | 33000 to 45000 N/rad. |
| $C_{\alpha R}$ | 33000 to 45000 N/rad. |

Table (4.1) Three DOF Vehicle parameter.

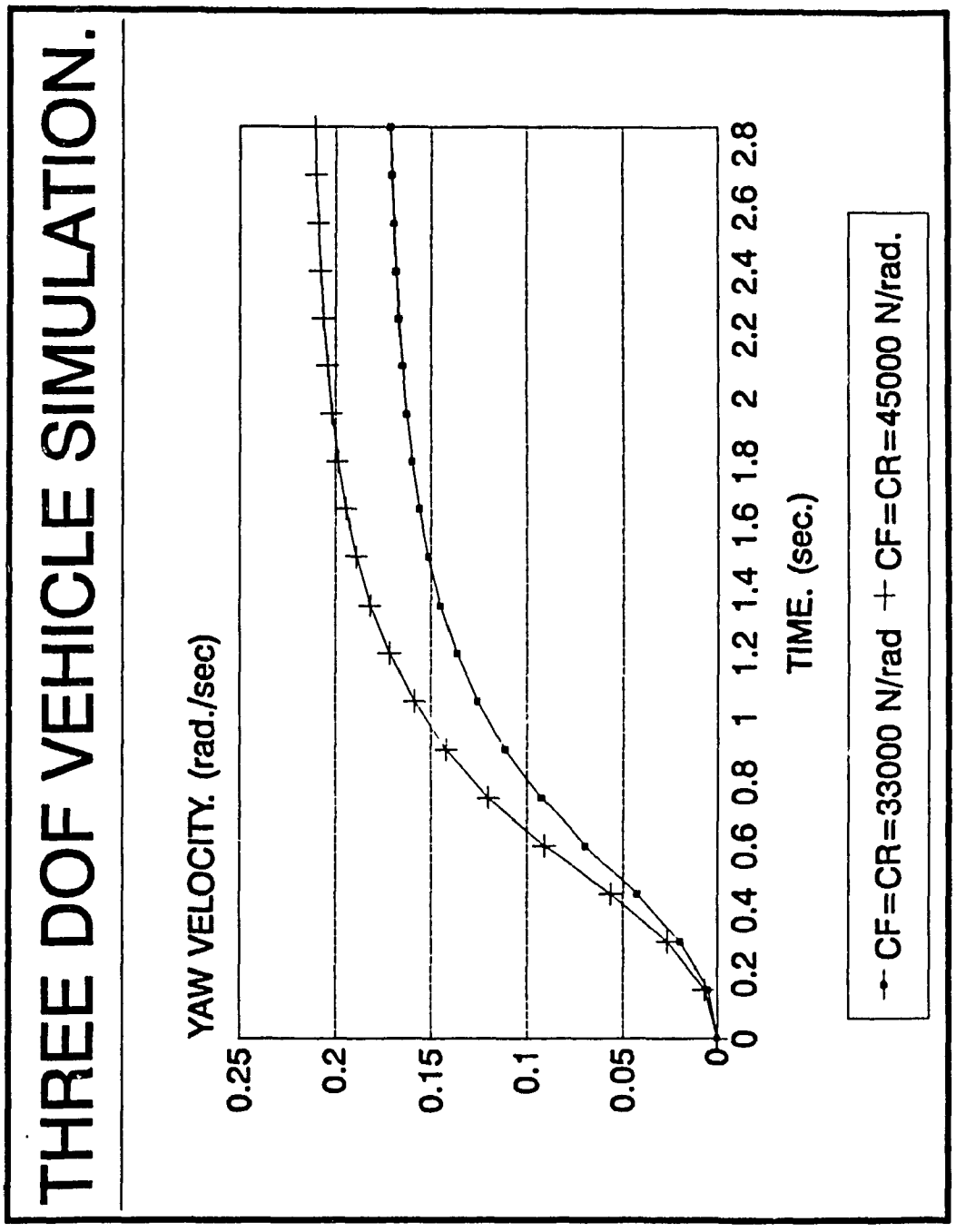


Fig. (4.3) Yaw velocity of the three DOF vehicle model.

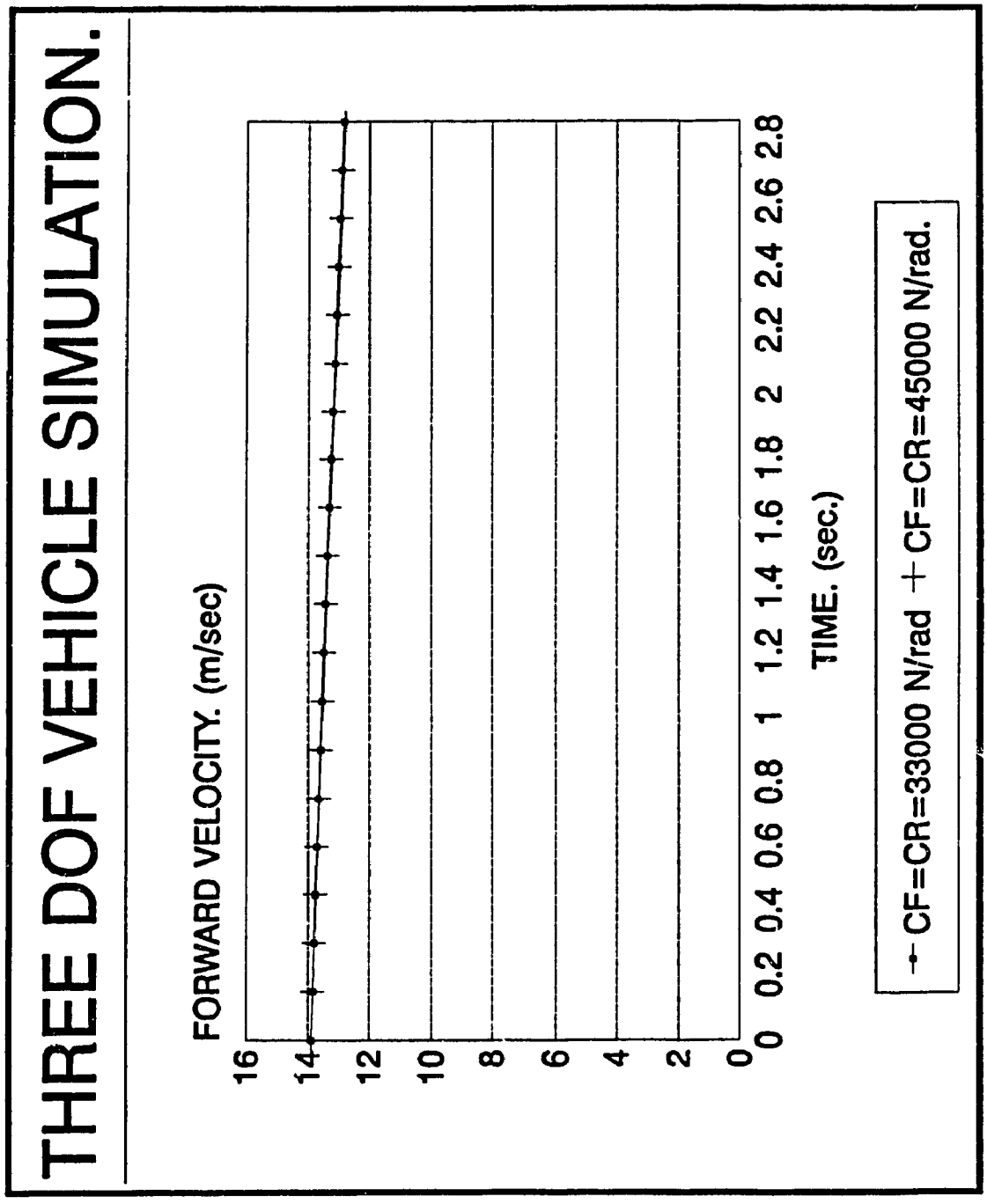


Fig. (4.4) Forward velocity of a three DOF vehicle model.

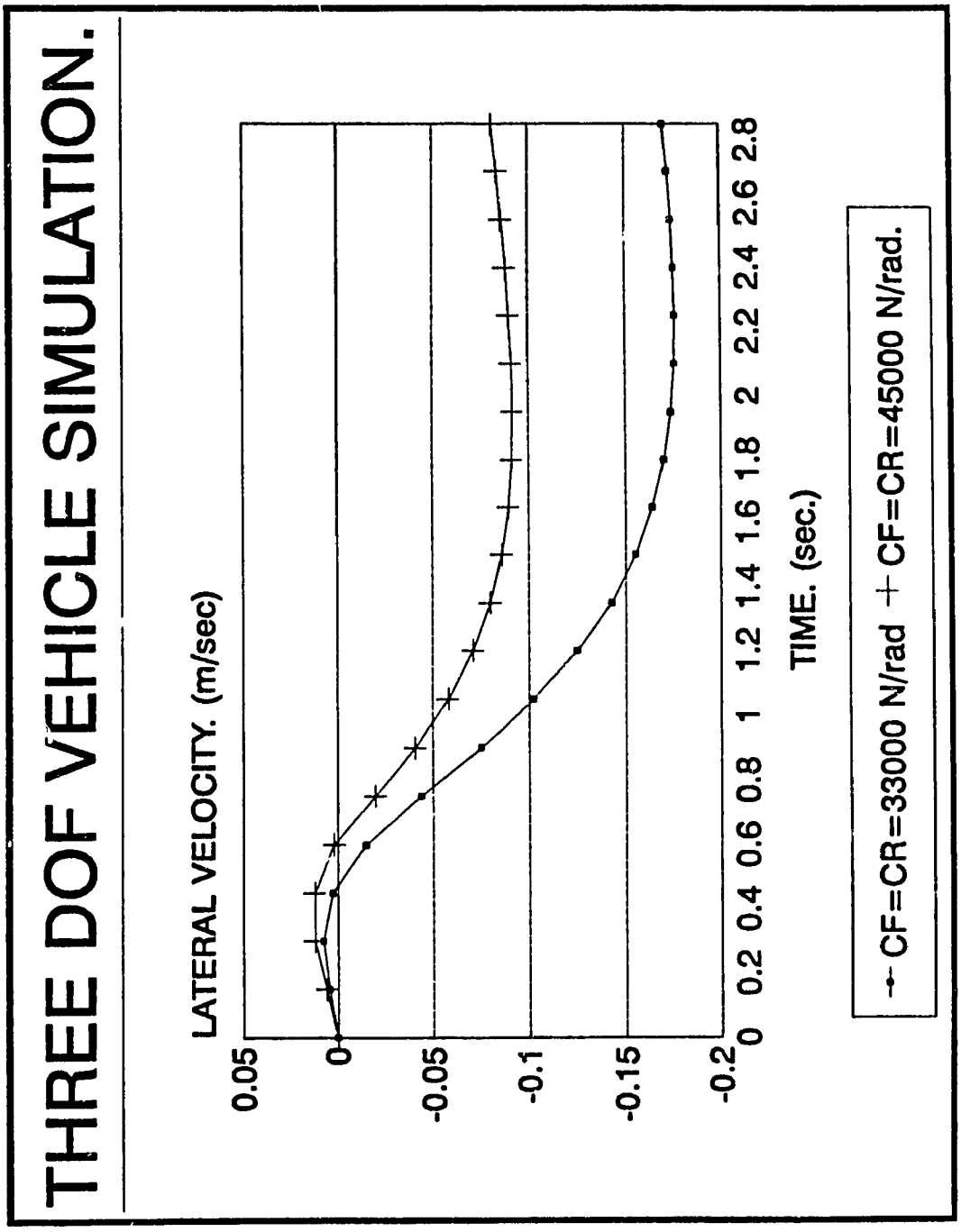


Fig. (4.5) Lateral velocity of a three DOF vehicle model.

Yaw velocity of the vehicle in response to a steering input is a good index for handling and steering response [11]. The simulation results obtained as yaw velocity for 49 sets of tire parameters were compiled for the training of the N.N.

## 4.4 N.N. FOR THE THREE DOF VEHICLE MODEL

As discussed in chapter 3, the N.N. selected for this application is the back-propagation network (BPN). The architecture and parameters for the BPN are also discussed in chapter 3.

The software used for the N.N. is Neural Works. The software is used with a 486 PC. The major advantage of the software is the simplicity of setting the parameters. The user has to choose the N.N. type from a menu and then enter the N.N. specifications and parameters. While training the user can observe the performance of the N.N. through the network mean square error graph.

As discussed in chapter 3, the transfer function, learning rate and N.N. parameters are selected based on trial. The parameters used in the present application are presented in Table (4.2).

The network is trained by providing 19 discrete values of

| | |
|---|---|
| Inputs (yaw velocity) | 19 |
| Hidden | 40 |
| Output (Tire stiffness) | 2 |
| Learning coefficient for input | 0.6 |
| Learning coefficient for output | 0.6 |
| Epoch | 10 |
| Learning rule | Normal Cumulative |
| Transfer Function | Sigmoid, |

Table (4.2) N.N. Parameters for the three DOF vehicle model.

yaw response in the time domain for a set of two tire stiffness. 19 values are used to ensure that the time domain response curve is described as a continuous smooth curve. Sets of data required for the successful training of N.N. depend on the complexity of the problem. For a stable physical system the number of sets required is small. On the other hand, a large number of training sets are required if the system is non physical. Following are the results during training stages in the present application.

### 4.4.1 TRAINING USING 9 SETS OF SIMULATION RESULTS

First, only 9 sets of data are used for the training of the N.N. The N.N. is tested using 49 sets of data. Some of the results are presented in Table (4.3), the first two columns represent the required front and rear tire stiffness the second two represent the N.N. calculated front and rear tire stiffness. It is clear from the table that the error is acceptable.

### 4.4.2 TRAINING USING 25 SETS OF SIMULATION RESULTS

25 sets of data are used to train the N.N. Table (4.4) show some results of the training process as described for table (4.3).

| Front tire stiffness. | Rear tire stiffness. | Front N.N. tire. | Rear N.N. tire. |
|---|---|---|---|
| 35000 | 39000 | 34626.95 | 39197.31 |
| 37000 | 43000 | 36736.76 | 43500.83 |
| 41000 | 41000 | 41387.36 | 41400.43 |
| 43000 | 45000 | 43329.35 | 44994.23 |

Table (4.3) Testing N.N. after 9 sets of training.

| Front tire stiffness. | Rear tire stiffness. | Front N.N. tire. | Rear N.N. tire. |
|---|---|---|---|
| 35000 | 39000 | 34924.35 | 39236.57 |
| 37000 | 43000 | 36909.79 | 43470.96 |
| 41000 | 41000 | 41296.05 | 41250.25 |
| 43000 | 45000 | 43137.28 | 44800.26 |

Table (4.4) Testing N.N. after 25 sets of training.

9 sets of data was found adequate for the training of the BPN in the present application. Small sets of data is sufficient since the system data represent a stable physical system. From the result listed in tables (4.3) and 4.4) it shows that N.N. achieved better results with more training sets.

Despite the N.N. ability to learn with small sets of data, 49 sets are used for completely training the N.N. This is to ensure that a wide range of input and response is experienced by the network. This will further aid in estimating tire property corresponding to minimum response at each discrete point learned by the N.N., as presented in section (4.6).

## 4.5 APPLICATION OF THE N.N.

The trained BPN is used as an inverse dynamic tool. For this an arbitrary yaw response of the vehicle within the range of yaw response obtained from simulation is provided to the N.N. The N.N. in tern provides the two parameters as front and rear tire cornering stiffness. The N.N. calculated tire stiffness is then used to simulate yaw response and the two responses are then compared. Figs. (4.6) to (4.9) present sample results for this part of the study. As the results show, in every case the N.N. is capable of predicting the tire

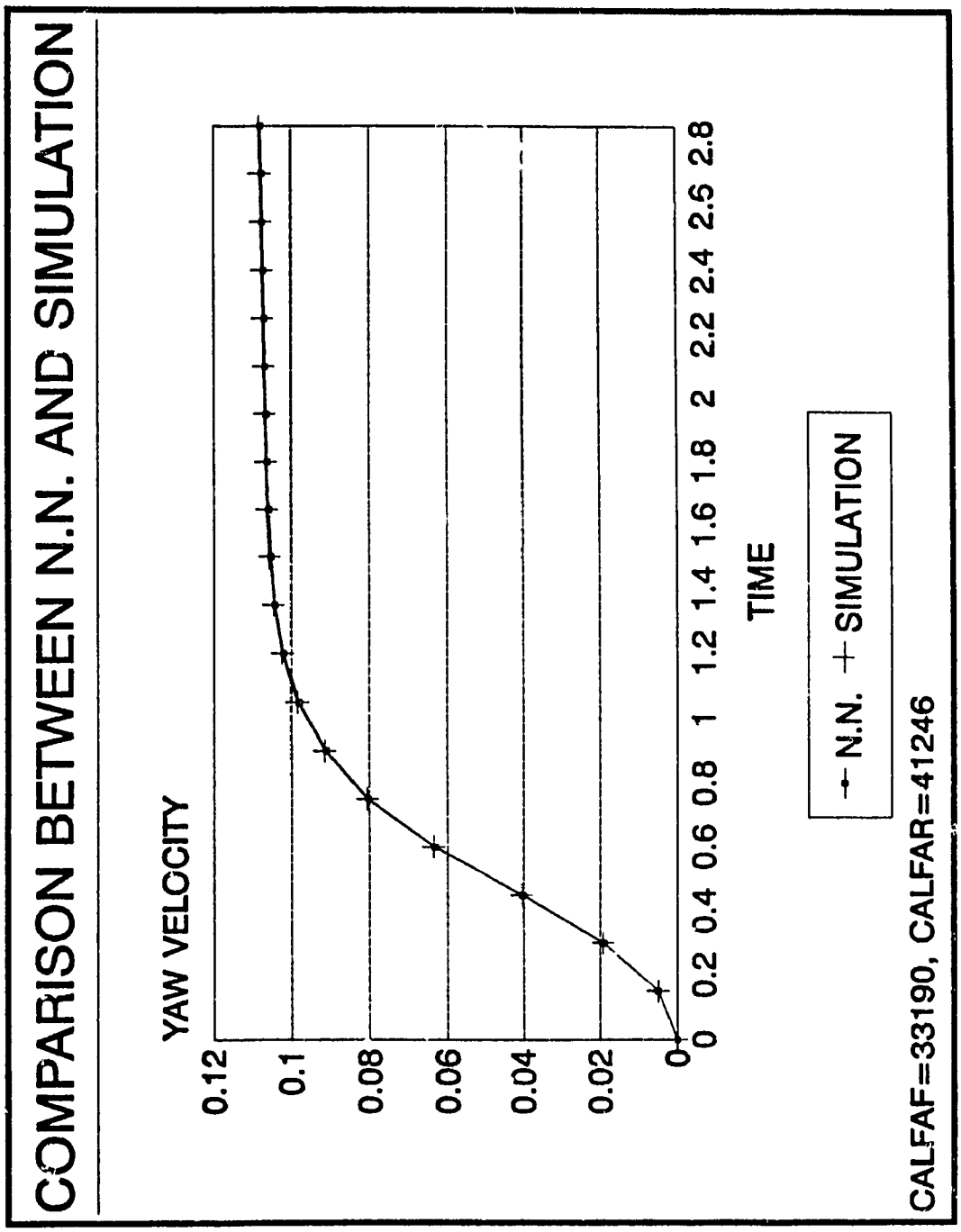


Fig. (4.6) Comparison between N.N. and simulation.

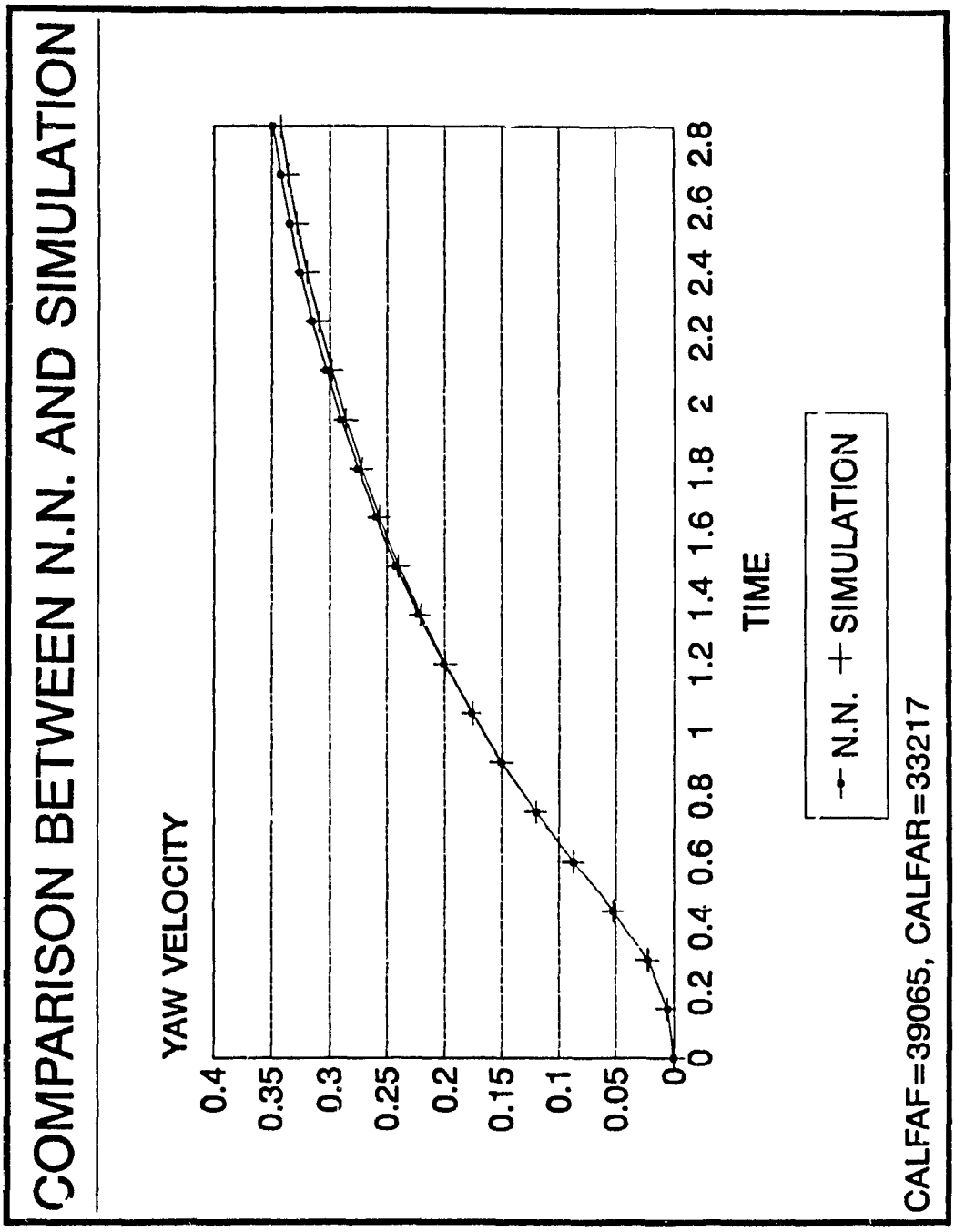


Fig. (4.7) Comparison between N.N. and simulation.

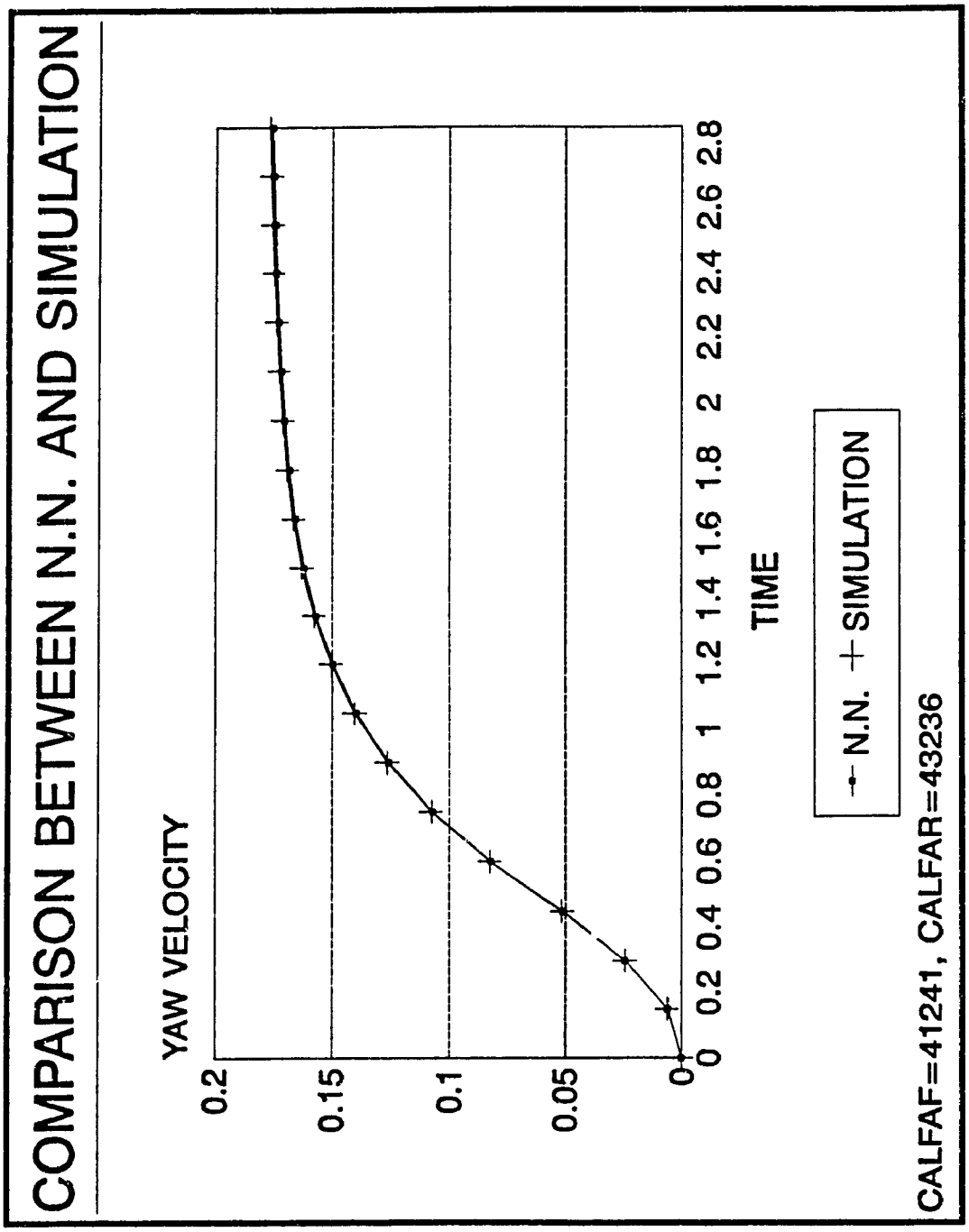


Fig. (4.8) Comparison between N.N. and simulation.

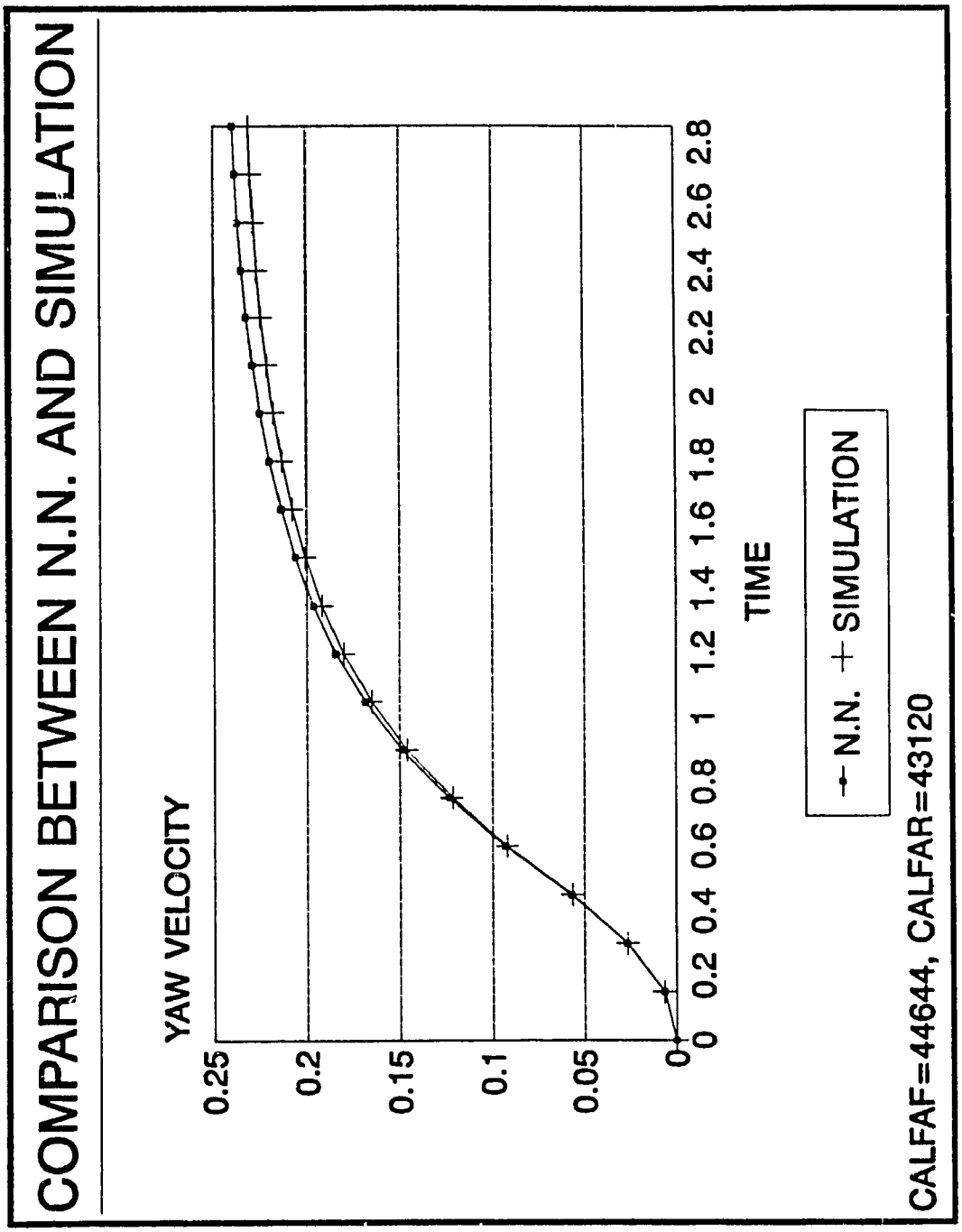


Fig. (4.9) Comparison between N.N. and simulation.

parameter quite effectively as long as the yaw response is within the training range.

To test the performance of N.N. in the presence of noise or errors in response data, some bad values are introduced in the input. The results are shown in table (4.5). Here the first set of result correspond to a response curve with three unrealistic very large values. The second set correspond to three response values set to zero. The final set correspond to three response values being negative. As the results show, the N.N. still tries to predict a tire parameter which are not very unreasonable (within 23%). The trained N.N. is found to predict very reasonable values for tire stiffness even when one or two values of the response curve are contaminated or has error.

## 4.6 APPLICATION OF N.N. IN OPTIMIZATION

Finally, the trained BPN is used in an attempt to find the optimal tire parameter that minimizes the yaw response. For this, the minimum values of yaw response within the range of simulation results at each of 19 discrete points (on time scale) is provided to the N.N. The N.N. predicted tire parameters are shown in Fig. (4.10). As the results show the N.N. predicted and simulated results are quite close with some

| Front tire stiffness. | Rear tire stiffness. | Front N.N. tire. | Rear N.N. tire. |
|---|---|---|---|
| 43000 | 41000 | 48499.96 | 39980.58 |
| 43000 | 45000 | 31474.71 | 48903.45 |
| 45000 | 35000 | 43950.57 | 43851.39 |

Table (4.5) Testing N.N. with noise.

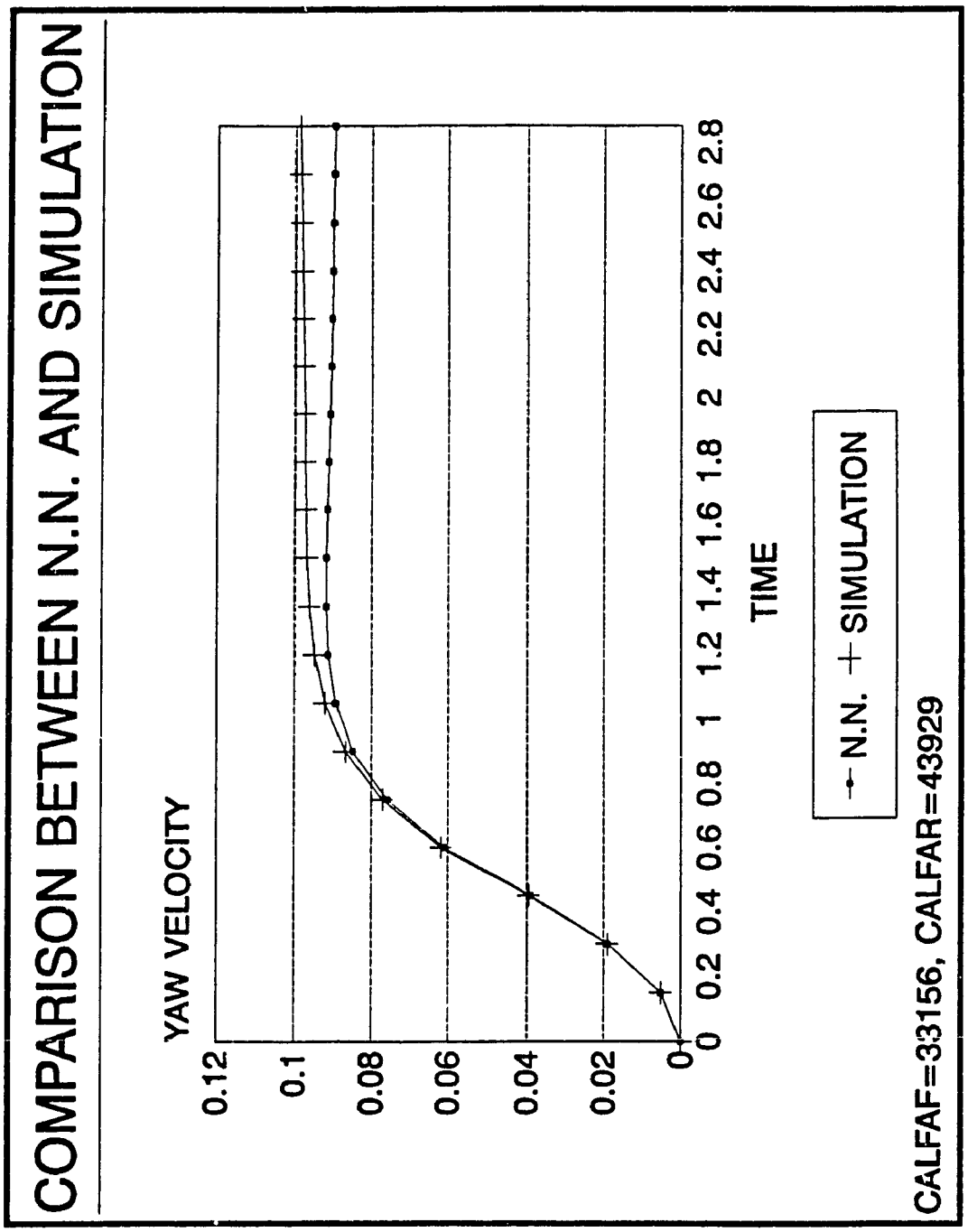


Fig. (4.10) Optimization of tire stiffness using N.N.

error in the steady state response of approx 4.5%. This error is very small, which demonstrate the potential of BPN in predicting the optimal parameter for such a system.

## 4.7 SUMMARY

In this chapter a three DOF vehicle model is developed to generate the data needed for the N.N. The vehicle model used is a simple vehicle model with the only variable being the tire parameters. The generated data is used to train the N.N. The training is carried out first using 9 sets of data then 25 sets and finally 49 sets. The training process proved that the N.N. is able to learn even with a small number of data sets. It has been also proved that the accuracy of the N.N. is increased with more data sets.

The trained N.N. is then used for predicting the tire parameters using the vehicle yaw response. Furthermore the N.N. is used to calculate the tire parameters that would optimize the vehicle response.

# CHAPTER 5

# 5. APPLICATION OF N.N. TO A SIX DEGREES OF FREEDOM VEHICLE MODEL.

## 5.1 INTRODUCTION.

Chapter 4 presents N.N. application of a simple vehicle model under steering input, where system parameters are cornering stiffness of tires and response is vehicle yaw velocity. The application in this chapter is extended to a six degrees-of-freedom (DOF) vehicle model representing four tires, four suspensions and a vehicle body. In this case the response of interest is the roll angle of the vehicle under a steering input. This is significantly more realistic model of the vehicle for curving analysis. The number of system parameters in this case can be many if all tire and suspension parameters are considered.

In this chapter, the six DOF vehicle model is presented and the equations of motions are developed. The data for the training of the N.N. is generated through simulation of the developed model. Systematic attempts are made to evaluate N.N. performance in single and multi-parameter simulation. Finally, application of N.N. is presented as a controller for vehicle roll to demonstrate its potential in controlling the roll

angle without affecting the ride quality.

## 6.2 SIX DEGREES OF FREEDOM VEHICLE MODEL

A six DOF model is adequate to determine the performance of the vehicle under steering input. The body fixed axis used in the modeling is the one defined by the Society of Automotive Engineers (SAE). The axis system along with various DOF is shown in Fig. (6.1), where the translational motions are defined for the vehicle centre of gravity (CG) along forward ($X$) , lateral ($Y$) and vertical ($Z$) directions. The rotational motions are defined about each of the above directions referred to as roll ($\Omega_X$) , pitch ($\Omega_Y$) , and yaw ($\Omega_Z$) motions, respectively.

The formulation of the mathematical model is carried out following the same steps as that for the three DOF model presented in chapter 5. In this case the transformation matrix between the fixed and body reference system is expressed in terms of change in rotations $\Delta\Omega$ , $\Delta\Omega_Y$ and $\Delta\Omega_Z$ in a time $\Delta t$ as [10, 11, 12, 25]:

$$\begin{pmatrix} c\Delta\Omega_Z c\Delta\Omega_Y & c\Delta\Omega_Z s\Delta\Omega_Y s\Delta\Omega_X - s\Delta\Omega_Z c\Delta\Omega_X & c\Delta\Omega_Z s\Delta\Omega_Y c\Delta\Omega_X + s\Delta\Omega_Z s\Delta\Omega_X \\ s\Delta\Omega_Z c\Delta\Omega_Y & s\Delta\Omega_Z s\Delta\Omega_Y s\Delta\Omega_X + c\Delta\Omega_Z c\Delta\Omega_X & s\Delta\Omega_Z s\Delta\Omega_Y c\Delta\Omega_X - c\Delta\Omega_Z s\Delta\Omega_X \\ -s\Delta\Omega_Y & c\Delta\Omega_Y s\Delta\Omega_X & c\Delta\Omega_Y c\Delta\Omega_X \end{pmatrix} \qquad (5.1)$$

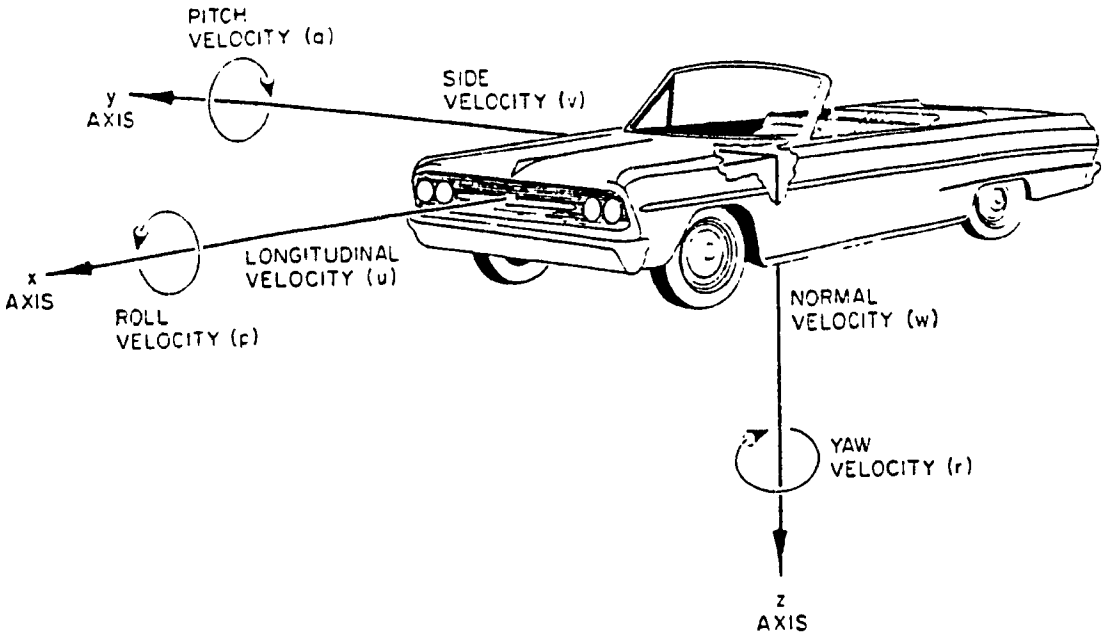


Fig. (5.1) Vehicle axis defined by S.A.E. [33]

where $s$ and $c$ represent sin and cos ,respectively. Assuming small change in the angles in time $\Delta t$ , and substituting $\sin\Delta\Omega-\Delta\Omega$ , $\cos\Delta\Omega-0$ , $\sin\Delta\Omega*\sin\Delta\Omega-0$ and $\cos\Delta\Omega*\cos\Delta\Omega-1$ in equation (5.1) lead to a simplified transformation matrix:

$$\begin{pmatrix} 1 & -\Delta\Omega_Z & \Delta\Omega_Y \\ \Delta\Omega_Z & 1 & -\Delta\Omega_X \\ -\Delta\Omega_Y & \Delta\Omega_X & 1 \end{pmatrix} \tag{5.2}$$

After a time $\Delta t$ , the change in velocity along each coordinate are $V_X+\Delta V_X$, $V_Y+\Delta V_Y$ and $V_Z+\Delta V_Z$ . The change in velocity with respect to the fixed coordinate can therefore be expressed as:

$$\Delta V-\begin{pmatrix} 1 & -\Delta\Omega_Z & \Delta\Omega_Y \\ \Delta\Omega_Z & 1 & -\Delta\Omega_X \\ -\Delta\Omega_Y & \Delta\Omega_X & 1 \end{pmatrix}*\begin{pmatrix} V_X+\Delta V_X \\ V_Y+\Delta V_Y \\ V_Z+\Delta V_Z \end{pmatrix}-\begin{pmatrix} V_X \\ V_Y \\ V_Z \end{pmatrix}-\begin{pmatrix} \Delta V_X-V_Y\Delta\Omega_Z+V_Z\Delta\Omega_Y \\ \Delta V_Y+V_X\Delta\Omega_Z-V_Z\Delta\Omega_X \\ \Delta V_Z-V_X\Delta\Omega_Y+V_Y\Delta\Omega_X \end{pmatrix} \tag{5.3}$$

The absolute acceleration can now be found by dividing the velocity component by $\Delta t$ and taking the limit when $\Delta t-0$ :

$$\begin{pmatrix} a_X \\ a_Y \\ a_Z \end{pmatrix}-\begin{pmatrix} \dot{V}_X-V_Y\dot{\Omega}_Z+V_Z\dot{\Omega}_Y \\ \dot{V}_Y+V_X\dot{\Omega}_Z-V_Z\dot{\Omega}_X \\ \dot{V}_Z-V_X\dot{\Omega}_Y+V_Y\dot{\Omega}_X \end{pmatrix} \tag{5.4}$$

## 5.3 EQUATIONS OF MOTION

The equations of motion for the six DOF vehicle model can be derived by summing forces and moments at the CG and applying Newton's second law. The location of all the forces acting on the vehicle are shown in Fig. (5.2). As shown in the figure, all the external forces are introduced at the tire-road interface except for aerodynamic drag $F_D$ acting at the centre of gravity. Here $F_{Xi}$ represents the longitudinal force due to drive or braking and rolling resistance. $F_{Yi}$ is the lateral force primarily due to cornering, and $F_{Zi}$ is the vertical force due to static and dynamic load of the vehicle transmitted through the suspension to the axle.

With reference to Fig. (5.2), the equations of motion can be expressed as:

$$M*a_X = F_{X1}\cos\theta_{FL} + F_{X2}\cos\theta_{FR} + F_{X3} + F_{X4} - F_{Y1}\sin\theta_{FL} - F_{Y2}\sin\theta_{FR} - F_D \tag{5.5}$$

$$M*a_Y = F_{X1}\sin\theta_{FL} + F_{X2}\sin\theta_{FR} + F_{Y1}\cos\theta_{FL} + F_{Y2}\cos\theta_{FR} + F_{Y3} + F_{Y4} \tag{5.6}$$

$$M*a_Z = M*g - (F_{Z1} + F_{Z2} + F_{Z3} + F_{Z4}) \tag{5.7}$$

$$I_X'\dot{\Omega}_X = Ma_Y h_B + \frac{S}{2}(F_{Z1} + F_{Z3} - F_{Z2} - F_{Z4}) - h_O(F_{Y3} + F_{Y4} + F_{Y1}\cos\theta_{FL} + F_{Y2}\cos\theta_{FR} + F_{X1}\sin\theta_{FL} + F_{X2}\sin\theta_{FR}) \tag{5.8}$$

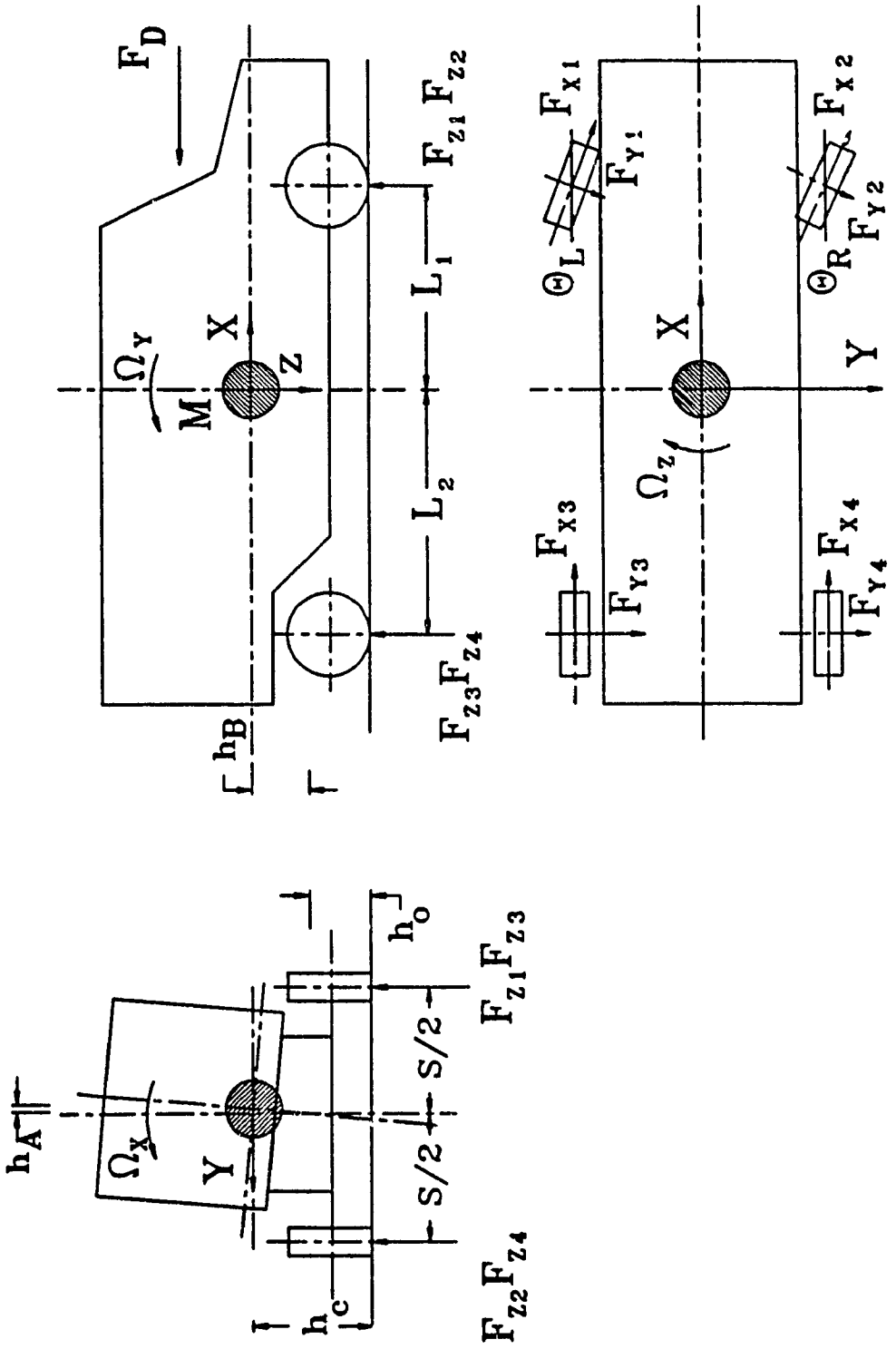


Fig. (5.2) Six degrees of freedom vehicle model.

$$I_Y\dot{\Omega}_Y - L_1(F_{Z1}+F_{Z2}) - L_2(F_{Z3}+F_{Z4}) + h_c(F_{X3}+F_{X4}+F_{X1}\cos\theta_{FL}+F_{X2}\cos\theta_{FR}-F_{Y1}\sin\theta_{FL}-F_{Y2}\sin\theta_{FR}) \quad (5.9)$$

$$I_Z\dot{\Omega}_Z - L_1(F_{Y1}\cos\theta_{FL}+F_{Y2}\cos\theta_{FR}+F_{X1}\sin\theta_{FL}+F_{X2}\sin\theta_{FR}) - L_2(F_{Y3}+F_{Y4}) - (\frac{S}{2}-h_A)(F_{X4}+F_{X2}\cos\theta_{FR}-F_{Y2}\sin\theta_{FR}) + (\frac{S}{2}+h_A)(F_{X3}+F_{X1}\cos\theta_{FL}-F_{Y1}\sin\theta_{FL}) \quad (5.10)$$

where, $I'_X$ is the moment of inertia of the vehicle about the roll centre and is defined as:

$$I'_X = I_X + Mh_b^2$$

Various forces in equations (5.5) to (5.10) are described as follows:

Longitudinal forces

In equations (5.5) to (5.10), $F_{Xi}$ represents the longitudinal force at the tire-road interface, expression for which is derived in section (2.2.2.1). Combining equations (2.1) and (2.7) the longitudinal force for a driving wheel can be expressed as:

$$F_{Xi} = F_{di} - f_r * F_{Zi} \qquad i=1 \text{ to } 4 \quad (5.11)$$

where $F_{di}$ is the tractive force and $F_{Zi}$ is the normal load at the ith wheel. In this study the tractive force effort is only considered for the rear wheel ( $F_{di}=0$ for $i=1,2$ ). The coefficient of rolling resistance $f_r$ is taken as a constant.

Lateral forces

The lateral forces in $F_{Yi}$ in equation (5.5) to (5.10) are due to cornering force as discussed in section (2.2.2.2). Neglecting camber effect, the lateral forces can be expressed as:

$$F_{Yi} = C_\alpha \alpha_i \quad i = 1 \text{ to } 4 \tag{5.12}$$

where $C_\alpha$ is the tire cornering stiffness as explained in section (2.2.2.2) and is considered to be same for each tire. $\alpha_i$ is the slip angle for the ith wheel. As described for the three DOF model (equations (4.9) and (4.10)), the slip angle for each tire can be expressed as a function of wheel steer angle and response variable:

$$\alpha_1 = \theta_{FL} - \frac{L_1 \dot{\Omega}_Z + V_Y}{V_X} \tag{5.13}$$

$$\alpha_2 = \theta_{FR} - \frac{L_1 \dot{\Omega}_Z + V_Y}{V_X} \tag{5.14}$$

$$\alpha_3 = \alpha_4 = -\frac{L_2 \dot{\Omega}_Z - V_Y}{V_X} \tag{5.15}$$

The wheel steering angle ( $\theta_{FL}$ and $\theta_{FR}$ ) in the above equations and in the equations of motion (equations (5.5) to (5.10)) can be expressed in term of mean input steering angle $\theta$ , as discussed in section (2.4.2) and presented in

equations (2.23) and (2.24):

$$\theta_{FL} = \frac{\theta}{\frac{S\theta}{2(L_1+L_2)}+1} \qquad (5.16)$$

$$\theta_{FR} = \frac{\theta}{1-\frac{S\theta}{2(L_1+L_2)}} \qquad (5.17)$$

where $S$ is the track width and ( $L_1+L_2$ ) is the wheel base as shown in Fig. (5.2). $\theta$ is the steering angle which can be described in section (2.4.3).

Vertical forces

The vertical forces ( $F_{si}$ ) in equations (5.5) to (5.10) are due to the vehicle mass and suspension forces. The vertical force for the front and rear wheels can be expressed as:

a) For the front suspension:

$$F_{si} = M * g \frac{L_2}{2(L_1+L_2)} + F_{si} \qquad i=1 \text{ to } 2 \qquad (5.18)$$

where $F_{si}$ is the suspension force at the ith suspension. Using expression derived in section (2.3.2) (equation (2.19)) the suspension force is:

$$F_{si} = K_P \Delta_i + C_P \dot{\Delta}_i + (-1)^i K_T \Omega_X \qquad i=1 \text{ to } 2 \qquad (5.19)$$

where

$$\Delta_i = Z - (-1)^i \frac{S}{2}\Omega_X - L_1\Omega_Y \qquad i=1 \text{ to } 2 \qquad (5.20)$$

$$\dot{\Delta}_i = \dot{Z} - (-1)^i \frac{S}{2}\dot{\Omega}_X - L_1\dot{\Omega}_Y \qquad i=1 \text{ to } 2 \qquad (5.21)$$

For the front suspension, $K_F$, $K_T$ and $C_F$ are the equivalent spring stiffness, torsion stiffness and damping coefficient, respectively. $Z$ represents bounce displacement of the vehicle CG.

b) For the rear suspension:

$$F_{si} = M * g \frac{L_1}{2(L_1+L_2)} + F_{si} \qquad i=3 \text{ to } 4 \qquad (5.22)$$

Using expression derived in section (2.3.2) (equation (2.18)), the suspension force is

$$F_{si} = K_R\Delta_i + C_R\dot{\Delta}_i \qquad i=3 \text{ to } 4 \qquad (5.23)$$

where

$$\Delta_i = Z - (-1)^i \frac{S}{2}\Omega_X + L_2\Omega_Y \qquad i=3 \text{ to } 4 \qquad (5.24)$$

$$\dot{\Delta}_i = \dot{Z} - (-1)^i \frac{S}{2}\dot{\Omega}_X + L_2\dot{\Omega}_Y \qquad i=3 \text{ to } 4 \qquad (5.25)$$

For the rear suspension, $K_R$ and $C_R$ are the equivalent spring stiffness and damping coefficient respectively. In deriving these equations it is assumed that the tire deflection is small and that the road is smooth.

The aerodynamic drag force is included in the model represented by $F_D$ in Fig. (5.2) and equation (5.5). The drag force assumed to act at the CG can be expressed as a function of velocity $V$, by [11]:

$$F_D = \frac{\rho}{2} C_D A V^2 \qquad (5.26)$$

where $\rho$ is the air density, $C_D$ is the coefficient of aerodynamic resistance and $A$ is the frontal area.

The moment arms $h_O, h_A, h_B$ and $h_C$ shown in Fig. (5.2) and used in equations (5.5) to (5.10), are variable distances that can be expressed in terms of static vehicle parameter and bounce motion ( $Z$ ):

$$h_O = A - B \qquad (5.27)$$

$$h_A = A * \Omega_X \qquad (5.28)$$

$$h_B = (B-Z)\,(1-|\Omega_X|)\,(1-|\Omega_Y|) \qquad (5.29)$$

$$h_C = (A-Z)\,(1-|\Omega_X|)\,(1-|\Omega_Y|) \qquad (5.30)$$

$A$ is the distance between the vehicle CG and the ground. $B$ is the distance between the vehicle CG and the roll centre. The location of the roll centre is discussed in section 2.3.1.

## 5.4 SIMULATION OF SIX DEGREES OF FREEDOM VEHICLE MODEL

The equations of motion derived in section 5.2 are solved

simultaneously using trapezoidal method. The parameters used for the simulation are representative of a passenger car [18] as presented in table (5.1). The parameters presented in the table are nominal values where the suspension parameter are retained as variable to attempt application of N.N. for multi variable training. These parameters are front and rear suspension stiffness $K_F$ and $K_R$ , torsion bar stiffness $K_T$ and front and rear suspension damping $C_F$ and $C_R$ .

The steering input in this case is considered to be the one presented in section 2.4.3 as Fig. (2.10). It represent a ramp function steering input of 0 to 5 degrees in 0.5 seconds.

Sample simulation results are presented in Figs. (5.3) to (5.8) for two simulations. The first one has the front and rear spring stiffness $K_F$-$K_R$-20000$N/m.$ , the torsion bar stiffness $K_T$-2000$N/rad.$ and the damping coefficient $C_F$-$C_R$-20000$Ns/m.$ For the second simulation, the suspension parameters are same as those presented in table (5.1).

Fig. (5.3) shows the roll angle of the vehicle during the simulation. It is clear from the Fig. that the roll angle is significantly affected by the variation of the suspension parameters. Fig. (5.4) shows the pitch angle of the vehicle. The pitch angle is also affected by the suspension parameter but to a lesser degree. Fig. (5.5) shows the yaw angle during

the simulation. The yaw angle is not affected by the suspension parameters as expected. Yaw angle response is primarily a function of tire property which is not changed in this case. Figs. (5.6) and (5.7) show respectively, the forward and lateral velocity of the vehicle during the simulation. Both of these velocities are not affected by the change of the suspension parameters. Fig. (5.8) shows the vertical velocity of the vehicle. Although the vertical velocity is low for the given steering input and parameters, the effect of suspension on this response quite apparent.

From the result presented, it is clear that during steering the critical vehicle motion is the roll angle. A large value of roll angle would make the vehicle unstable which may lead to roll over. The vehicle roll angle is therefore, selected to be a candidate for the N.N. application and control. In the following sections the absolute values of the roll angle is used for the training of N.N. for various sets of above parameters.

| | |
|---|---|
| Mass = 830 Kg. | $S$=1.3$m$. |
| $I_X$=150$kgm.^2$ | $C_\alpha$=30000$N/rad.$ |
| $I_Y$=1200$kgm.^2$ | $K_F$=30000$N/m$. |
| $I_Z$=1100$kgm.^2$ | $K_R$=30000$N/m$. |
| $L_1$=1$m$. | $K_T$=8000$N/rad.$ |
| $L_2$=1.4$m$. | $C_F$=30000$Ns/m$. |
| $V$=80$Km/h$. | $C_R$=30000$Ns/m$. |
| $F_{di}$=400$N$. | Distance between CG and ground $A$=0.5$m$. |
| $f_r$=0.02 | Distance between CG and roll centre $B$=0.3$m$. |
| Frontal area $A$=2$m.^2$ | $h_o$=o.2$m$. |

Table (5.1) Six degrees of freedom vehicle model parameters.

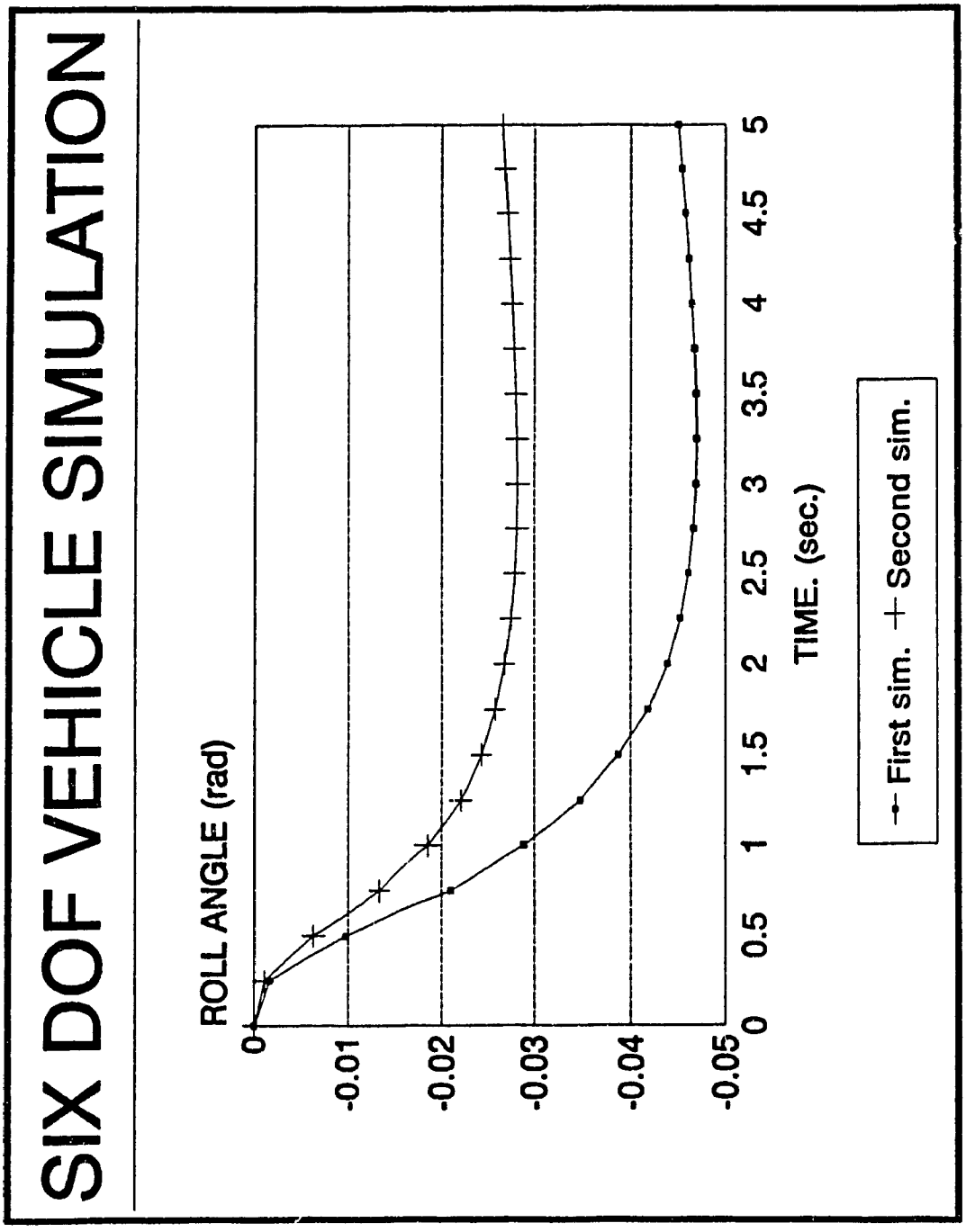


Fig. (5.3) Six DOF vehicle model roll simulation.

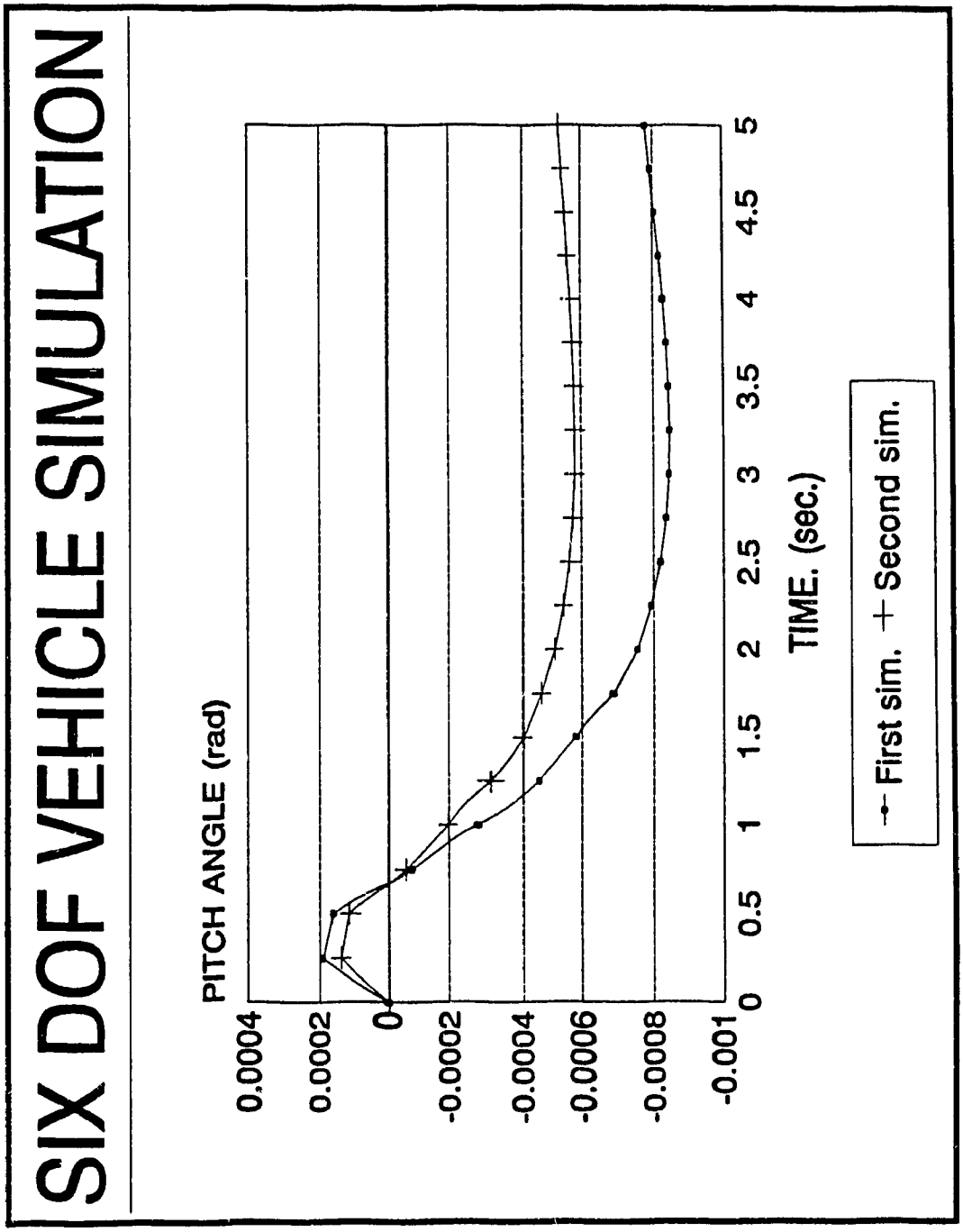


Fig. (5.4) Six DOF vehicle model pitch simulation.

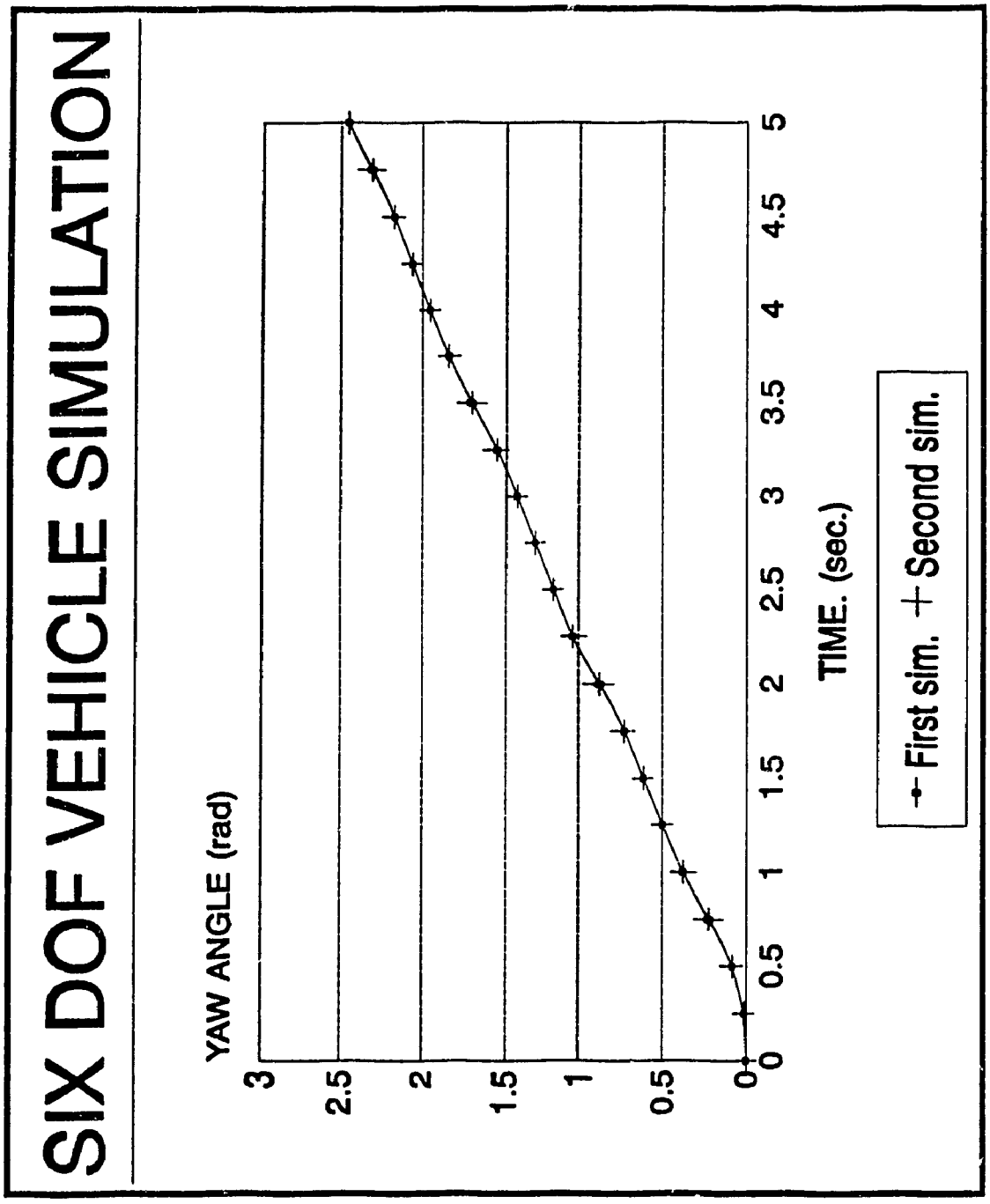


Fig. (5.5) Six DOF vehicle model yaw simulation.

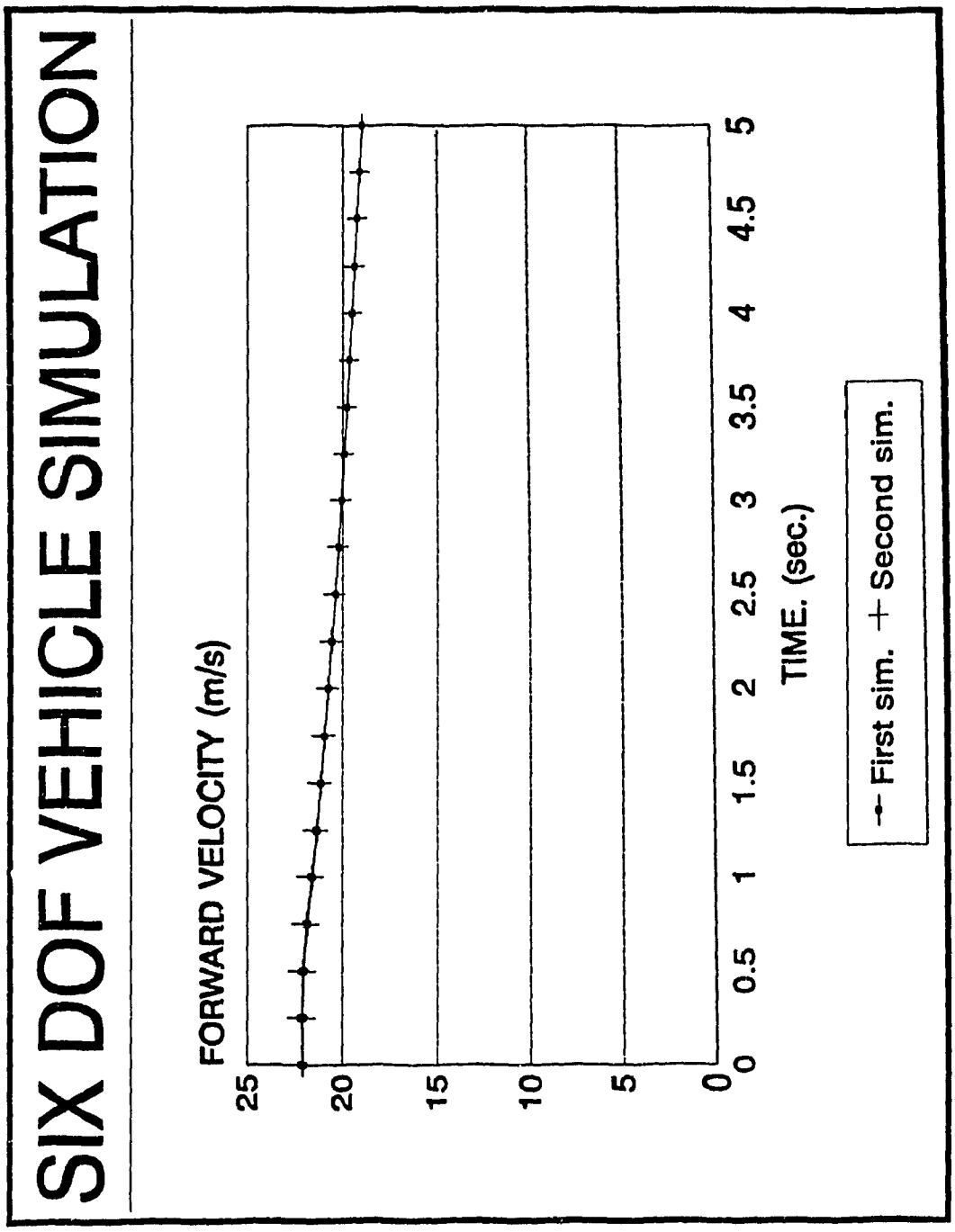


Fig. (5.6) Six DOF vehicle model forward velocity simulation.

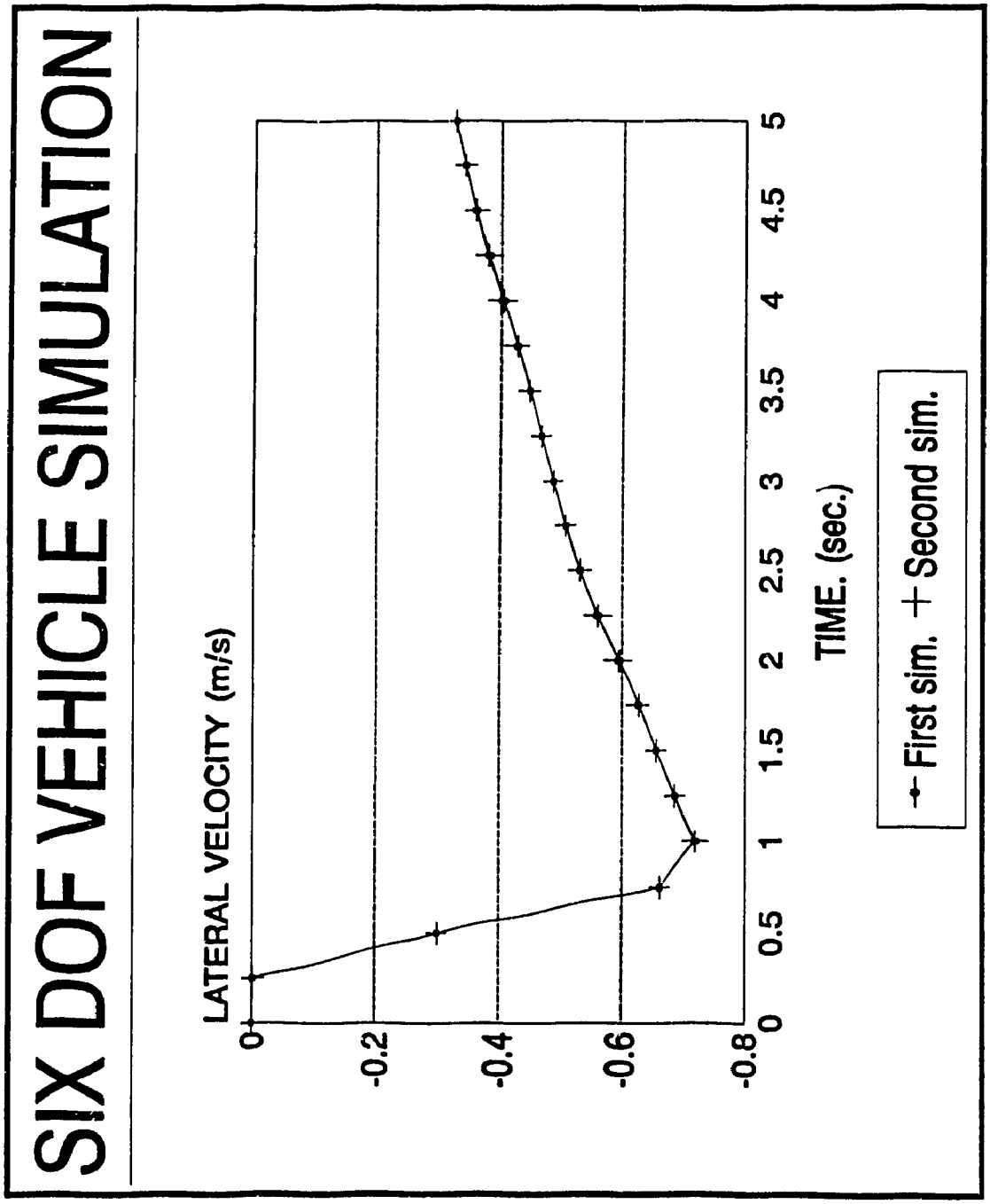


Fig. (5.7) Six DOF vehicle model lateral velocity simulation.

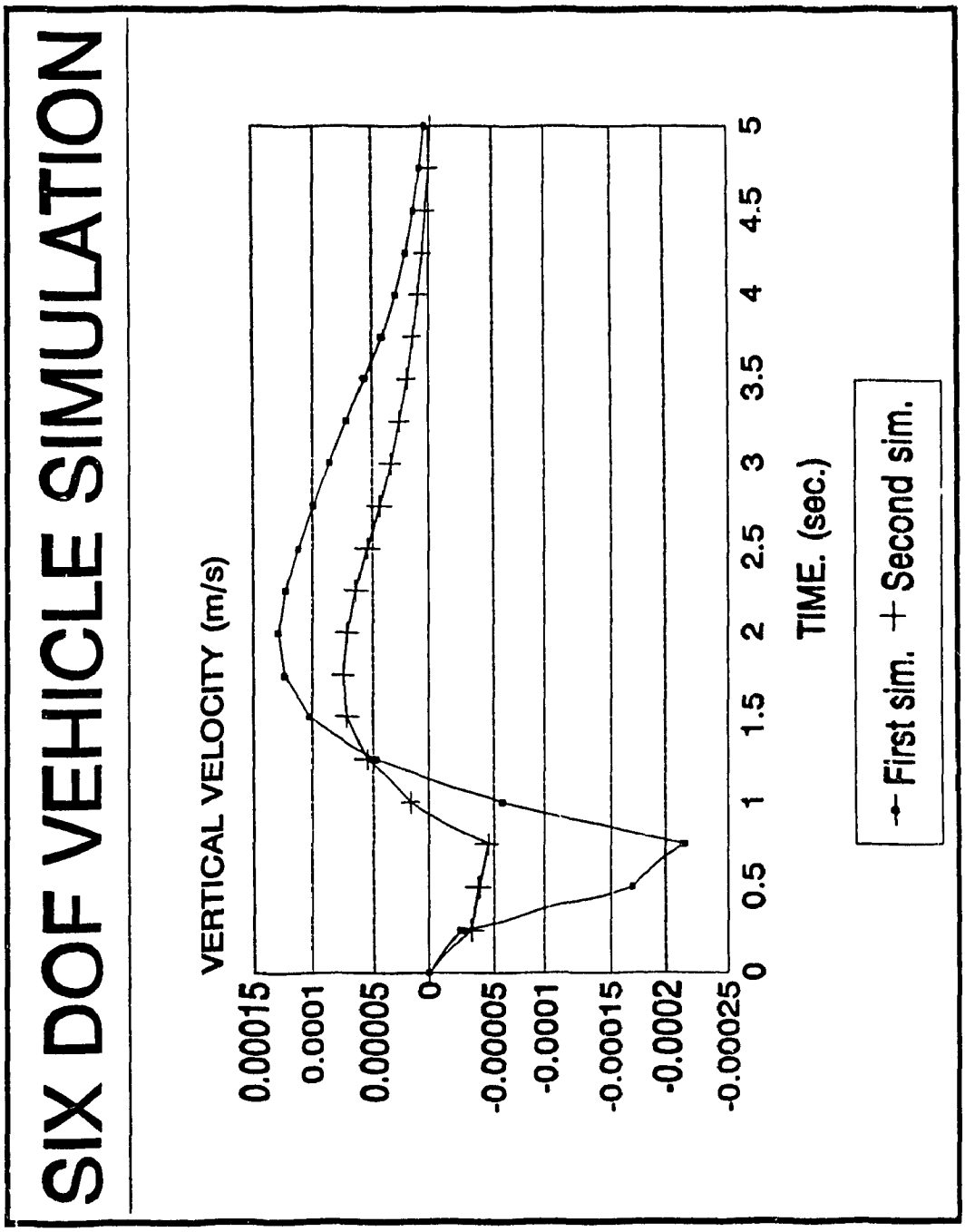


Fig. (5.8) Six DOF vehicle model vertical velocity simulation.

## 5.5 N.N. FOR SIX DOF MODEL

In the formulation, set up and training of N.N. in this application, the objective is to establish relationship between the roll angle and the set of suspension parameters $K_F$, $K_R$, $K_T$, $C_F$ and $C_R$ .

The initial attempts of training the network for the five variables were found unsuccessful. After investigating several aspects of the learning process, it was found that the data file created to train the network contained identical roll angle response to the steering input for different set of suspension parameters. For an example $K_F$=30000, *and* $K_R$=35000 leads to identical response as that corresponding to $K_F$=35000, *and* $K_R$=30000 while all other parameters remained constant. The roll angle time response for the above two cases is presented in table (5.2).

As discussed previously, such situation where different input may lead to same output causes a confusion in the learning process leading to failure to learn. The training and application schemes are, therefore, modified. First, attempt is made in training for one parameter at a time, namely, suspension stiffness, or torsion bar stiffness, or suspension damping, where front and rear suspension are identical and all other parameters are constant and equal to

| | Time in sec. | Roll angle. |
|---|---|---|
| $K_P$- 30000 N/m. | 0.0000E+00 | 0.0000E+00 |
| $K_R$- 35000 N/m. | 0.5000E+00 | 0.6384E-02 |
| | 0.1000E+01 | 0.1817E-01 |
| | 0.1500E+01 | 0.2336E-01 |
| | 0.2000E+01 | 0.2569E-01 |
| | 0.2500E+01 | 0.2655E-01 |
| | 0.3000E+01 | 0.2666E-01 |
| | 0.3500E+01 | 0.2641E-01 |
| | 0.4000E+01 | 0.2598E-01 |
| | 0.4500E+01 | 0.2548E-01 |
| | 0.5000E+01 | 0.2495E-01 |
| $K_P$- 35000 N/m. | 0.0000E+00 | 0.0000E+00 |
| $K_R$- 30000 N/m. | 0.5000E+00 | 0.6384E-02 |
| | 0.1000E+01 | 0.1817E-01 |
| | 0.1500E+01 | 0.2336E-01 |
| | 0.2000E+01 | 0.2569E-01 |
| | 0.2500E+01 | 0.2655E-01 |
| | 0.3000E+01 | 0.2666E-01 |
| | 0.3500E+01 | 0.2641E-01 |
| | 0.4000E+01 | 0.2598E-01 |
| | 0.4500E+01 | 0.2548E-01 |
| | 0.5000E+01 | 0.2495E-01 |

Table (5.2) Time versus roll angle.

their nominal values. After successful implementation for each, the network is extended for two parameters, namely suspension stiffness and damping, where front and rear suspension are the same.

The type of N.N., learning rules and procedure used are discussed in details in chapter 3 and are same as those used for the 3 DOF model in chapter 4. The N.N. parameters used for this study are presented in table (5.3). The results for the six DOF model in each of the different case are presented in the following sub-sections.

### 5.5.1 N.N. FOR SUSPENSION STIFFNESS

For this part of the study, simulation results are obtained using the six DOF model for different values of suspension stiffness while all other parameters are held constant and equal to their nominal values. Front and rear suspension stiffness are taken as identical. The suspension stiffness and vehicle roll response to the prescribed steering input is used as the data set for training the N.N. 31 set of data are used for the training, where each set includes a value of suspension stiffness and 10 points on the roll angle response curve. 10 Points are found adequate to describe the response as a smooth continuous curve. The N.N. parameters are listed in table (5.3) while the vehicle suspension parameters

are listed in table (5.4).

The trained network is used for prediction of suspension stiffness for an arbitrary roll response described by 10 points along the time scale. This is achieved by applying inverse dynamics capability of BPN. The BPN predicted suspension stiffness is then used to simulate the roll response. Simulated roll response is compared with that of response described to the N.N. as presented in Figs. (5.9) to (5.11). As the results show, the N.N. is capable of predicting the relationship quite accurately. These results also show the trend that roll angle decreases with an increase in suspension stiffness. On the other hand, this will adversely affect the ride quality.

| | |
|---|---|
| Number of inputs (roll angle). | 10 |
| Hidden. | 10 |
| Output. | 1 |
| Learning coefficient for input. | 0.3 |
| Learning coefficient for output. | 0.15 |
| Learning rule. | Delta rule. |
| Transfer function. | Sigmoid. |

Table (5.3) N.N. parameters for one parameter vehicle model.

| | |
|---|---|
| $K_F$-$K_R$ | From 10000 to 40000 N/m. |
| $C_F$-$C_R$ | 30000 Ns/m. |
| $K_T$ | 8000 N/rad. |

Table (5.4) Vehicle suspension data for N.N. application to spring stiffness.

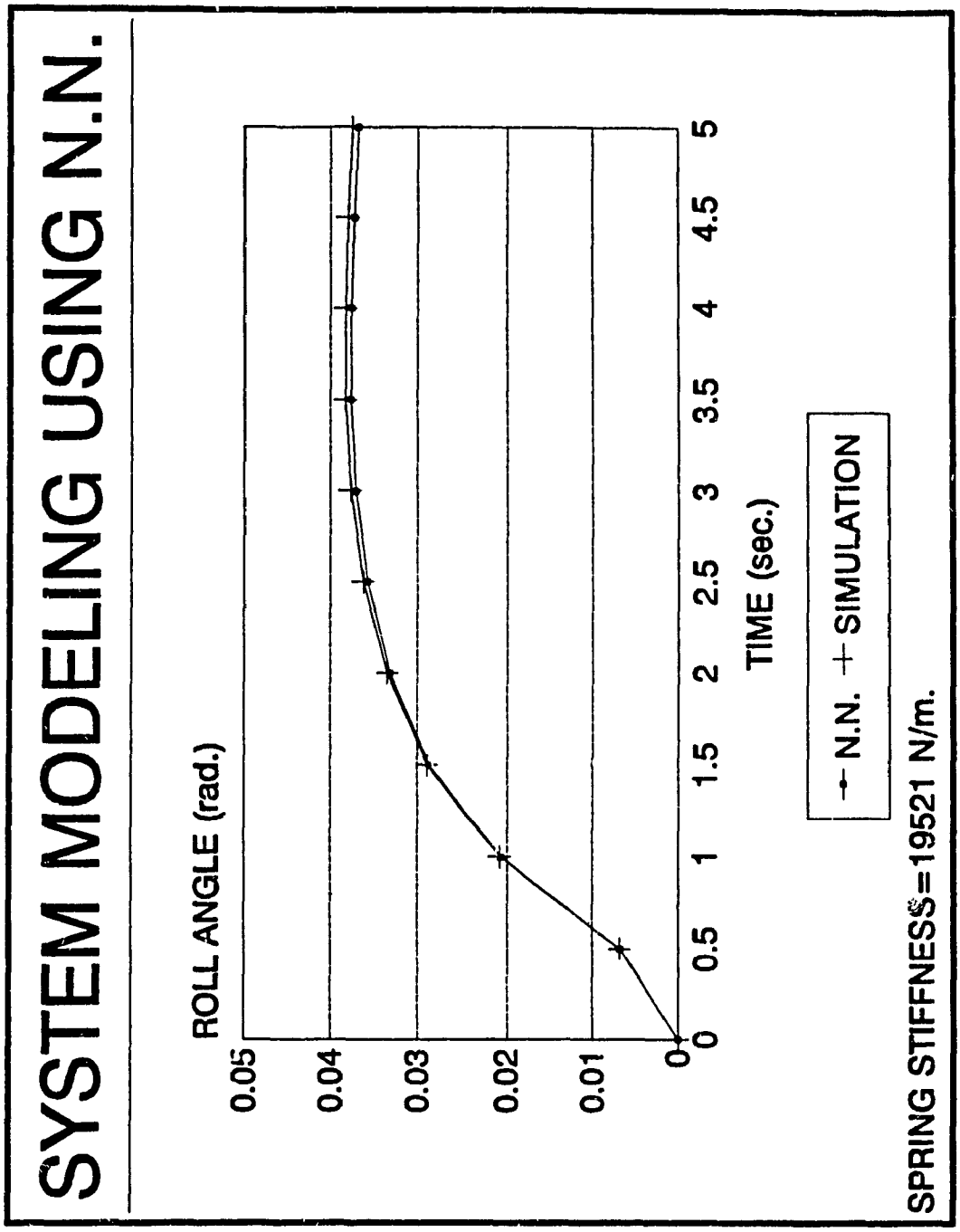


Fig. (5.9) N.N. versus simulation.

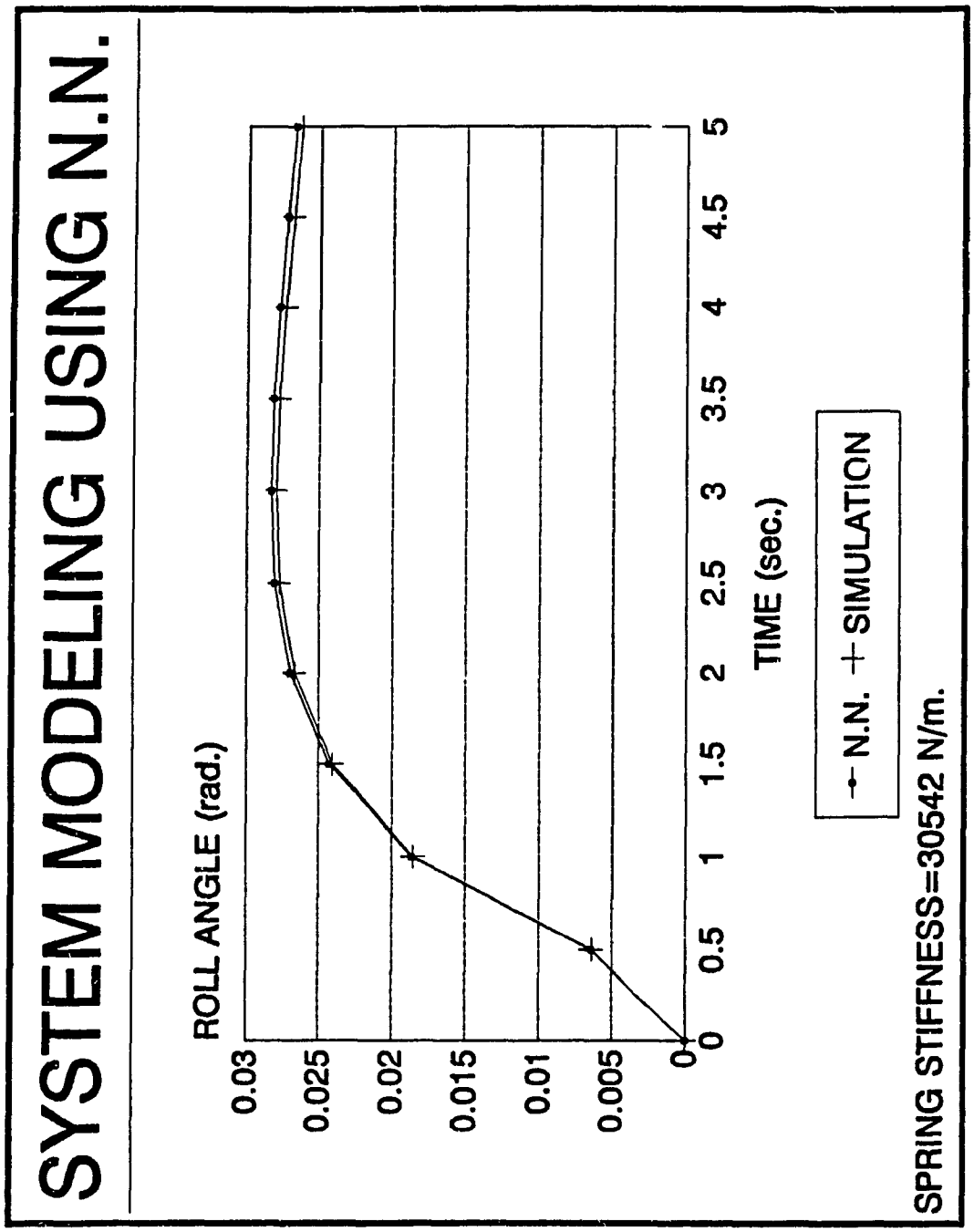


Fig. (5.10) N.N. versus simulation.

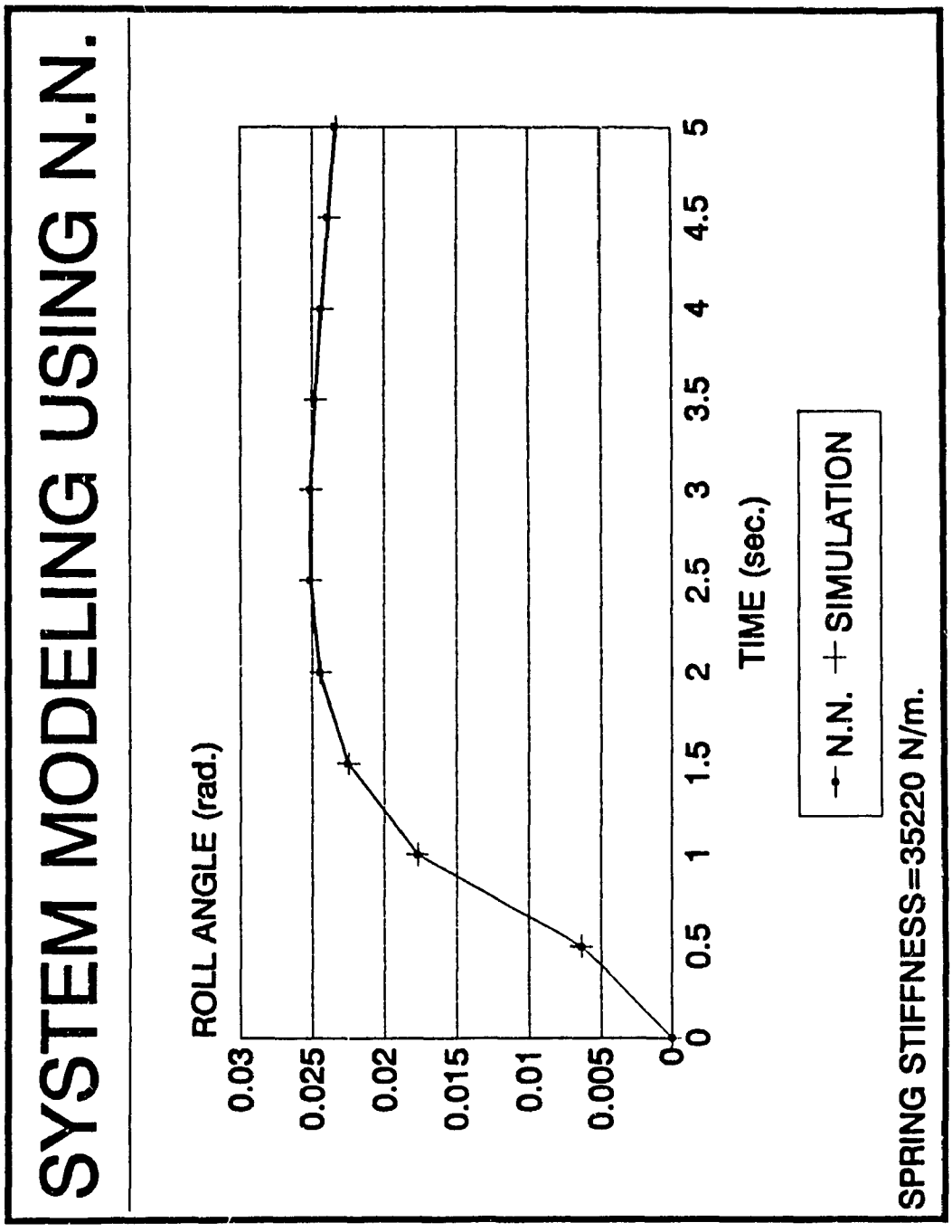


Fig. (5.11) N.N. versus simulation.

### 5.5.2 N.N. FOR SUSPENSION TORSION BAR STIFFNESS

Similar to the previous section, simulation is carried out for the vehicle model for different values of suspension torsion bar stiffness, while all other parameters remain constant. The value of torsion bar stiffness is varied between 1000 to 10000 N/rad. to generate roll response data.

The 19 sets of data generated during the simulation are used to train the N.N. The N.N. parameters are the same as the previous section and are presented in table (5.3). The trained N.N. is used for predicting the suspension parameter which in this case is the torsion bar stiffness. The Figs. (5.12) to (5.14) show the success of the N.N. in predicating the torsion bar stiffness.

From the results, it is clear that the roll angle would decrease with the increase of the torsion bar stiffness. The torsion bar stiffness only increases the suspension stiffness when the vehicle is under roll. That means that a higher torsion bar stiffness would not affect the ride quality of the vehicle when both left and right wheels move simultaneously.

The problem that prevent the designers from increasing the torsion bar stiffness is that the diameter of the bar

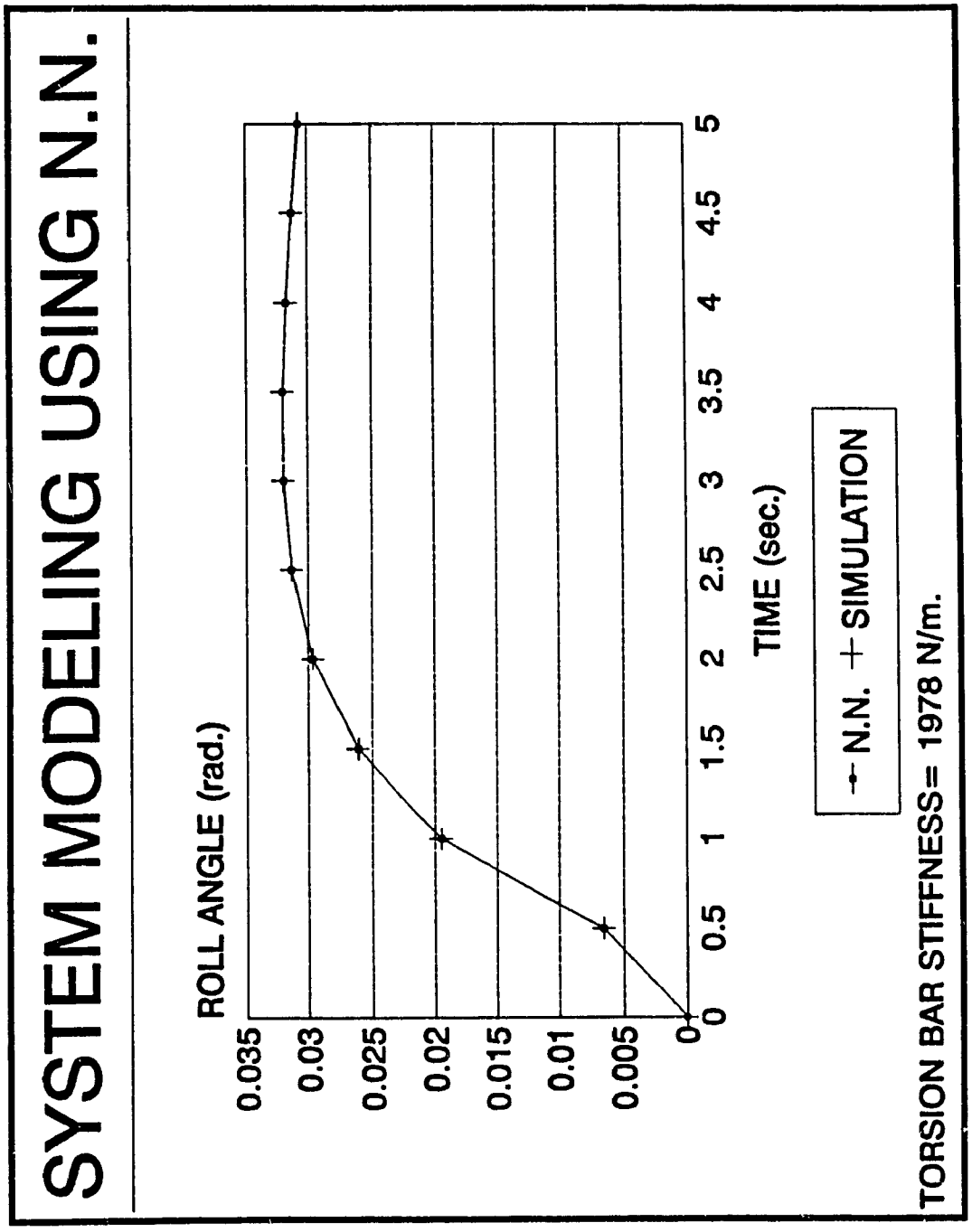


Fig. (5.12) N.N. versus simulation.

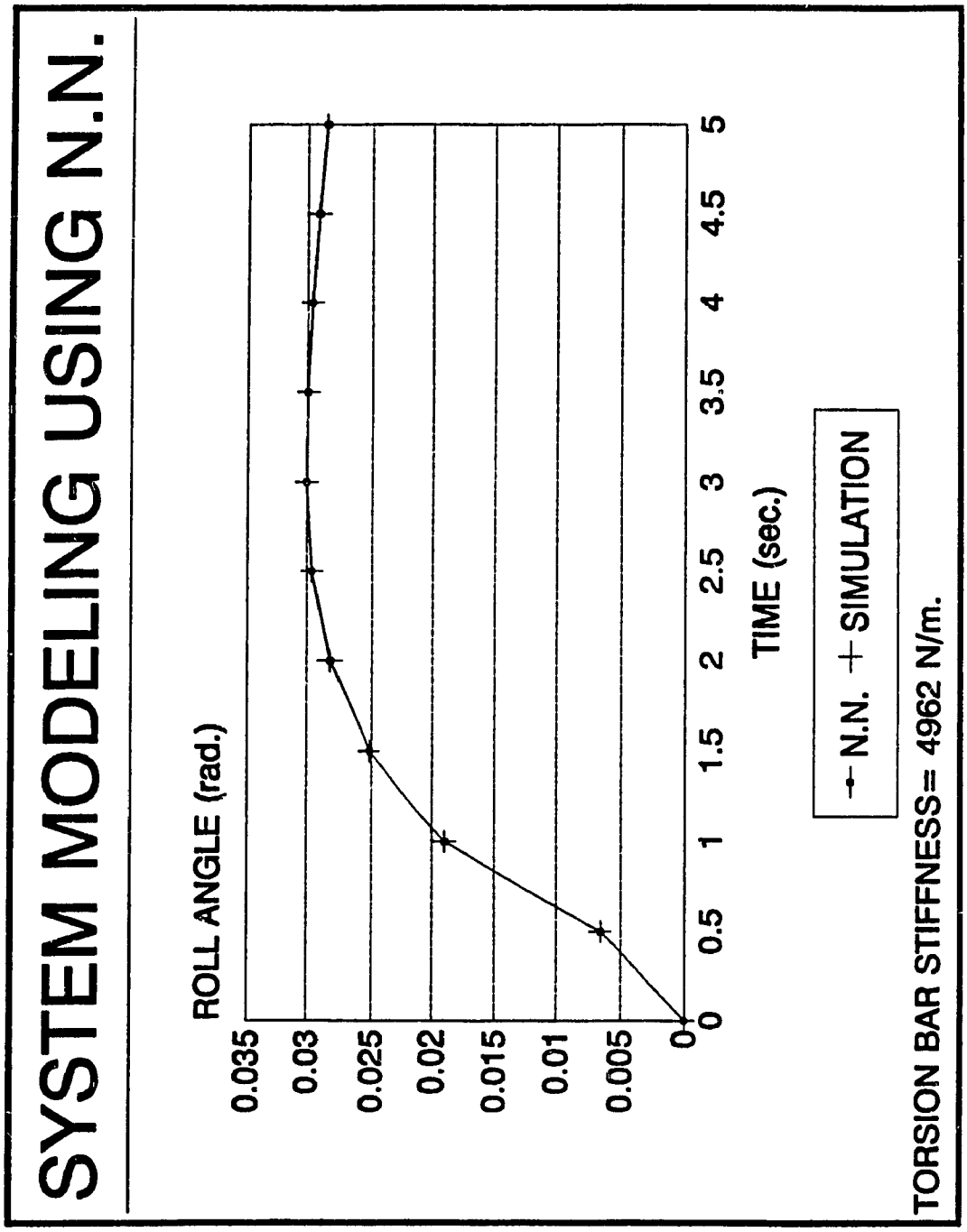


Fig. (5.13) N.N. versus simulation.

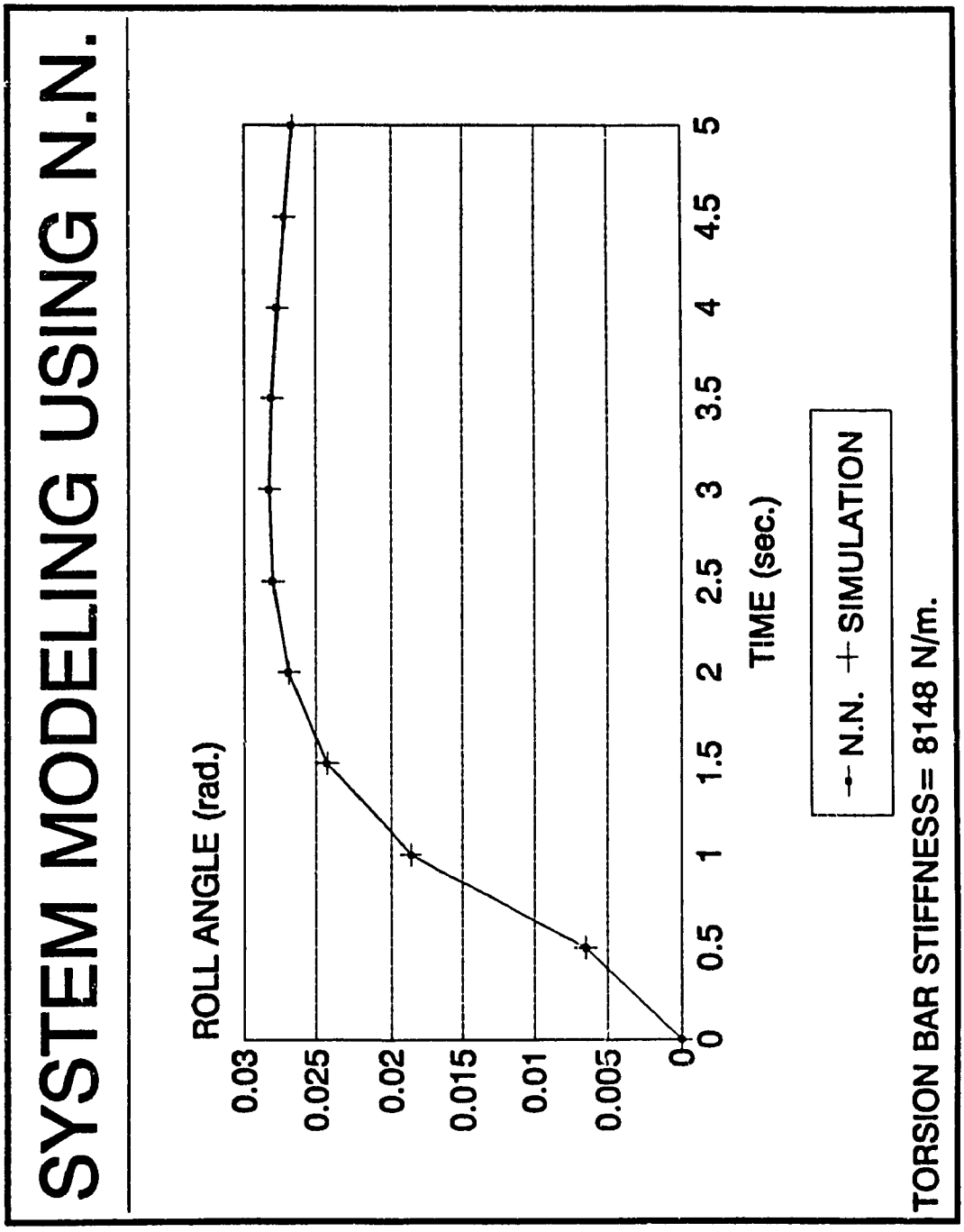


Fig. (5.14) N.N. versus simulation.

would increase and would not be feasible for passenger vehicles.

### 5.5.3 N.N. FOR SUSPENSION DAMPING

In this section the simulation is carried out for different damping coefficients while other parameters are maintained equal to their nominal values. The value of the suspension damping coefficient is varied between 10000 and 40000 Ns/m. to generate the roll response data.

The 31 sets of data generated during the simulation are used to train the N.N. Similar to previous sections, the trained N.N. is used to predict the damping coefficient given a certain roll behaviour. The N.N. parameters used for this part are also same as those shown in table (5.3). The Figs. (5.15) to (5.17) show the success of the N.N. in predicting the damping coefficient accurately given a roll behaviour.

It is clear from the results of the simulation that the roll behaviour is improved as the damping coefficient increases, but again that would adversely affect the ride quality of the vehicle.

In most modern vehicles the damping coefficient is not constant and in some vehicles controlled damping is used

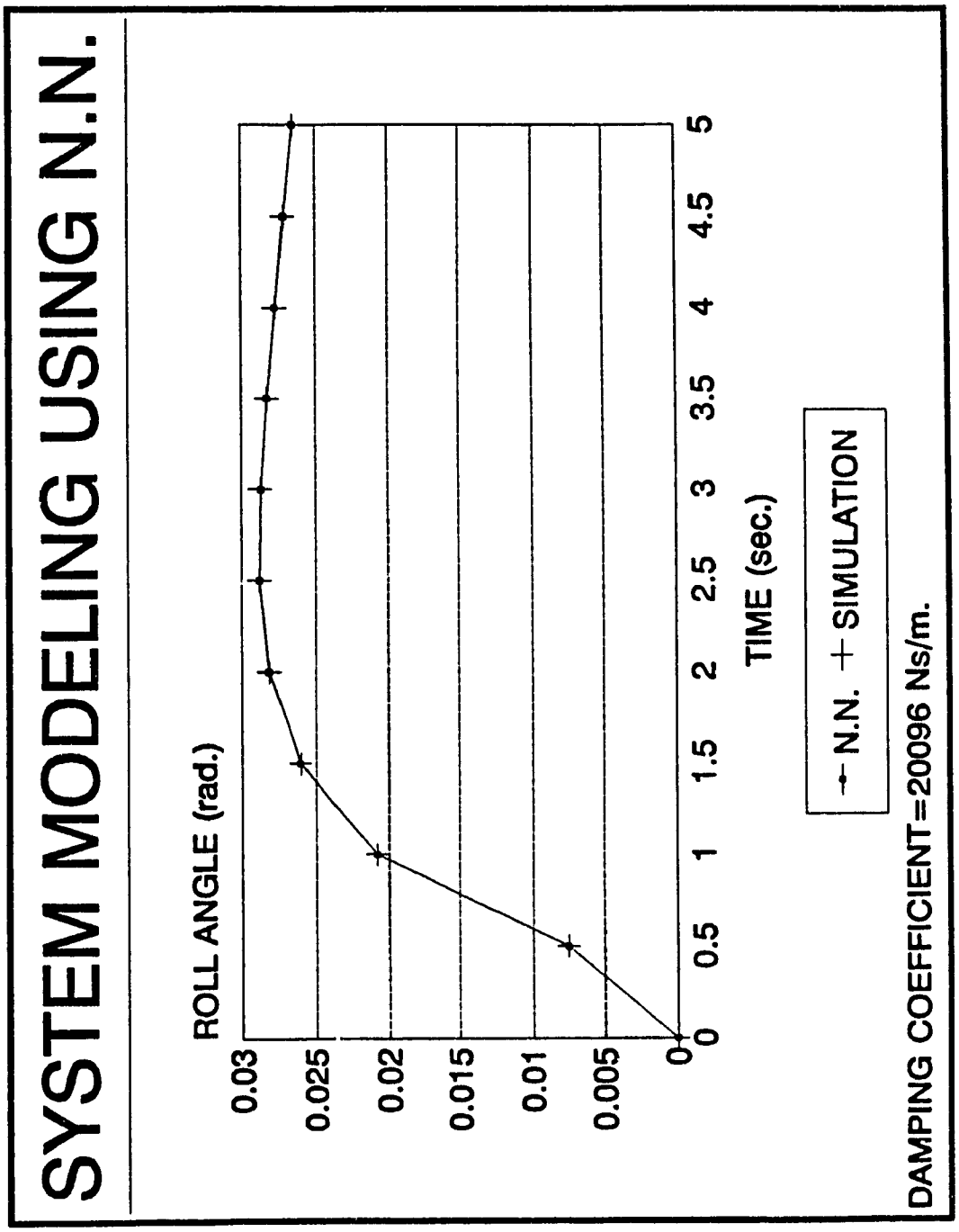


Fig. (5.15) N.N. versus simulations.

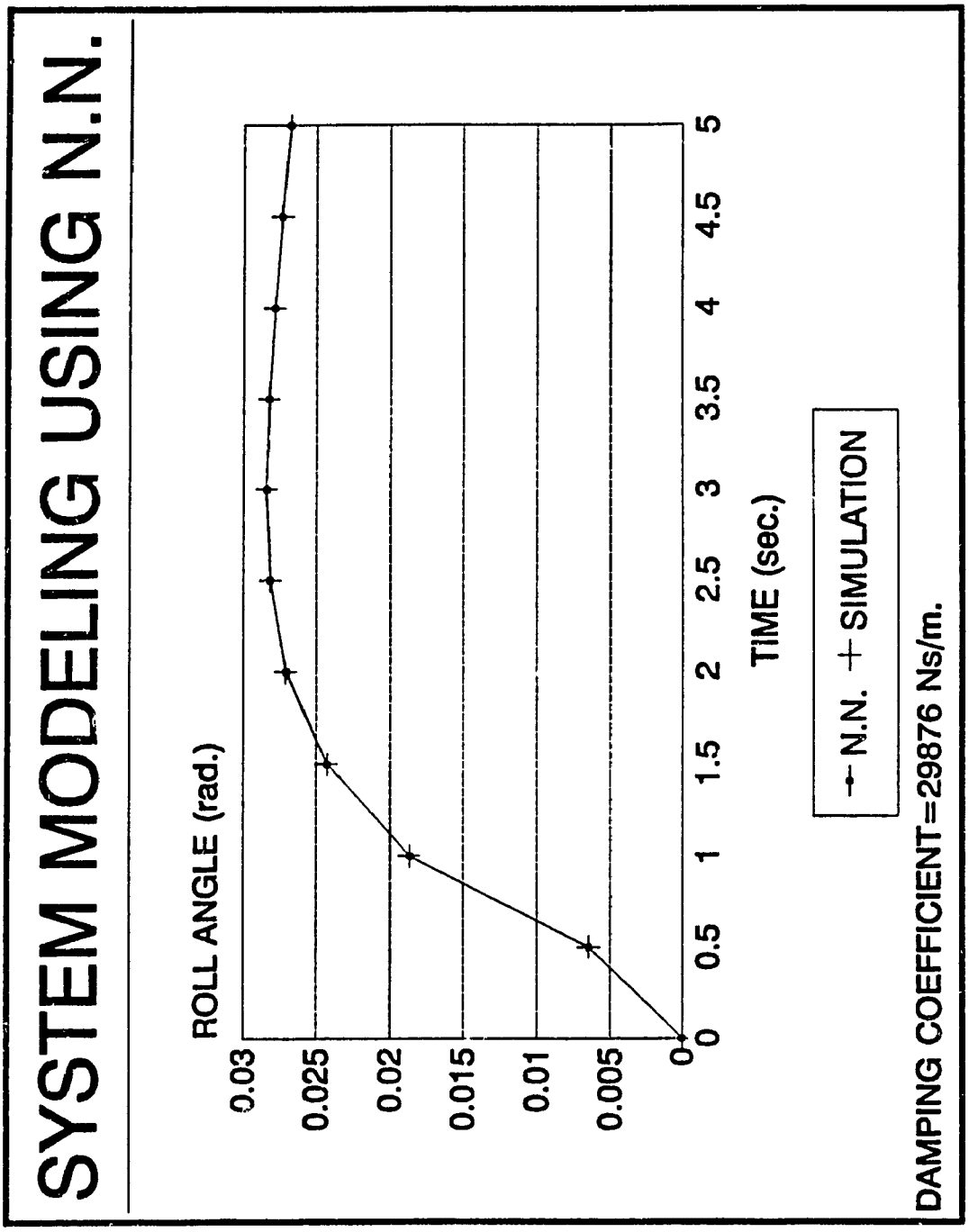


Fig. (5.16) N.N. versus simulation.

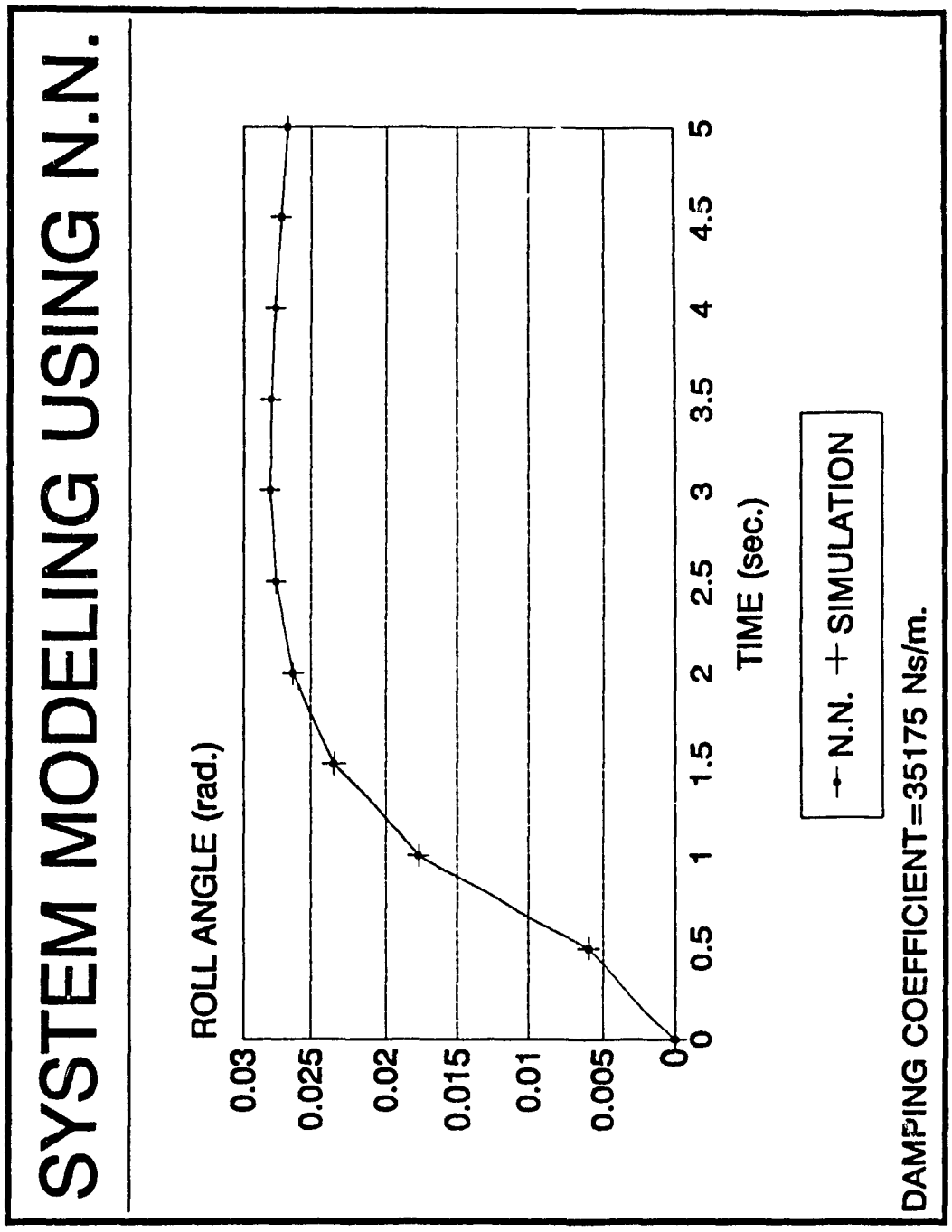


Fig. (5.17) N.N. versus simulation.

depending on the vehicle speed and relative motion between the suspension and the vehicle body. These adaptive systems are referred to as semi active and active suspensions.

### 5.5.4 N.N. FOR SUSPENSION STIFFNESS AND DAMPING COEFFICIENT

In this section the number of variable parameters for the suspension is increased to two. Identical parameters are used for front and rear suspensions where the suspension stiffness and damping coefficient are varied. The torsion bar stiffness in the simulation is maintained equal to its nominal value. Various combination of suspension stiffness in the range of 10000 to 40000 N/m., and suspension damping coefficient in the range of 10000 to 40000 N.s/m are used to generate the data set. A data set consists of 10 values of roll response in the time domain for a set of suspension parameter.

The N.N. parameters used for this part of the study are the same as those presented in table (5.3), except in this case the number of output is two. Data sets generated from 169 simulations are used for the training of N.N. The trained N.N. is then used as an inverse dynamical model of the vehicle to predict the spring stiffness and the damping coefficient given a certain roll behaviour. Figs. (5.18) and (5.19) show the N.N. success in predicting the suspension parameters accurately.

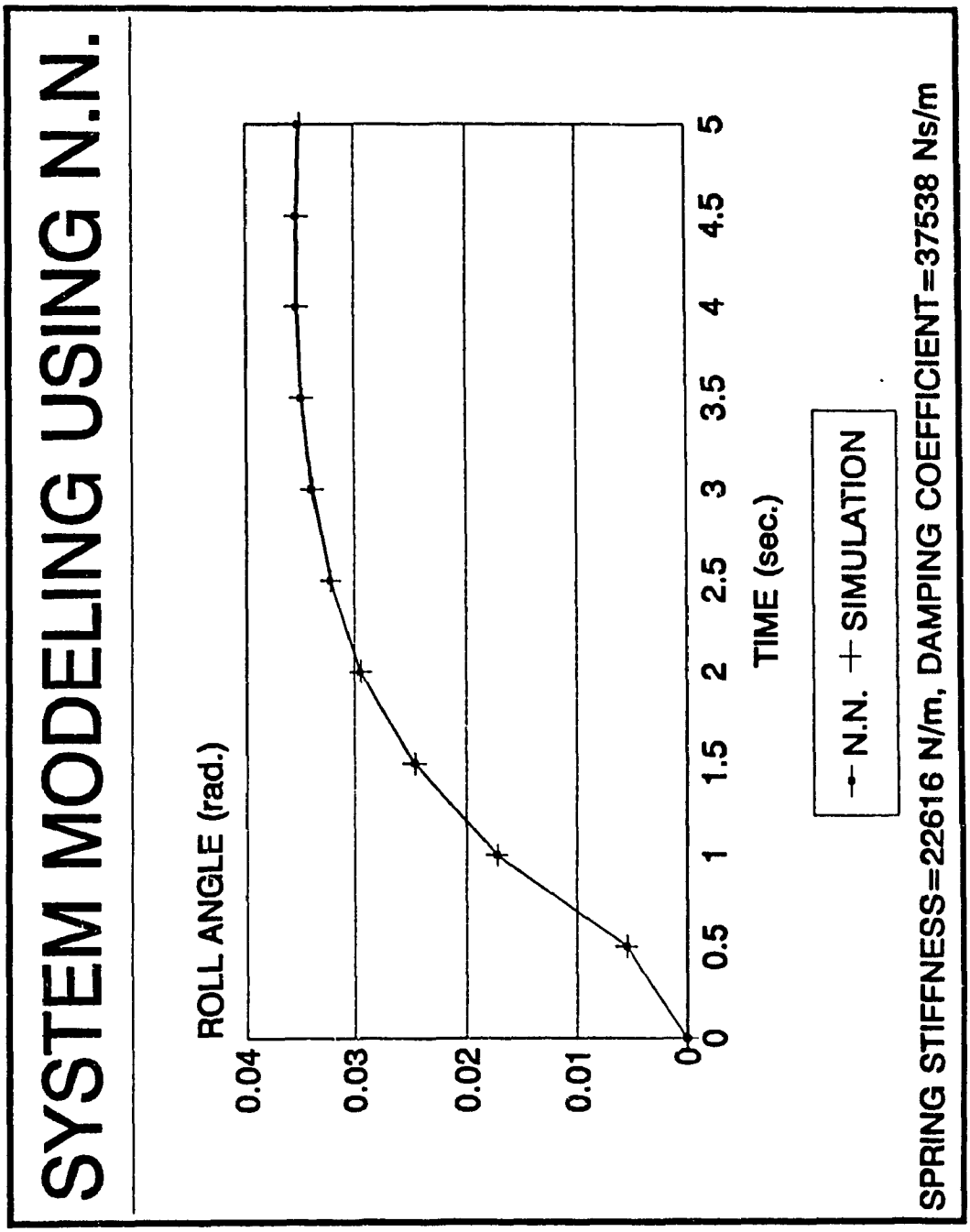


Fig. (5.18) N.N. versus simulation.

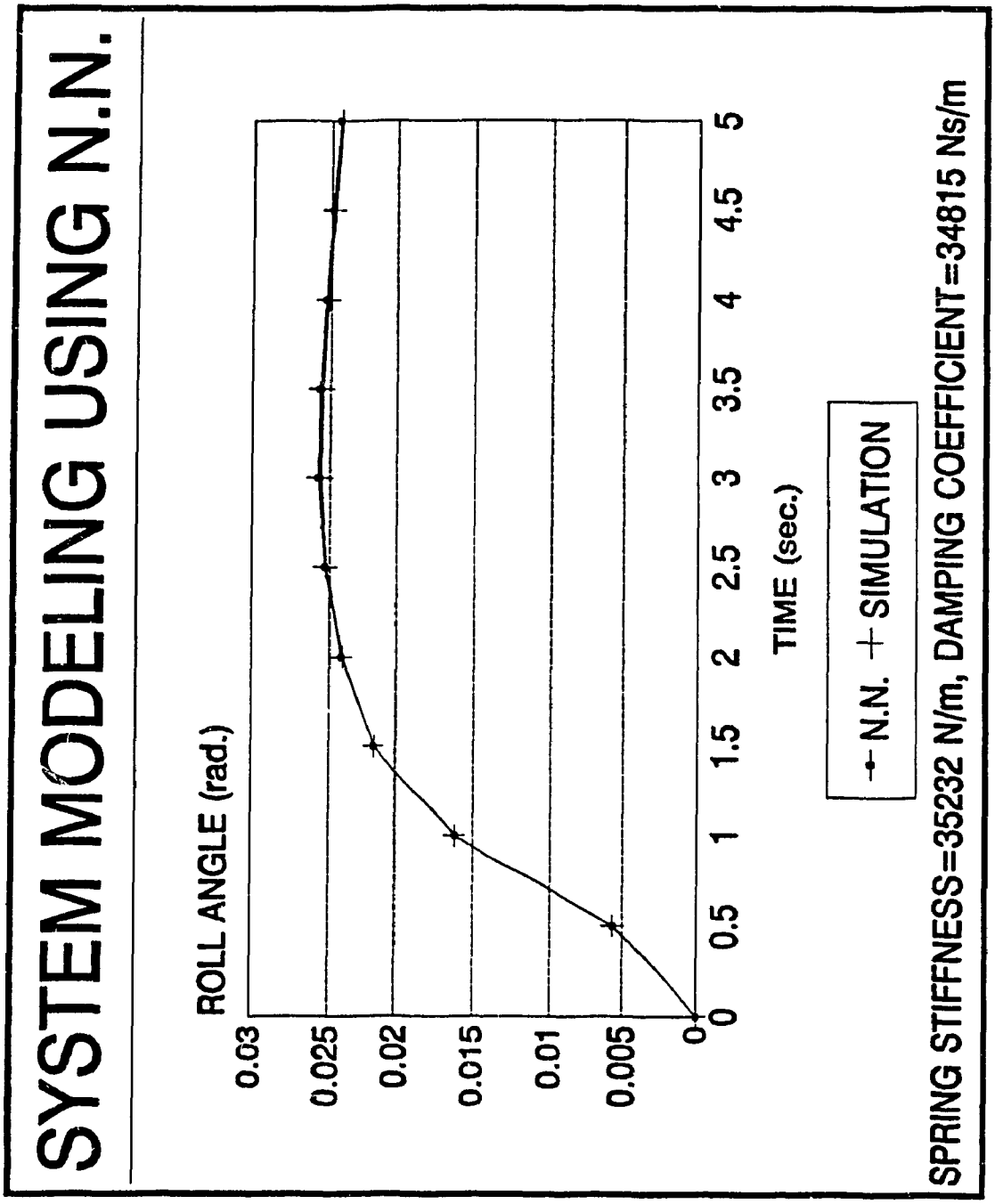


Fig. (5.19) N.N. versus simulation.

As in the previous sections the results show that the roll angle of the vehicle could be decreased by increasing the spring stiffness and the damping coefficient, but that would decrease the riding quality of the vehicle.

## 5.6 APPLICATION OF N.N. AS A CONTROLLER FOR VEHICLE RESPONSE

The inverse dynamic capability of back-propagation N.N. (BPN) has the potential to be applied as a controller for the control of the vehicle response. In this application, attempt is made in controlling the roll response of the six DOF model subjected to a steering input. For this case, the parameter to be controlled is selected to be the suspension damping.

A scheme for control and selection of input and output for the N.N. is based on providing a practical means to generate control signal at an early stage of the response. The selected control scheme, training of the N.N. and simulation results are presented in the following subsections to demonstrate the present application.

### 5.6.1 THE CONTROLS SCHEME

As mentioned above, the objective is to control the roll angle response of the vehicle to a steering input. The control is to be achieved by an early prediction of suspension damping

required to reduce roll response. Therefore, the suspension damping coefficient is the output parameter for the N.N.

In order to provide an early control, the complete time response of the roll angle as obtained in previous applications cannot be used. In this application only one value of the roll response at an early stage of response with rate of steering input and vehicle velocity is used as a measure of roll response.

Based on this, the control scheme is designed to predict a suspension damping for a reduction in the roll angle response. Therefore, various input parameters for the N.N. for a given steering input are selected as:

- Roll angle response $\Omega_x$ at $t=0.25s.$ measured from the time steering input is initiated.
- The steering rate used, which is defined as:

$$\dot{\theta} = \frac{\Delta\theta}{\Delta t}$$

  where $\Delta\theta$ is change in the steering angle for $\Delta t=0.25s.$ .
- And the forward velocity of the vehicle, $V$ .

Based on the roll angle ( $\Omega_x$ ) response at $t=0.25s.$ , a desired roll angle must be defined to the N.N. to predict the damping coefficient required to achieve it. A decrease in roll

angle ( $\Omega_{xd}$ ) is therefore defined as:

$$\Omega_{xd}=\left|\frac{\Omega_x-\Omega_{xi}}{k}\right| \quad k>1 \tag{5.31}$$

where $\Omega_x$ is the roll angle at $t=0.25\ s.$ , and $\Omega_{xi}$ is the initial roll angle which is the roll angle at the beginning of the steering input. The parameter $k$ defines a factor by which the roll angle is reduced. $k$ should be selected such that a feasible response and damping coefficient are predicted. The proposed control scheme is, therefore, defined as an open loop control model as shown in Fig. (5.20). Here the input to the trained N.N.controller are the steering rate, decrease in roll required, and the velocity. The controller output is the suspension damping required.

### 5.6.2 TRAINING OF THE N.N. FOR CONTROL

As discussed above, the input parameters for the N.N. required in this application are roll response at $t=0.25s.$ , forward velocity and steering rate. The output desired from the N.N. is the suspension damping coefficient for a prescribed reduction in roll response.

The six DOF model developed is used to generate the data sets for training the N.N. The data sets are generated for: forward velocity in the range of 57 to 144 Km/h.; steering input for the range of 1 to 5 deg. as a ramp function in 0 to

0.5 sec.; and damping coefficient in the range of 20000 to 40000 Ns/m. All other parameters for the model are maintained equal to their nominal values except for suspension stiffness which is taken as 20000 N/m.

One hundred simulation are carried out for various combinations if the above parameters. Similar to previous sections BPN is used with the N.N. parameters same as those presented in table (5.3) except in this case the number of input 3, hidden 5 and output 1. The data for the training of N.N. are scanned from the simulation results as described below:

$$Input\ 1 - \Omega_x\ Net. - \Omega_x(t) * 10 \quad where\ t - 0.25$$

$$Input\ 2 - V_x Net. - \frac{V_x(t)}{100} \quad where\ t - 0$$

$$Input\ 3 - \dot{\theta} - \frac{\theta(t_1) - \theta(t_2)}{t_1 - t_2}$$
$$where\ t_1 - 0\ and t_2 - 0.25\ \text{sec.}$$

$$Output - C_F - C_R$$

where a factor of 10 and 100 are used in the previous input 1 and 2, respectively, in order to balance the magnitudes.

### 5.6.3 N.N. SIMULATION RESULTS

The trained N.N. is used as a roll controller for the six

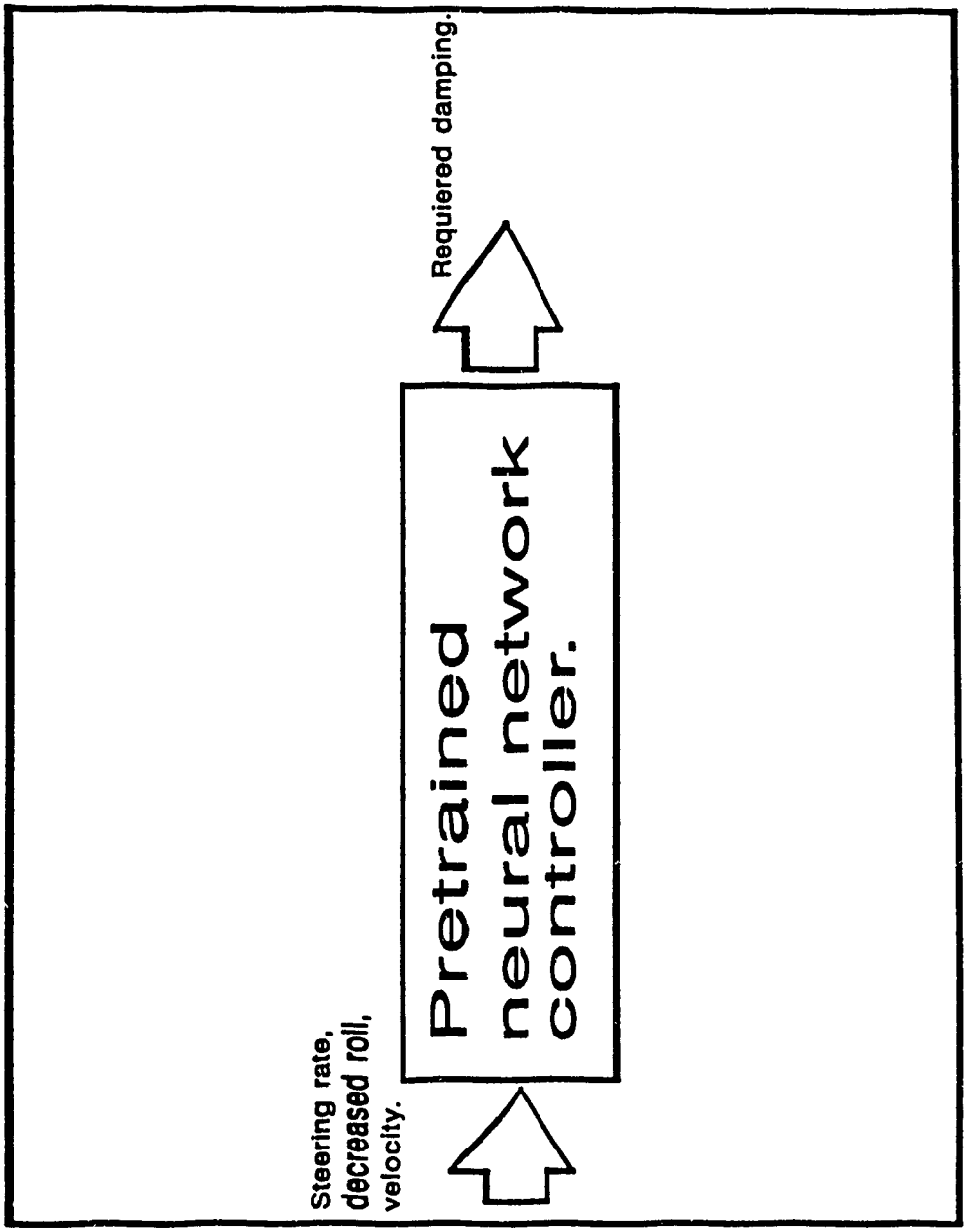


Fig. (5.20) N.N. application for control.

DOF model used in this investigation. Simulation is first carried out in time domain without the controller for nominal parameters and $C_F$-$C_R$-25000$Ns/m$ . For a Steering rate 2 deg./s, Figs (5.21) and (5.22) present the roll angle response for velocity 57.6 Km/h and 100.8 Km/h, respectively. These figures also present the roll response with N.N. controller where the N.N. predicted damping coefficient required is also listed.

The roll reduction parameter $K$ in equation (5.31) for this study is selected based on forward velocity and steering rate, as they both have strong influence on the roll. This value should however be selected such that a feasible damping coefficient is predicted to achieve the reduction. The value of $K$ in this study is based on:

$$K\text{-}1.25 \quad IF \quad V \leq 86.4 \; km/h \;\&\; \dot{\theta} \leq 4°/s.$$
$$K\text{-}1.66 \quad IF \quad V \leq 86.4 \; km/h \;\&\; \dot{\theta} > 4°/s.$$
$$and \quad K\text{-}2.00 \quad IF \quad V > 86.4 \; km/h$$

To demonstrate the effectiveness of the controller, high steering rate is also simulated. Fig (5.23) presents the roll response results for $C_F$-$C_R$-25000$Ns/m$ at 57.6 Km/h for a steering rate 10 deg/s. The result also show the effectiveness of the N.N. controller in reducing the roll response by modifying the damping coefficient to 41286 Ns/m in the presence of a steering input.

In this controller scheme, the required damping is

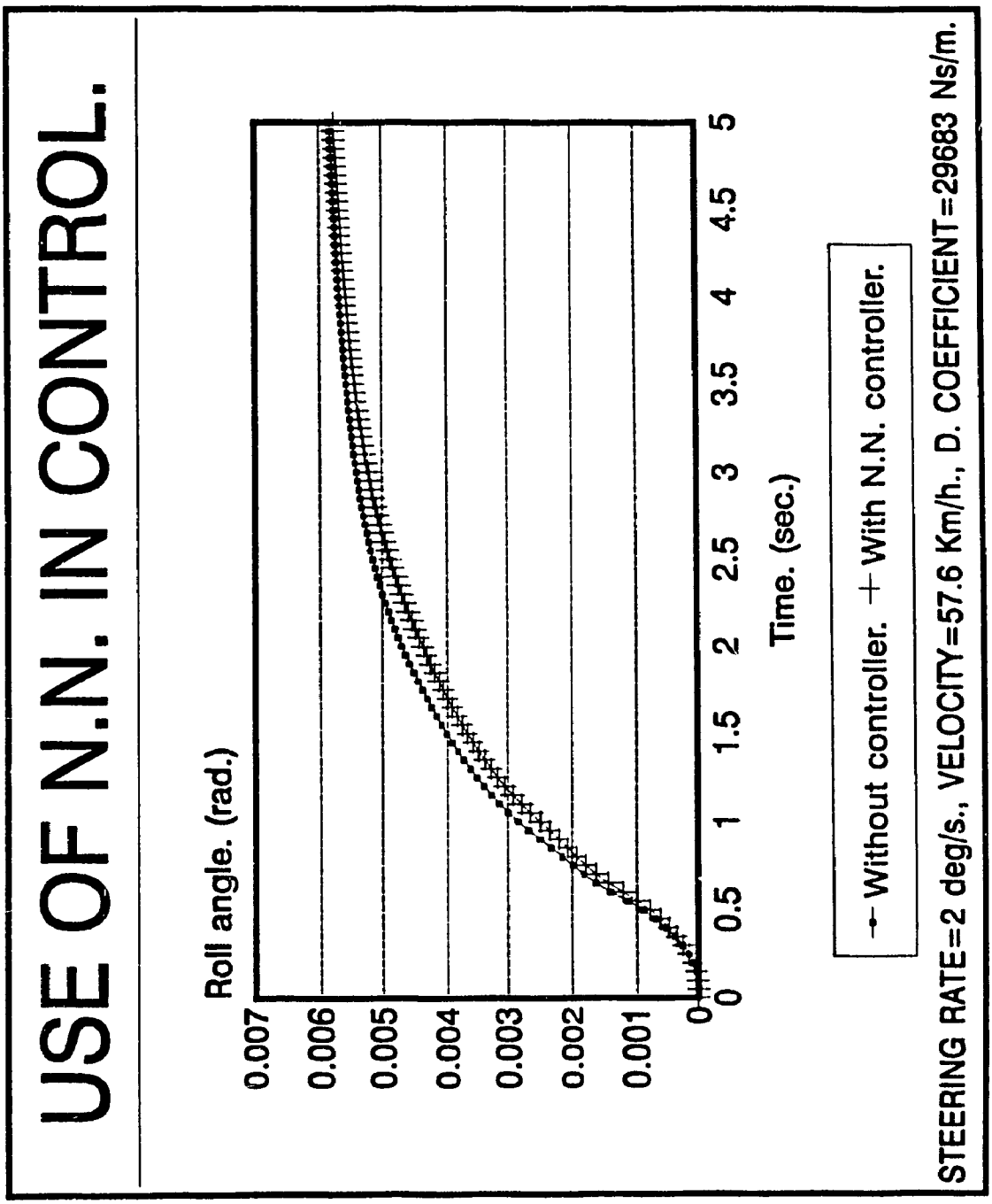


Fig. (5.21) N.N. controlled vehicle versus uncontrolled vehicle.

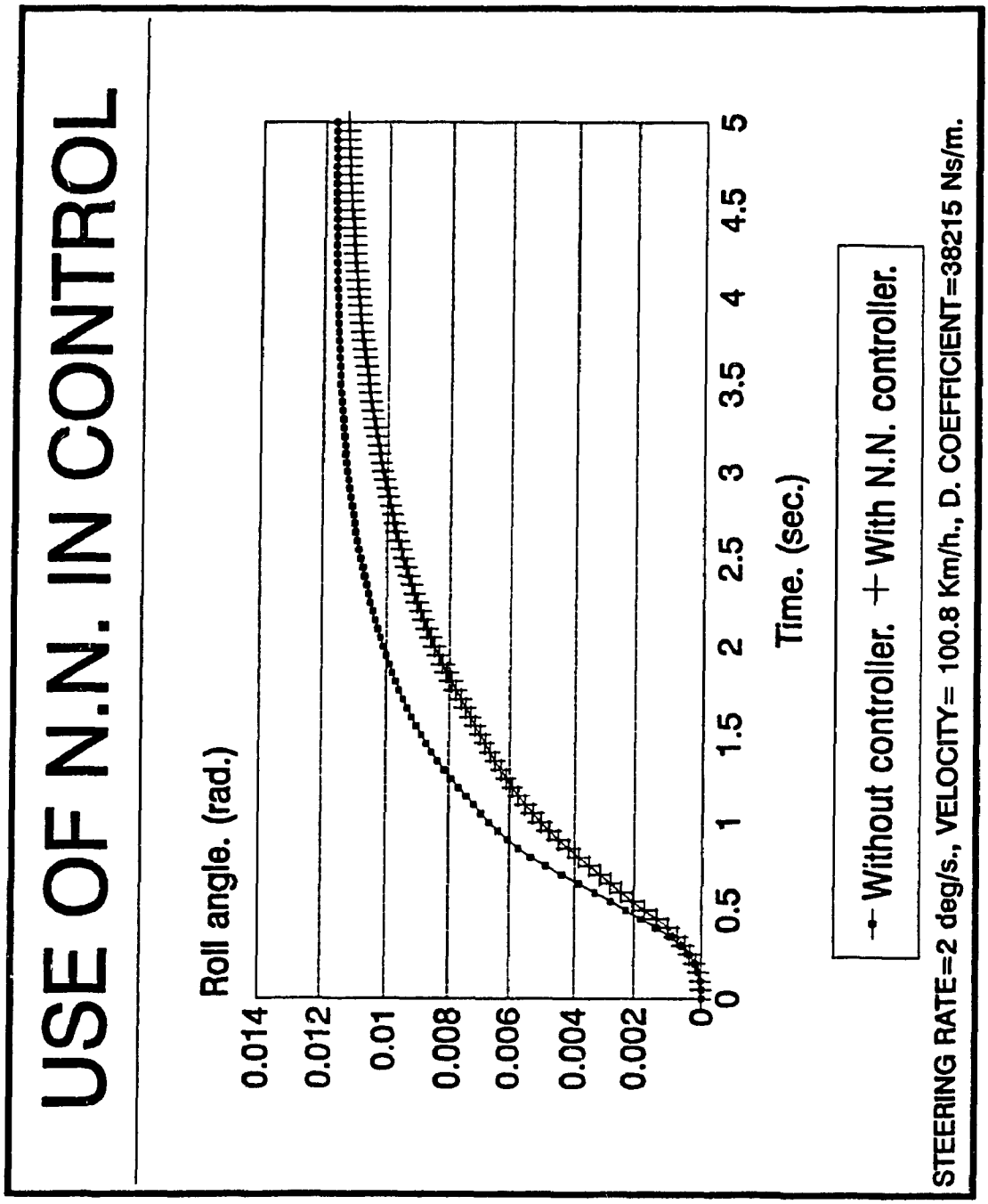


Fig. (5.22) N.N. controlled vehicle versus uncontrolled vehicle.

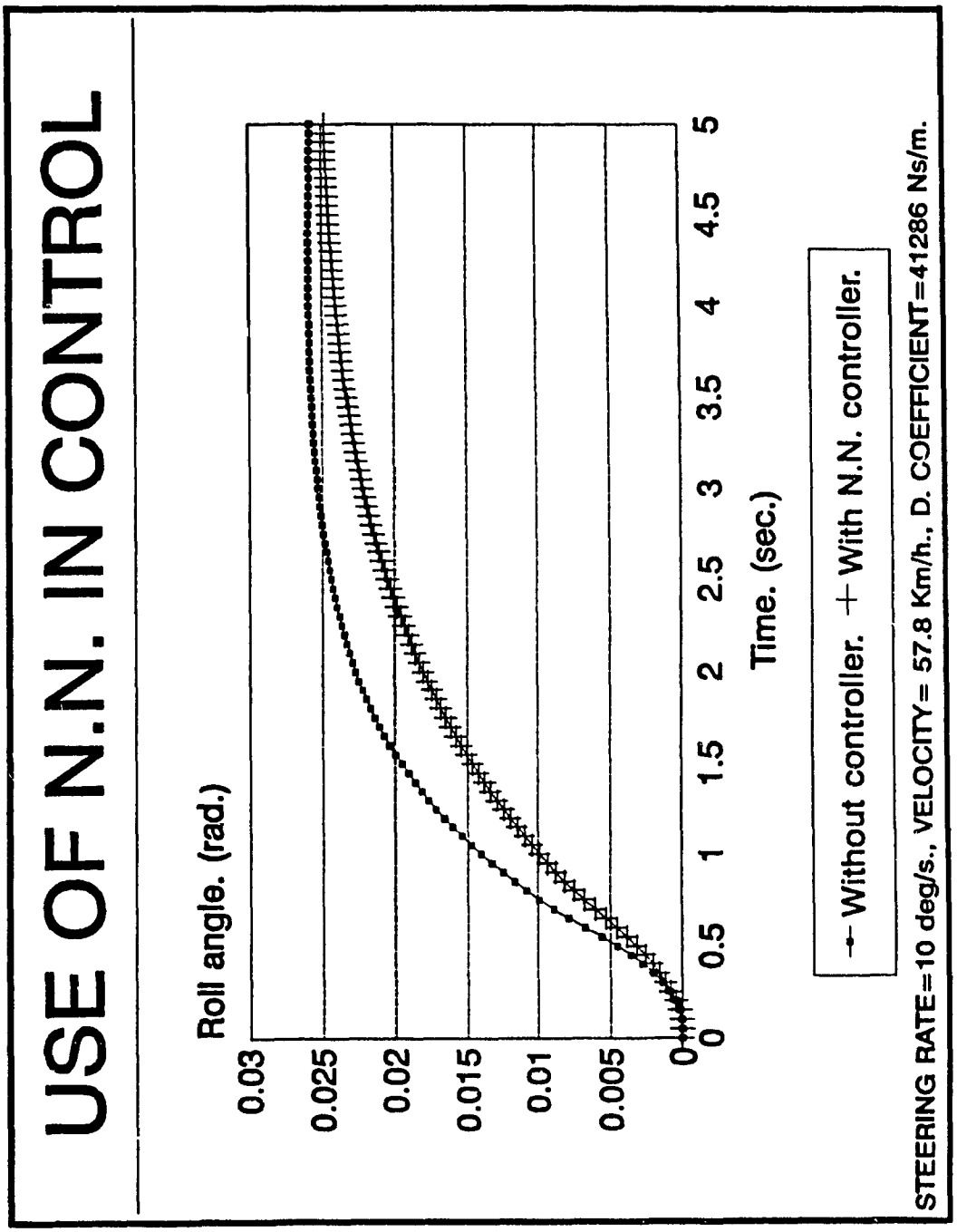


Fig. (5.23) N.N. controlled vehicle versus uncontrolled vehicle.

calculated and maintained only during the steering input and until it is back to zero.

Such a controller would not compromise between stability and ride quality which is not the case for most of the controllers used on passenger vehicles. Most of these controllers would monitor vehicle speed and relative velocity between the sprung and unsprung mass and calculate the damping coefficient accordingly. This would result in stiffer suspension at high speeds.

## 5.7 SUMMARY

This chapter presents a six DOF model and its simulation results for different suspension parameters when subjected to a steering input. Based on the influence of the suspension on the time response of vehicle roll, back-propagation neural network is trained to predict vehicle suspension parameters for a given roll response. Problem is encountered during, multi parameter training due to identical response from different suspension.

The N.N. is trained and tested for prediction of one and two suspension parameters. The results showed excellent capability of N.N. in simulating such dynamical system.

In the second part of this chapter the N.N. is used to build an open loop controller that is able to predict the damping coefficient that will reduce the roll angle. That type of controller would not compromise between the ride quality and the stability of the vehicle as most of the controllers used in vehicles do.

# CHAPTER 6

# 6. CONCLUSION AND RECOMMENDATION FOR FUTURE WORK

## 6.1 GENERAL

Designing a vehicle is a very complicated task. The choice of tires parameters is usually done by trial and error. The suspension parameters are usually a compromise between the vehicle stability and ride quality.

In this study an attempt is made to demonstrate the effectiveness of neurocomputing and neural network in applications to vehicle dynamics study and selection of parameters. The neural network after training is able to predict the tire parameter that would give the highest stability for a certain vehicle. A properly trained network could also predict the tire and/or suspension parameter for any feasible vehicle response.

The capability of N.N. can further be used as a mean for parameter control as demonstrated in this investigation. In general, N.N. is found to be a very efficient tool for simulation of complex dynamical system. However, difficulty is encountered due to inherent limitations. Its potential is significant in application to control of vehicle system

dynamics. A major limitation being the inability for the N.N. to learn when different combination of parameters lead to identical response. From this preliminary study it can be concluded that N.N. has significant potential in application to vehicle dynamics, specially for a tire model. There is also tremendous potential for application in a wide range of control in vehicle system.

## 6.2 MAJOR HIGHLIGHTS AND CONCLUSIONS

The study presented in this thesis is a systematic investigation on the potential of N.N. in application to vehicle system dynamics and control. Instead of an in-depth study on one aspect such as tire model, the study explores the potential on various aspects of vehicle system including control. The major highlights of the thesis are summarised as follows:

1) The major component of vehicle system namely: tire; suspension, and steering are discussed in detail. Their characteristics are discussed and formulated towards the development of vehicle models. Several assumptions made to simplify the model, and the interpretation of the results are outlined.

2) A detail survey of neurocomputing and Neural Network (N.N.) is presented toward the selection of N.N. type and

parameters required. Back-propagation network (BPN) for its capability in the present study is discussed. Although a commercial N.N. software is used, the architecture, learning rules and formulation of BPN are presented and discussed.

3) Simplified three DOF vehicle model is developed and simulated for influence of tire parameters on the vehicle response to a steering input. Based on the simulation results, N.N. is formulated and trained to predict tire parameters for a given vehicle yaw response.

4) The application of N.N. is extended to a N.N. suspension system model using more realistic six DOF vehicle model with four suspensions. Due to vehicle symmetricity, different combination of parameter lead to identical vehicle response. Difficulty is therefore experienced in training the N.N. in multi variable application. It is however found effective in one and two variable training and simulation.

5) The trained N.N. in all cases is successfully implemented as an inverse dynamic tool to predict vehicle parameter for given response. Further the N.N. is capable of predicting parameter for any described response as long as the response is feasible and within the learning range

of the N.N. The N.N. can be considered as an intelligent dynamic simulation tool as it can identify and ignore error or noise in the response. When intentioned noise in the response curve is introduced in this study, the N.N. only predicted inaccurate parameter when the noise is extremely large and frequent.

6) This study finally presents an application of BPN inverse dynamics as a controller to predict suspension damping required for a prescribed reduction in roll response to a steering input. The proposed control scheme although simple and open loop is found to be quite effective in achieving control.

## 6.3 RECOMMENDATION FOR FURTHER STUDIES

In view of the N.N. potential in vehicle dynamics application, a list of future work recommended are as follows:

1) Improve the tire model and introduce non linearities. Due to complex and poorly defined tire characteristics, potential of N.N. is significant for tire modeling.
2) Improve the suspension model and introduce non linearities to the spring and damper.
3) Validate the controller described in this study through fabrication of prototype and implementation.

4) Extend the use of N.N. to other aspects of vehicle engineering as:

   a) Vehicle brakes and Anti Skid control.

   b) Control suspension and use of N.N. in active suspension.

   c) Control of the automatic transmission and determining the best time to shift.

   d) Control of engine performance.

   e) Control of power steering of the vehicle.

## REFERENCES.


1. McCulloch, W. S., and Pitts, "A logical calculus of the ideas immanent in nervous activity", Bulletin of Math. Bio., 5, 115-133, 1943.
2. Von Neumann, J, "Probabilistic logics and the synthesis of reliable organisms from unreliable components", in Shannon, C. E., and McCarthy, J.[Eds.], Automata Studies, 43-98, Princeton University Press, Princenton NJ. 1956.
3. Von Neumann, J, "The general and logical theory of automata", in Jeffress, L. A. [Ed.], Cerebral mechanisms in behavior, 1-41, Wiley, New York, 1956.
4. Hebb, D., "The organization of behavior", wiley, New York 1949.
5. Rosenblatt, F., "The perceptron: A probalistic model for information storage and organization of the brain", Psychol. Rev., 65, 386-408, 1958.
6. Zurada Jacek M., "Introduction to artificial neural systems", West publishing company. 1992.
7. Hecht-Nielsen Robert, "Neurocomputing", Addison-Wesley publishing company. 1991.
8. Freeman James A. and Skapura David M., "Neural networks", Computation and neural systems series. 1991.
9. Domany E., van Hemmen J.L. and Schulten K., "Models of neural networks", Springer-Verlag. 1991.
10. Ellis J.R., "Vehicle dynamics", London business book

limited. 1969.

11. Wong J.Y., "The theory of ground vehicles", John Wiley & sons, Inc., 1978.
12. Gillespie Thomas D., "Fundamentals of vehicle dynamics" SAE Inc. 1992.
13. Liu Peijun, "An Analytical study of ride and handling performance of an interconnected vehicle suspension", M Thesis, Mechanical Engineering Department, Concordia University, 1994.
14. Newton K., Steeds W. and Garrett T.K., "The motor vehicle", eleventh edition, Butterworth International editions. 1989.
15. Rakheja, S. and Ahmed, A. K. W., "An algorithm for simulation of nonlinear mechanical system with symmetric and asymetric dissipative and restoring elements", computational methods in engineering, Vol. 2, pp. 915-920, 1992.
16. Bevan Thomas, "The theory of machines", Longmans 1962.
17. Lugner Peter, "Horizontal motion of automobiles", Dynamics high speed vehicles. (83-146) 1992.
18. Lugner Peter, "The influence of the structure of automobile models and tire characteristics on the theoretical results of steady-state and transient vehicle response", The dynamics of vehicles on roads and tracks. (21-39) 1977.
19. Hunt K.J. and Sbarbaro D., "studies in neural network

based control" , Neural networks for control and systems. (94-122) 1992.

20. Moran A. and Nagai M., "Optimal preview control of rear suspension using nonlinear neural networks", Vehicle system dynamics, 22(1993), (321-334)
21. Palkovics L. and El-Guindy M., "Neural network representation of tyre characteristics: the neuro-tyre", Int. journal of vehicle design, Vol. 14, nos 5/6. 1993.
22. Lukin P., Gasparyants G. and Rodinov V. "Automobile chassis design and calculations", MIR Publishers Moscow. 1989.
23. Bastow Donald, "Car suspension and handling", second edition, Pentech press limited. 1987.
24. Bosch, "Automotive handbook", second edition, VDI Verlag. 1986.
25. Schielen Werner O., "Modelling by multibody systems", Dynamics of high speed vehicles. (39-49) 1992.
26. Kane Thomas R. and David A. Levinson, "Dynamics theory and applications", McGraw-Hill series in mechanical engineering. 1985.
27. Lippman Richard P., "An introduction to computing with neural nets", IEEE ASSP magazine, April 1987 (4-22)
28. Narendra Kumpati S. and Parthasarathy Kannan, "Identification and control of dynamical systems using neural networks", IEEE Transaction on neural networks Vol. 1 No. 1 March 1990 (4-27)

29. Trom J.D., Lopez J.L. and Vanderploeg M.J., "Modelling of a mid-size passenger car using a multibody dynamics program", Transactions of ASME Vol. 109 December 1987 (518-523)

30. Liu T.S. and Chen J.S., "Nonlinear analysis of stability for motorcycle-rider systems", Int. journal of vehicle design, Vol. 13, No. 3, 1992 (276-294)

31. Padgett Mary Lou and Roppel Thaddeus A., "Neural networks and simulation: modelling for applications", Simulation 58:5 (295-205) 1991

32. Toboldrt William K. and Johnson Larry, "Automotive encyclopedia", The Goodhert-Wilcox company, Inc. 1983.

33. Vehicle Dynamics Terminology -SAE J670e, SAE Handbook, (34.297-34.306), 1988.

34 P. Werbos, "Beyond regression: New Tools for Prediction and Analisys on the Behavioral Sciences", PhD thesis Harvard, Cambridge, MA, August 1974.

35 D.B. Parker. Learing logic. Technical report TR-47, Center for computational Research in Economics and Computational Science, MIT, Cambridge, MA, April 1985.

36 James McClelland and David Rumelhart, "Parallel distributed processing", volumes 1 and 2. MIT Press, Cambridge, MA, 1986.